1. Introduction and objective

According to United Nations Food & Agricultural Organization (FAO), “By 2050 the world’s population will reach 9.1 billion, 34 percent higher than today. Nearly all of this population increase will occur in developing countries. Urbanization will continue at an accelerated pace, and about 70 percent of the world’s population will be urban compared to 49 percent today (Alexandratos and Bruinsma, 2012). To feed this larger, more urban and richer population, food production must increase by 70 percent.” To support this food production growth, 80% must come out of increased yields from agriculture through agricultural innovation, as the possible expansion of agricultural land is limited

The World Bank report also showed that 80 percent of the cropped area in the world depends on rainfall alone. However, with highly variable rainfall, long dry seasons, recurrent dry spells and droughts; water is a key constraint in many dry sub-humid, tropical, arid as well as in temperate zones. Added up to high temperature, shallow soil depth with low nutrient status, the case is worst in the Sub-Saharan African regions.

In the 2010-2011, drought in the Horn of Africa has affected over 13 million people. Because of steep climatic gradients, topographic contrasts and general data scarcity in this region, developing soil moisture understanding method is a crucial input for drought analysis (Anderson et al., 2012).

Ethiopia, one of the world’s arid and semiarid regions, is faced with inadequate, irregular and erratic nature of rainfall. Moreover, recurrent drought lack of efficient use of scarcely available water amplified the impact of water scarcity in agricultural production and productivity. The reduction of agricultural production results from a combination of many factors, such as crop management, crop genetics and biotic stress. Achieving more agricultural production to meet the growing demand for food, feed and fuel and fiber for the rapidly increasing population is a continuing and ever increasing challenge (Yenesew and Tilahun, 2009).

In agriculture, soil moisture has a substantial contribution for plant growth as water storage, nutrient transport, and micro-biological activities in combination with higher temperature.

With annual rainfall of more than 2000 mm, Ethiopian highlands represent a water tower in the drought-prone Horn of Africa. Most of the Ethiopian summer rainfalls are evolved as air masses carrying moisture from various continental and oceanic sources, converge and ascend above the Ethiopian mountain plateau (Viste and Sorteberg, 2013).

Average annual rainfall in the study area ranges from 900mm to 1600mm. But the nature of the rainfall is erratic occurred for short duration with high intensity and unpredictable (Yonas et al., 2010). Therefore, soil moisture is dominantly related to rainfall amount and intensity.

Antecedent soil moisture has an influence on the leaching of nitrate and phosphorus in agricultural fields (Lewis, 2010), and added up that high rainfall rates caused rapid increase and decline in soil moisture, indicating faster water flow in larger soil pores.

Climatic variability in combination with soil characteristics and topography variations is the main cause to the dynamics of soil moisture in the soil where crops are grown. The variability of soil moisture, the main element that governs the decline of crop production and productivity, can be improved with variation of these variables using different controlling mechanisms. One of the mechanisms to control future soil moisture is predicting using different hydrological models. Many researchers have been predicting soil moisture and found reasonable results. Yonghui et al., (2003), has predicted soil moisture patterns in the Australian continent in the summer season that mainly related to soil type. Shao et al., (1996) has predicted soil moisture using WAVES and found as an important indicator of vegetation change.

Soil moisture is applied for climate prediction (Conil, Douville and Tyteca, 2009), and was used soil for flood prediction (Basara, 2001). An example, under saturated conditions, soil cannot retain any surplus run-on or precipitation, hence a sharp rise in flooding risk. Bronnstert et al (2011), has studied the impact of soil moisture on flood simulation, and convinced as; physical based hydrological flood models need soil moisture as an initial condition.

It was also noted by Senevirane and Orth (2012), that knowledge of initial soil moisture are important to predict sub-seasonal temperature forecasting.

Ethiopia receives an apparently adequate rainfall for crop production if one considers country-wide average annual rainfall. However, the production of sustainable and reliable food supply is becoming almost impossible due to temporal and spatial imbalance in the distribution of rainfall and the consequential non-availability of water at the required period. Often, crop failure occurs because of unavailability of water at some critical growth stages.

The research question of this study is then ‘how much soil moisture is left in the soil during drying process or recession of the summer (wet) season whose rainfall distribution is uni-modal as well as uncertain in its occurrence’ and ‘How readily available topographic data can be used to predict soil moisture patterns and their spatial distribution’.

Most of the standard geostatistical methods cannot test for the effects of the soil microclimate covariates and they assume data stationarity, as a result, the impact of these factors on soil moisture is applied on SPAW.

If precision agriculture is needed, understanding and determining the availability of spatial soil moisture redistribution is important; because it is a factor that controls nutrient transport and crop evapotranspiration. Better estimation of soil moisture patterns is use full as a reliable input for hydrological models, validation of remotely sensed soil moisture data and is a base for the hydrological forecasting system as the antecedent moisture conditions. Clear understanding of factors affecting daily soil water status is necessary to increase or modify vegetation or water yields.

The temporal distribution of soil moisture within the root zone is a complex interaction of more variables which are related to the historical and present information on climate, plants and parent material (soil).

One of the models employed as a prediction technique for soil water storage for variety of environmental settings is the Soil Plant Atmosphere Water (SPAW) model, which simulates daily soil moisture storage change.

In case of farmed catchments, the factors controlling the spatial variation of soil moisture may change in space and time according to land management and land use. Therefore, this study is aimed to investigate the following two objectives.

- To predict temporal soil moisture content using physical based hydrological model (SPAW)
- Spatial prediction and mapping of soil moisture distribution with ArcGIS package using field topography as basic information

2. Literature Review

2.1. Soil water definition and empirical determination

Soil water content interchangeably named as soil moisture content is water contained in a soil starting from very dry soil whose water is 0 to fully saturated soil where the pores inside the soil are 100% filled.

Soil moisture is also defined as the amount of water level in the layer of the soil which interacts with the atmosphere through evaporation and transpiration. The volumetric water content is estimated with the equation:

$$\theta_v = \frac{Volume\ of\ soil\ water}{total\ volume\ of\ soil} \quad (1)$$

Where θ_v is soil water content ($m^3\ m^{-3}$)

Globally, soil moisture is approximated to be 70 x 10^3 km^3 or 0.005% of the earth's total water volume (George et al., 2013).

Soil moisture can be viewed from different perspectives. Soil moisture is part of the hydrological cycle, controls soil temperature, contributes in plant growth and biochemical fluxes in terrestrial hydrosphere. It basically influences hydrological cycle, evaporation, infiltration and runoff processes.

The soil, plant, and atmosphere act as a continuum along which soil water moves in response to gradients in energy. The energy potential of the water relative to that of pure water helps determine the amount of water stored in the soil, moved through the soil, and moved into and through the plant to the transpiring surface of the leaf. Water will flow from a region of high potential to that with low potential (Tolk, 2003).

The difference between soil moisture and water potential is because the first is about the volume of water stored in the soil while the latter is defined as the soil water energy status used to attract water towards itself.

Soil texture and soil bulk density are the important soil characteristics to determine the soil water content and the soil water potential.

Water potential is the sum of energies from gravitational potential, osmotic potential, matric potential, and pressure potential that is required to move water from lower to higher potential level. Matric potential is a sum of soil capillarity and surface adsorption that depends on the physico-chemical nature of soil. Osmotic potential is a chemical nature of water in a soil solution due to the presence of dissolved substances. Pressure potential represents the solution pressure within the plant cells. Pressure potential is insignificant for soil water movement while gravitational potential has significance until water is drained to reach field capacity. For the movement of water through the plant, the gravitational and matric potentials are less important.

Moist soil subjected to a vacuum (negative pressure or tension) tends to lose water from pore spaces according to the pore distribution and strength of attraction forces in between soil and gravity or the other stated potentials.

The total matric potential of soil then is mathematically expressed as

$$\psi_t = \psi z + \psi m + \psi o + \psi p \qquad (2)$$

Where ψz is the gravitational potential, based on elevation above the mean sea level; ψm is the matric potential, ψp is the pressure potential or the hydrostatic pressure below a water surface and ψo is the osmotic potential.

Conditions in the soil – plant – atmosphere continuum affect the amount of water extracted by the plant before wilting. Matric potential is influenced by soil texture, whose capillary soil pore size and adsorptive properties vary, and this controls the amount of water held within and moves through the soil at low soil water potentials. Distribution of roots throughout the soil, which is the function of soil properties such as soil texture and soil strength, is important to extract soil water.

Soil with a high osmotic pressure has a low water potential and there is thus a low water potential gradient between plant and soil (Casey, 1972). Therefore, osmotic potential gradient between soil solution and the root have to be maintained; hence water will be absorbed to the plant roots. A water potential gradient between the plant leaf and the roots helps to move water through the plant to the leaves. Water is then evaporated or transpired through the stomata of the leaves due to the vapor pressure differences between the leaf and the surrounding air. If atmospheric water demand exceeds the water supply to the plant surface evaporation demand, the plant will face water stress and biological activity will decline. Unless resupplied with water, the plant cells will lose pressure potential, or turgor, and the leaves will permanently wilt and ultimately die.

2.2. Soil moisture controlling factors

Different variables or factors influence the amount of soil moisture distributed in time and space. These factors are climatic and meteorological, topographic, both inherent and dynamic soil properties, vegetation cover and land use.

2.2.1. Climatic and Meteorologic

The exchange between soil and the atmosphere that is between precipitation and evapotranspiration dominates the change of soil moisture in the soil (Wilson et al., 2004).

Evapotranspiration as affected with solar radiation and wind influences the change of moisture content in the soil. Evaporation is the physically based process of transferring water stored in the soil or on the surface of canopies, stems, branches, soils and paved areas to the atmosphere (Verstraeten, 2008). It is dominant when vegetation cover is low and evaporation dominates the loss of water from high vegetative cover.

Evaporation is affected with wind speed, relative humidity, temperature and solar radiation which let the water leave the soil and move to the atmosphere near or away from the source. These variables more or less affect soil moisture in the soil if protection mechanism is employed.

Wind removes out water from the soil based on the humidity level of the coming wind. If the humidity of the air/wind is low compared to the humidity level near or at the soil surface, there is a possibility an amount of water can be removed from the soil surface. Rainfall characteristics like duration and intensity also cause variation in the amount of water infiltrated to the soil. More intensive rain produces overland flow quickly and this causes the macro-pores to be filled up with upcoming washed out silt.

2.2.2. Soil

According to USDA soil texture classification, the particle diameter in between 2mm and 0.02mm is said to be sand, between 0.02mm to 0.002mm is silt and the size less than 0.002mm is clay. Important soil characteristics that control the spatio-temporal variability of soil moisture are soil texture, organic matter content, bulk density and soil macro-porosity.

Variation in soil properties affecting soil moisture may occur vertically as soil horizons with varying water holding capacities change and laterally along hillslopes with changing depths of soil horizons due to geomorphic processes (Conacher and Dalyrmple, 1977; Buol *et al.,* 1989).

Generally, soil properties affect the shape of the soil moisture characteristic equation. Several studies have predicted soil moisture content at fixed matric potentials based on texture, bulk density and/or organic matter content alone with correlation coefficients ranging from 0.80 to 0.97. In general, the greater the clay content, the greater the water content at any particular suction, and the more gradual the slope of the curve. In contrast, an inverse relationship is generally found between soil moisture content and sand. Based on these relationships, in this study a storage index was developed to represent soil moisture holding capacity integrated over a given soil depth (Yeakley et al., 1998).

2.2.3. Topography

Topography is an obvious source of soil moisture variability since it determines surface and to a lesser extent subsurface flow paths, as well as hydraulic gradients driving flow (Western, 2004).

Topography related parameters that affect the distribution of soil moisture in the top soil layer include slope, aspect, curvature, specific contributing area, and relative elevation. Slope influences processes such as infiltration, subsurface drainage, and runoff. It also influences the evapo-transpiration from the soil by controlling the solar radiance received. The specific contributing area is the upslope surface area that drains through the unit length of contour on a hill slope. Then the higher contributing area to the specific point the more wetter its soil is. Relative elevation can influence soil moisture distribution because of its effect on soil water redistribution.

2.2.4. Vegetation

The existence of water in soil with different proportion varies along space and through time because of multiple factors of which one of the factors is root water uptake during crop growth to meet evapo-transpiration demand through its leaves. Crop/vegetation type and cover are therefore important factors that influence the degradation of soil moisture or as a reason to increase the rainfall infiltration rate hence increased soil profile moisture. It can provide shadow and minimize the evaporation from bare soil surface.

Water is available to crops in different water potential status that depends on the water uptake properties of crops. However, in more conventional way, crops extract water in the range from field capacity to wilting point which is named as plant available water which is retained with capillary pores. But, these ranges also deviate based on the soil characteristics in which these crops are planted. Loam soil has higher water holding capacity, while clay has medium capacity. Sand has small range of water holding capacity hence limited available water for crops. Grayson et al (2004), noted that moisture content in the above 50cm soil profile is affected both by atmosphere and active soil roots.

Water consumption characteristics of crops like *Tef (eragrostis Tef),* Faba bean, Sorghum and Chickpea has an importance on the study area.

Tef is a fine stemmed tufted annual grass that looks a bunch of grass with large crown and many tillers whose 1000 seeds weigh from 0.3 to 0.4 g (Likyelesh, 2005). The root depth of *Tef (eragrostis Tef)* reaches up to 1m with frequent range of 0.6m to 1.0m. (Mulu et al., 2001).

Chickpea and faba bean are among field crops grown in the experimental field. Chickpea root depth can reach up to 1.5m to 2.0m deep where its major part is around 60cm (Duke, 1981). Though it is for irrigation, the maximum root depth of chickpea is between 0.6m to 1.0m while the root depth of faba bean and sorghum ranges from 0.5m to 0.7m and 1.0 to 2.0m respectively (Allen et al., 1998).

Generally, roots of many cool season food legumes seldom penetrate deeper than 1 meter even on those soils where the rooting depth of cereal crops is deeper (Gregory, 1988).

Combination of the above stated factors with varying proportions influences the distribution of soil moisture content in time and space in the real world. All of these influences will have an impact on the soil moisture pattern but some will be more important than others in a particular setting. For example, we would expect the spatial patterns of wilting point and possibly soil depth to be important during dry conditions. Under saturated conditions, the spatial pattern of soil porosity will be important. Through well understood information on these factors, soil moisture can be predicted to a minimum error level.

2.3. Soil moisture measurement techniques

Physical and chemical soil properties are affected with the dynamic of soil moisture content. Measurement of soil water content is needed in every type of soil study; hydrology, agronomy and civil engineering.

Though the technique we use depends on the purpose to which we apply, there are several techniques of soil moisture measurement. Many authors classified these techniques in to different groups according to the objective they want to address. Verstraeten et al (2008), and Robock (2000), have classified current soil moisture measurement methods in to gravimetric, nuclear-based, electro-magnetic, tensionmeter-based, hygrometric, and emerging techniques.

But the generalized techniques are classified in to direct and indirect or in to in-situ and remote sensing soil moisture measurement techniques of soil moisture measurement.

For direct (gravimetric) soil moisture measurement techniques, evaporation, leaching or chemicals, are employed for water removal from the soil. Then soil moisture is estimated from the difference between the removed water and the dry soil.

Indirect methods, which are mostly automated, can be done frequently hence has high temporal resolution in contrast to manual soil moisture sampling methods.

2.3.1. In-situ soil moisture measurement techniques

In-situ measurement methods are undertaken in the soil to be measured; but remote sensing techniques are employed to measure soil moisture while they are away from the exact place of measurement. Though measurement is taken directly in the soil, these techniques other than gravimetric method do not measure water quantity in the soil. Except gravimetric method all the methods in the indirect techniques are based on a factor that is indirectly influenced with the water quantity in soil. The techniques are either those measure soil water potential like tensiometer, or that measure reflection like remote sensing moisture measurement techniques while some of them depends on soil water dielectric and also radiologic methods.

Regular gravimetric observation of soil moisture was started in the 1930s in the former Soviet Union (FSU) at a network of agro-meteorological stations. Several neighboring countries adopted the Russian method of soil moisture observation, among them Mongolia, China, India, and a few eastern European countries (Robock et al., 1999).

In this technique, soil sample is taken from the sampling field using core samplers with known weight. This is done with sufficient care in order to extract the natural soil in terms of its physical structure. The sample is weighed with its sampling cylinder and put in an oven for 24hours at a temperature of 105 degree centigrade. It is again weighed for its dry weight. The difference between the initial sample weight and the dried sample weight is the weight of water in unit mass measurement. This mass value can be converted into volumetric water content multiplying with the bulk density of the soil.

Mathematically, it can be represented as:

$$\%Mwt = \frac{(W_{wet} - W_{dry}) * 100}{(W_{dry})} \quad (3)$$

Volumetric soil moisture (gm/cm^3), which is equivalent to

$$\%M_{wt} * Y_d$$

Where **Yd** is oven dry bulk density

The gravimetric method is the accurate measurement technique and is indispensable for calibration of other instruments and techniques.

Being a member of the in-situ soil moisture measurement techniques**,** the soil moisture sensing probe or soil moisture sensor is a device that measures or estimates how much water the soil contains at a given depth and time. It does not measure soil moisture directly rather derives soil moisture indirectly by measuring other soil properties that depend on soil moisture, such as soil water tension or the ability of soil to conduct or store electricity.

Despite of the difference in capacity, accuracy and reliability, field soil moisture measurement can be held with field sensors. These automated sensors endowed in point measurement have been using intensively since the last few decades due to their important role in guiding the soil water management. Unlike the ability to capture high temporal resolution of soil moisture, the spatial distribution is poor because doing so can lead to high cost. Due to this fact, a consensus is important to prefer among manual (gravimetric) automated (field sensors) soil moisture measuring techniques.

Tensiometer, a kind of artificial root that measures soil matric potential (ψm) in the crop growing medium, also measures the potential water requirement of the soil. It consists of a shaft with degassed water in which porous ceramic cap in its bottom end and a vacuum pressure transducer at the top (IAEA, 2008). The term matric potential describes the potential water need of the soil towards itself in unsaturated soil water condition. It is a negative pressure because work is needed to withdraw water against the soil matric forces.

Time Domain Reflectometry (TDR) and Frequency Domain Reflectrometry (FDR) use dielectric properties of soil. Propagation time of a pulse travelling along a wave is measured. This time depends on the dielectric properties of soil surrounding guide and therefore on the soil water content.

Capacitance sensors are also alternatives of soil moisture measurement equipments to others due to their advantage to human health. Capacitance sensors detect the soil moisture by measuring the permittivity (dielectric constant) of the soil either by inserting electrodes into the soil (Gaskin and Miller, 1996) or lowering sensor(s) into access tubes (Dean et al., 1987; Whalley et al., 1992) based on the large difference in permittivity of water.

Despite the unavailability of these techniques at small cost, remote sensing methods are now accessible with the capacity to capture high temporal and spatial resolution soil moisture data. But these signals are limited to the upper few centimeters of soil profile.

2.3.2. Remote sensing method

In-situ soil moisture measurement techniques provide information at only few selected points; otherwise are expensive with high labor requirement to do for high temporal and spatial soil moisture distribution. Therefore, remote sensing is a viable option for such interests.

With remote sensing methods, large area can be assessed for soil moisture content that is at basin level or at continent level. The best advantage of remote sensing technique

soil moisture measurement is; it has large spatial coverage and can be measured day and night.

Unlike their ability to produce high spatial resolution soil moisture with its large area coverage, the temporal resolution with remote sensing techniques is limited compared to automated and manual techniques. Besides, remote sensing methods measure soil moisture only at the very top soil profile part.

2.4. Soil Moisture and Hydrological Modeling

A model is any device that represents a field condition in real world. It is similar to but simpler than the system it represents. One purpose of a model is to enable the analyst to predict the effect of changes to the system. Besides, a model should be a close approximation to the real system and incorporate most of its salient features.
A simulation is a tool to evaluate the performance of a system, existing or proposed, under different configurations of interest and over long periods of real time (Maria, 1997*).*

Ernest (1994), defined simulation as "The use of a mathematical or logical model as an experimental vehicle to answer questions about a referent system."
Model representation is the process of describing system behavior and in-so-doing converting the model that exists in the mind of the system designer conceptual model into a model that can be communicated to others communicative model (Ernest H., 1994).

Besides to the above specified techniques for soil moisture determination and measurement, hydrological modeling is also a mechanism of soil moisture prediction. The models can be physically based, distributed models, conceptual lumped or semi-distributed models (Lee et al., 2007). Fully distributed, physically based hydrologic models explicitly predict the spatial pattern of soil moisture by simulating the water balance at many points in the landscape based on combinations of differential equations (Western and Grayson, 2001).

There are land surface models used to estimate soil moisture with limited data input of soil physical parameters (Mohr et al., 2000; Yang, 2010).

Soil Plant Atmosphoric Water (SPAW) model is a daily water budget physical based model for agricultural field or watershed including reservoir model. It requires climatic, soil and crop input variables for specific farm or field in one dimensional vertical plane. The objective of this model, SPAW, is to understand and predict agricultural hydrology and their ineraction with the soil and crop production with less computational time and limited input data (Saxon, 2006).

SPAW is designed to do field water and pond water simulation and can perform vertical water balance at daily basis. Simulation is done for single crop that can be grown from few to hundred hectares of land. In case simulation is required for agricultural fields at watershed level, outputs from single crop are summed up to get watershed output (Saxon, 2006).

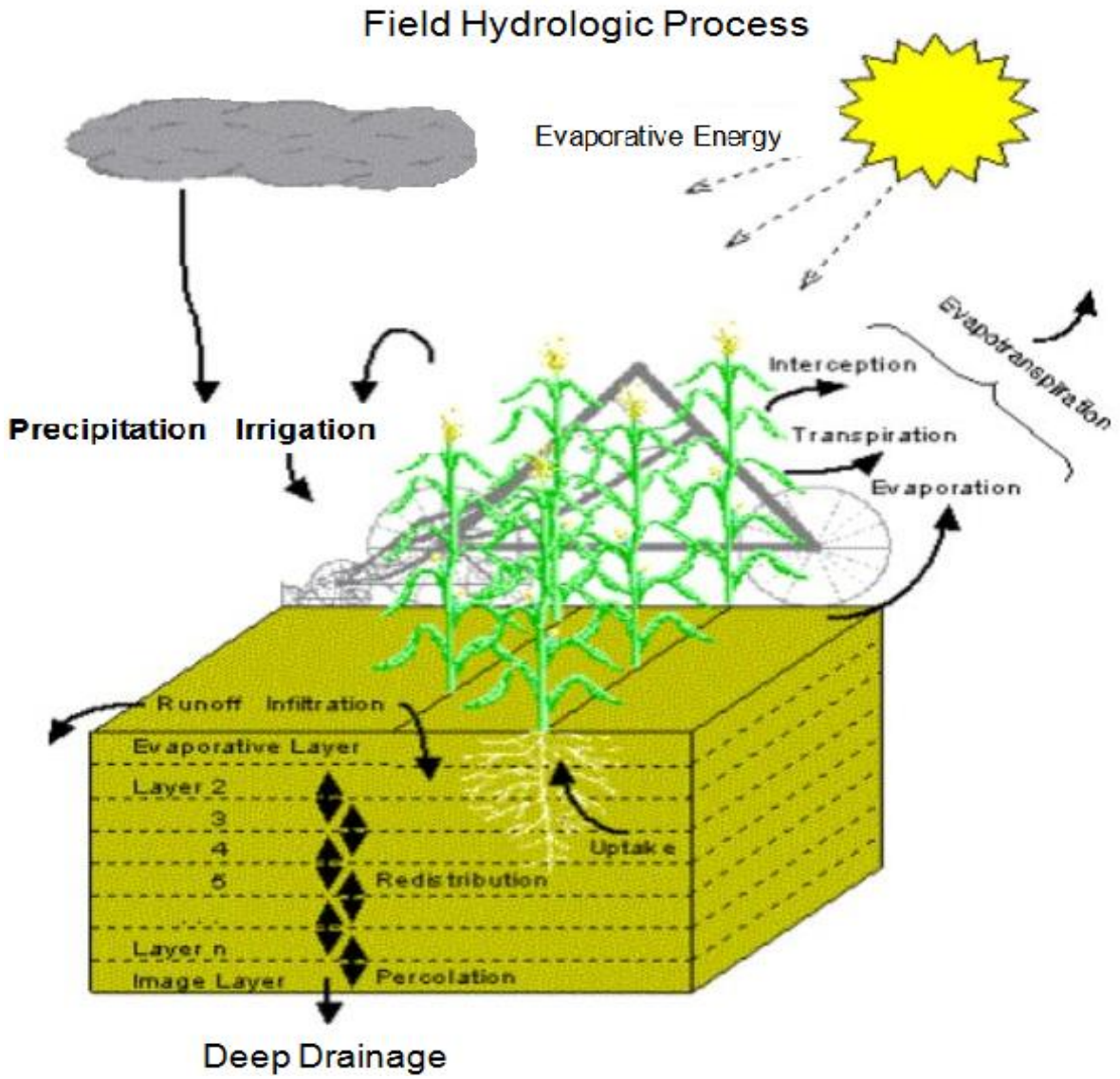

Figure 2.1. Schematic of Hydrologic processes within the SPAW-Field system of an agricultural field (Saxon, 2006).

One dimensional vertical daily runoff is estimated over the simulation field by the USDA/SCS Curve Number method (Saxon, 2006).

It was developed to provide daily and above soil water profile estimates on agricultural field in the Western United States. Besides to soil moisture, it estimates runoff, actual evapotranspiration stress index, deep drainage, percolation, infiltration, percolation.

The principal inputs are daily potential evapotranspiration (PET), precipitation, crop description of canopy, phenology, and rooting plus soil profile descriptions.

Soil layers are divided according to the soil layer uniformity and the user interest. Then, soil texture, bulk density, organic matter content and gravel content are entered to the corresponding soil layer.

Potential evaptranspiration is estimated either from climatic variables using Penman or Penman Monteith, or determined from actual or estimated daily evaporation in each day. PET demand is first fulfilled with the amount of intercepted rainfall before extracting from plant and plant environment. Special consideration of this model is that soil evaporation is represented by inclusion of separate thin soil profile i.e. 1.27cm from where water is readily evaporated and limited by PET. A lower soil layer is specified below the last real soil layer of interest and termed an “image” layer because it is similar to the last real layer. The image layer controls deep percolation or upward flowing water back to the profile. If the water content of the image layer exceeds its field capacity, that water is cascaded downward to become groundwater recharge and its lost from the control volume. If the last real layer becomes drier than the image layer, water will move up from the image layer according to the Darcy calculation; however, the image layer cannot pull water up from below itself if it gets dry.

Root water extraction is represented using typical root distribution for the plants with time and depth. By adding root depth of the specific crop, the program partitioned them in percent to the typical root mass distribution.

The Soil Plant Atmosphere and Water model works in the procedure that potential initial evapotranspiration demand is met with the intercepted water in the crop canopy. The remaining part is divided between evaporation and transpiration based on the crop cover.

Evaporation from the surface takes place in two forms i.e. constant rate where supply of energy limits soil evaporation and the other is a falling rate stage, where soil hydraulic properties control the movement of water to the atmosphere. The rest potential energy for soil evaporation is transferred to the plant transpiration potential.

2.5. Temporal and spatial soil moisture characteristics

Temporal soil moisture variation is driven with the variation of agro-climatic variables. This is mainly dominated with the water input sources which could be either precipitation or irrigation. As these variables are stopped to pursue, its continuity to stay in soil will depend primarily on soil type and topography as well as weather variables. Yeakley et al. (1998), found that both topography and storage before rainfall recession has main controls on the rate of soil moisture reduction during drying period.

Due to the heterogeneity of soils, atmospheric forcing, vegetation, and topography, soil moisture is spatially variable (Kasteel et al., 2007).

Spatial variation of soil moisture was found to vary with terrain attributes like relative elevation, slope and topographic wetness index; (Yu-Hua et al., 2013). Vegetation factors such as type, cover, distribution, and growth period affect soil moisture variation (Jennifer et al., 2004; Hupet and Vanclooster, 2002).

Soil moisture content can vary in deterministic or stochastic ways or in a combination of the two (Western *et al*., 1999; Seyfried and Wilcox, 1995).
Spatially, soil moisture can be assessed in two scales .e. at regional scale and field scale. At the regional scale, it is thought to interact with the atmosphere, to affect the climate and its change, Manabe and Delworth (1990), then to have a controlling function in the hydrological cycle in general. Soil moisture has an effect on the generation of runoff and erosion, plant growth at the field scale. In this scale, soil moisture values are mostly found through ground measurements, Walker et al. (2004), which are typically point measurements collected in locations that can possibly represent the whole field area and at specific time instants.

2.6. Soil moisture spatial interpolation using Geostatistical tool

SPAW model considers the major factors to predict soil moisture in a specific location such as soil physical characteristics; organic matter content, soil texture, agro-climatic parameters and crop parameters with its management practices. But spatial distributed

soil moisture cannot be simulated using this model. Geostatistical technique can predict distribution of spatial information in a given area whose distributed information is important.

Spatial point information is enabled to make continuous surface using geostatistical techniques called kriging. It is a branch of statistical theory concerned with problems of spatial serial data, interpolation and mapping of distributed data, and related problems (Eldeiry and Garcia, 2010).

When additional variable has an impact on the main variable to be interpolated co-kriging is used for better prediction. It works well where the primary variable of interest is less densely sampled than than the additional variable (Eldeiry et al., 2010). Co-kriging is the extension of kriging. Therefore, co-kriging is a method for estimation that minimizes the variance of the estimation error by exploiting the cross-correlation between several variables. The estimates are derived using secondary variables as well as the primary variable.

The co-kriging estimate is a linear combination of both the variable of interest and the secondary variables and is given by:

$$\hat{Z}(x_0) = \sum_{i=1}^{n} W_i Z(\underline{xi}) + \sum_{j=1}^{m}\sum_{i=1}^{n} V_{ij}(\underline{xij}) = 0 \qquad (4)$$

Subject to one of the following sets of linear constraints;

$$\sum_{i=1}^{n} W_i = 1, \quad \text{or} \quad \sum_{j=1}^{m}\sum_{i=1}^{n} Vij = 0, \quad \text{or} \quad \sum_{i=1}^{n} W_i + \sum_{j=1}^{m}\sum_{i=1}^{n} Vij = 1$$

Where, ***Wi*** is the weight associated with the ***n***-nearest neighbors, ***Vij*** are cokriging weights of the relevant to the ***m*** secondary variable, ***Uij*** are spatially correlated to the principal variable.

The equation implies co-kriging is a combination of the primary and the secondary data values.

The “co-regionalization” (expressed as correlation) between two variables, can be exploited to advantage for estimation purposes by the cokriging technique. In this sense, the advantages of co-kriging were realized through reductions in costs or sampling effort (Webster and Oliver, 2001; Stefanoni and Hernandez, 2006).

Mutua and Kuria (2012), have found better result of rainguage values using cokriging taking elevation data as secondary variables than applying kriging. Noshadi and Sepaskhah (2005) also tested the same technique, co-kriging, to estimate reference crop evapotranspiration (ETo) using elevation as covariate in comparison with ordinary kriging and residual kriging.

2.7. Requirement of soil moisture prediction

Recent studies based on soil moisture predictability illustrated potential contributionton of soil moisture for weather and climate forecasts (Koster et al., 2011; van den Hurk et al., 2012) or its potential usefulness for agricultural decisions (Calanca et al., 2011).

Soil moisture is a function of many variables and is a factor by itself for other variables. It is of important to control for actual evapotranspiration in the hydrological cycle. The relationship between these two variables is stated as:

$$ET = f(\theta)PET \quad (5)$$

Where θ is the water content of the root zone and $f(\theta)$ is based on the relative water content and PET is potential evapotranspiration.

Relative water content (θrel) can be defined from;

$$\theta_{rel} = \frac{(\theta - \theta_{fc})}{\theta_{fc} - \theta_{pwp}} \quad (6)$$

On time soil moisture prediction has promising contribution for drought monitoring.

Soil moisture is important preliminary information to predict runoff from a catchment. Lewis (2010) has found antecedent soil water content has an influence on runoff from an agricultural field whose runoff rate was high in wet soil than in dry soil. Cited from Zhang Wei and Nearing (2011)**,** surface runoff was strongly controlled by soil moisture, with a threshold value of the volumetric water content varying from 41 to 46 %, below which no runoff occurred.

3. Material and methods

3.1. Description of study area

The study was carried out in the Highlands of Ethiopia, Amhara region called North Gonder. The experimental agricultural field is found 40km East of Gonder town. It is part of the Gumera-Maksegnit experimental watershed which is found in Lake Tana basin, the main tributary of Blue Nile. The annual mean maximum temperature of this watershed is 32ºc while its annual mean minimum temperature is 32ºc. Overall, it receives mean annual rainfall near to 1000mm. The dominant land use is cultivated land with crops varying from cereals to legumes. The points in the sampling field locations showing a distribution of soil moisture where time series values are held.

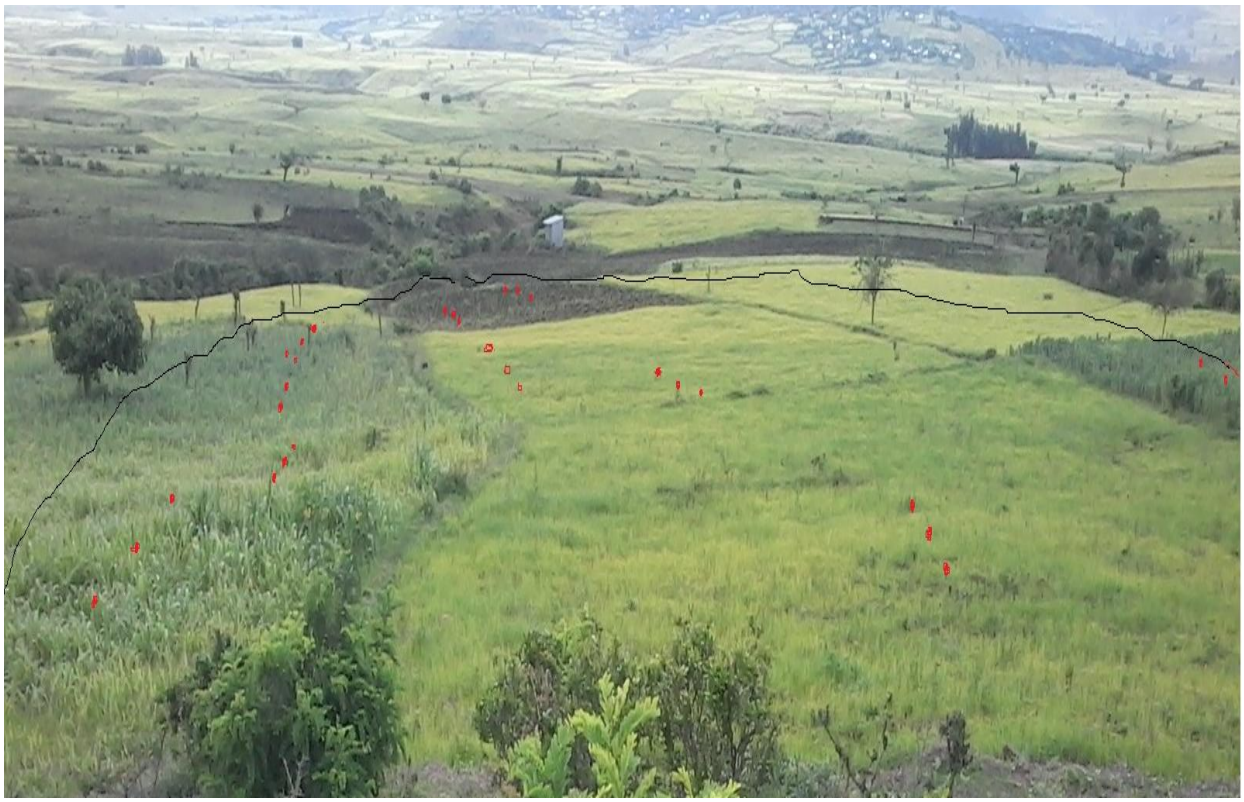

Figure 3.1. A photo showing an agricultural field selected for prediction of spatial and temporal soil moisture distribution in summer season of 2013. (Red points are SM sampling locations)

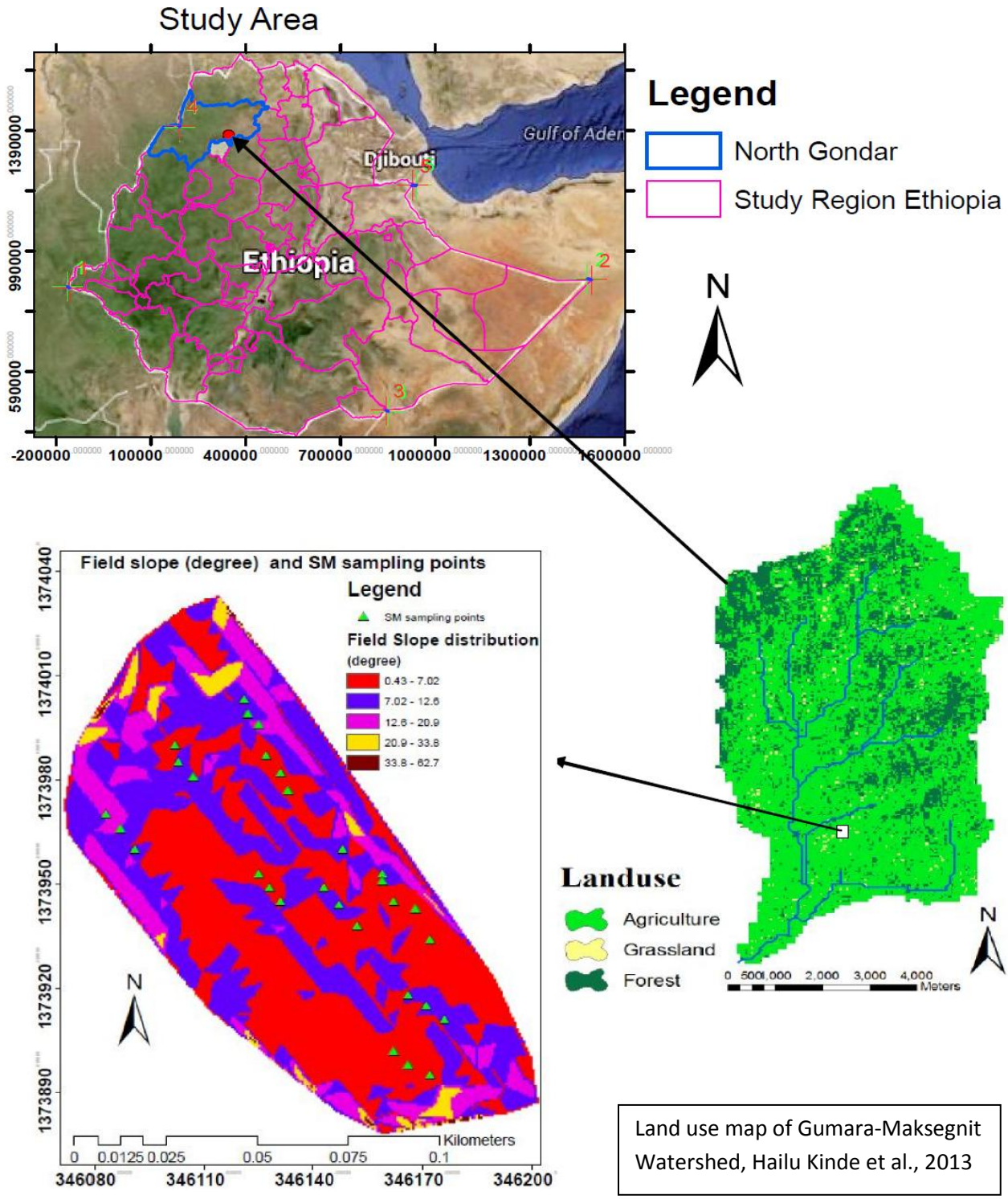

Figure 3.2. Description of study area in Gumara-Maksegnit Watershed, North Gondar, Ethiopia

The livelihood of the area mainly depends on Agriculture that includes livestock and crop production. Farmers use small scale agricultural system using oxen plowing method to produce their crops. The area earns a uni-modal rainfall distribution hence farmers produce crops once a year except some farmers have the possibility to produce twice a year if they can able to produce grain crops that uses residual moisture in clay and clay loamy soils. The agricultural system is generally fragmented in landholding, low agricultural management inputs such as fertilizers, pesticides, uneven rainfall distribution which some of it has erratic nature.

The study field has an area of 1 hectare whose elevation ranges from 2022masl to2001masl while the slope steepness is from 0.4 to 62 in degrees. In the study year i.e. summer season of 2013, it was covered with crops of Sorghum (*Sorghum bicolor (L.) Moench*), Faba bean (Vicia faba L.) teff (*eragrostis Tef*) and chickpea (*Cicer arietinum* L.), that was planted in the late of the season. Their coverage is 14.3%, 8.8%, 42% and 15.6% respectively with additional 16.2% mixed cropping of faba bean and sorghum while the rest part with 3.1% was covered with other vegetative types. The relative vegetative/canopy cover was different for each crop based on the management input of the owners and other factors.

3.1.1. Rainfall

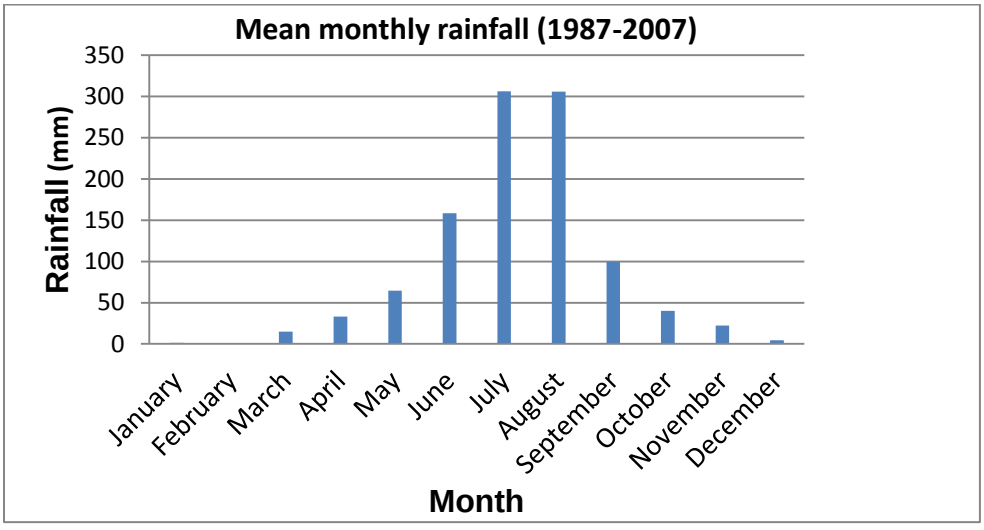

Figure 3. 3. Mean monthly rainfall (mm) of Gumera-Maksegnit Watershed

The mean annual rainfall of the area ranges between 641 mm and 1678 mm based on 20 years (1987-2007) data from Ethiopian Meteorological Agency (EMA). Its mean annual rainfall is 1052mm. Besides to its erratic nature, the distribution of rainfall in time and space is unpredictable which ceases early and late in onset. This causes losses in crop as well as livestock husbandry production and productivity potential (Yonas et.al. unpublished, 2010).

The distribution of rainfall in and near the study location prevails in the Ethiopian summer season in between early of June to the mid of September. Nyssen et al. (2004), has stated the detail characteristics of the rainfall events as "88% of the rainfall intensities were below 30mm/hour while the rest is more than this value".

Numerous topographic obstacles cause the winds to raise and create clouds; hence orographic type of rain occurs on many parts of Ethiopia. Besides, convective movements of air masses, caused by differential heating of the earth surface, and resulting rains of high intensity and often short in duration are most widespread in Ethiopia (Krauer, 1988). Generally, clouds are formed at the end of the morning, as a result of evaporation and convective cloud formation due to daytime heating of the land, and it rains in the afternoon (Nyssen et al., 2004).

3.1.2. Temperature

The mean monthly maximum temperature ranges from 25.ºc to 32ºc with a mean value of 28.5ºc, while the mean monthly minimum temperature ranges from 10.6ºc to 16.1ºc with a mean of 13.6ºc.

Table 3.1. Mean monthly minimum temperature (ºc) and mean monthly maximum temprature (ºc) of Gumera-Maksegnit watershed, data from (1987-2007)

Month	Jan	Feb	Mar	Apr	May	Jun	July	Aug	Sep	Oct	Nov	Dec
Minimum (ºc)	10.6	13.6	14.7	16.0	15.5	14.8	14.1	14.2	13.3	12.8	11.7	9.4
Maximum temp. (ºc)	28.8	30.5	32.0	31.0	30.6	27.6	24.4	25.3	26.8	28.3	29.2	28.3

3.1.3. **Topography**

The topography in Ethiopia, especially in the northern highlands, is known for its variability ranging from highest to the lowest of slope steepness. It is exposed for land degradation due to this nature besides to manmade and natural factors. Soil moisture is not maintained for long period as is in the low land areas because of its low infiltration resulted from most part of the rainfall is converted to surface runoff. High wind impact is also the reason to raise the evapo-transpiration demand. The study Watershed is part of also shares similar topographic indices. It is found in the rectangle from 347000E to 344250E of Easting and 1371250N to 1383500N of Northing.

But, the field where the study had conducted owns small mean slope value approximating to 12 (degree) with maximum elevation of 2022 and minimum of 2001mabs while the elevation range of the Gumara-maksegnit watershed circumscribing the field is between 1923 and 2860masl.

3.1.4. Soil

The soil type near and around the study area is clay to sand in texture and black to brown in color. The bulk density of the soil is 1.23g/cm^3 while the soil structure is blocky with coarse size. The organic matter content of the soil is 1.4% which is very low. Soil depth is beyond 1m while the infiltration rate of soils in three locations is shown in figure (3.4).

Double ring infiltrometer consisting of two rings with inner and outer diameters was used to measure the infiltration rate of soils in the study field. Sizes of inner and outer rings were 26cm and 15cm respectively. The patchworks of grass on the sites were removed and the surface was leveled; then, the bottoms of the rings were inserted 4cm to the soil. Three experiments were conducted in each identified soil type.

Soil samples for determining particle size distribution were collected from two horizons of which soil depth ranges of 0 - 30cm and 30-100cm by compositing distributed at10 locations. Particle size distribution was measured using traditional sieving methods to quantify the coarse grains (gravel) and then using hydrometer method to determine the particle fractions.

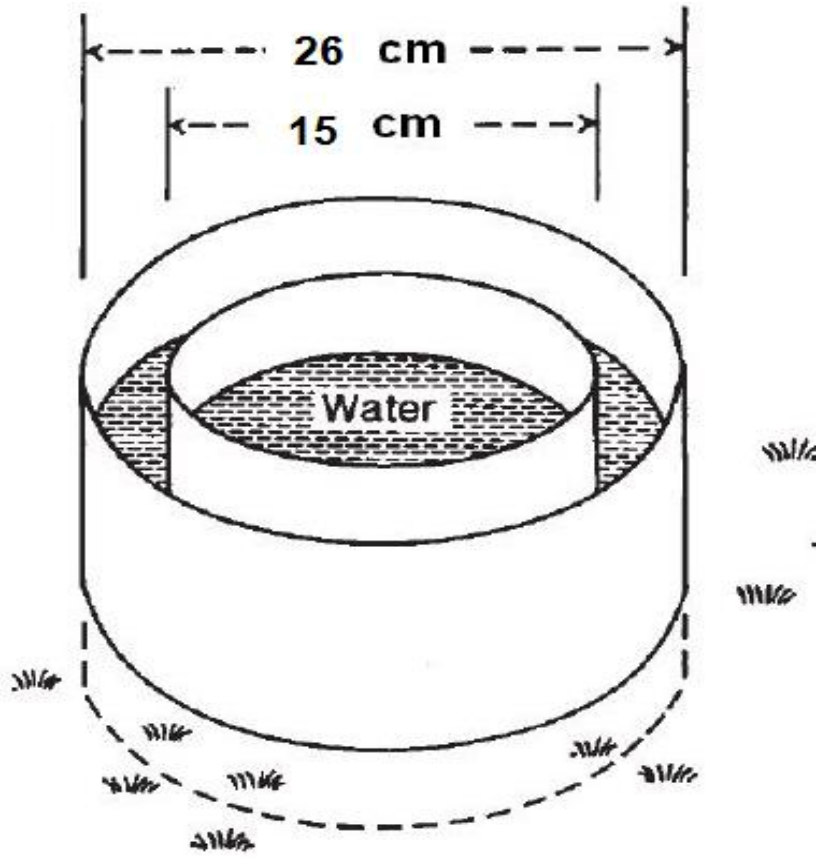

Figure 3.4: Double ring infiltrometer measurement set up used in all locations of the study field

3.1.5. Crop type and land use

According to the watershed survey held in 2010 by Yonas et.al, the major crops grown in the area include sorghum, *tef*, wheat, and barley among cereal crops; faba bean, lentil, chickpea, and vetch among pulse crops; garlic, shallot, and potato among horticultural crops; *nug* and linseed among oil crops; fenugreek (a spice), and hopp. Tef and sorghum are the main staple crops. The average productivity of tef is about 0.92 ton/ha, Sorghum is the second important crop with an average yield of 1.4ton/ha. This yield is too low than the national average yield.

Though crop varieties are currently being improved, most of the existing varieties are less drought and disease tolerant.

The land use of the study area is mainly cultivated land while grazing land is the next in terms of areal size. The grazing land is characterized as overgrazed because of high pasture load. Unlike large size of the pasture herds, their productive is very low due to lack of fodder and low management input to them. Due to the erratic nature of rainfall in combination with excessively grazed land characteristics, the upper soil is washed out hence is less fertile.

3.2. Soil moisture Measurement, Sampling Technique and Instrumental Calibration

Field measurements of surface soil moisture were carried out inside Gumera-Maksegnit watershed, where watershed characterization was done in 2010 Amhara Region Agricultural Research institute Gondar Agricultural Research Center in cooperation with Boku University of Natural Resource and Life Sciences, and International Center for Agricultural Research in the Dryland Areas (ICARDA). The characterization was mainly based on soil texture which is inherent, bulk density, soil depth, soil structure, soil structural stability and structural shape as well as land use, land cover and slope.

A small agricultural field whose surface runoff is drained to common outlet and cropped with different crops was selected to undergo soil moisture study. The field was initially cropped with four different crops of which one is mixed cropping of faba bean and sorghum. Figure 3.1, shows photo of this field covered with these crops.

Sampling location was selected with a consideration of the field based upon topographic and soils as well as crop distribution that can adequately predict field scale soil moisture in order to make the spatial soil moisture interpolation convenient. In this selected field, sampling points were chosen according to the crop and the slope distribution. These points were situated along the slope. The sampling technique was cluster method (Sampath, 2001) with 3 points each. As a result, there were 10 sampling clusters in the study field with 4 different types of crop covers. The specific sampling points of the soil moisture content were chosen based on the crop type and the topographical arrangement capable of representing the field. Accordingly, 9 sampling points were selected in a tef (*eragrostis Tef*) cropped field, 6 sampling points were selected in

sorghum cropped field, 6 sampling points were selected in mixed cropping of sorghum and faba bean, 3 points were in a field covered with faba bean, while 6 points were distributed in a field covered with chickpea that was sown in the late season. These points are those generally clustered for the purpose of minimizing error found from analyzing the soil moisture content from similar crop type and slope steepness. Indeed, the slope for each cluster of sampling points is not absolutely the same due to an obstruction during installation of the access tubes in locations where the slope is the same.

A thin wall access tubes made of fiber glass were inserted in locations preferred for sampling. Then, PR6 sensor was manually lowered down to the access tubes hence soil water contents were measured at 6 depths of 1meter soil profile. In each sampling day, it took 2 to 3 hours to finish reading for all sampling points. Theta profile probe PR2/6 (Delta-T Devices, Cambridge, England) was used to survey soil moisture on 30 points since July 30, 2013 once per week in 9 successive weeks while two samplings were done once per month in the day of 2nd October, 2013 and 9th November, 2013. This instrument is constructed as a cylindrical plastic shaft embedded the capacitor electrodes at pre-fixed intervals. It records voltages based on the electromagnetic (EM) properties of soil as influenced by soil water content. It measures at 6 depths down to 100cm in total and at 10, 20, 30, 40, 60 and 100 centimeter of depths. This was done by inserting 100cm deep access tube according to the procedures recommended with the producer of the instrument.

Soil moisture reading was taken once every week in the determined dates. In order to get stable reading value, two readings were taken per each depth. Values recorded in these points are required to upscale spatially through interpolation using geostatistical tool; and temporally using hydrological modeling i.e. SPAW.

The distance between sampling points was based on the convenience of soil profile for access tube installation besides to the purposely selected slope, soil and crope type; hence the minimum distance was 2 meter while the maximum was 7m. The general set up of the sampling points for soil moisture measurement are already displayed in figure 3.1.

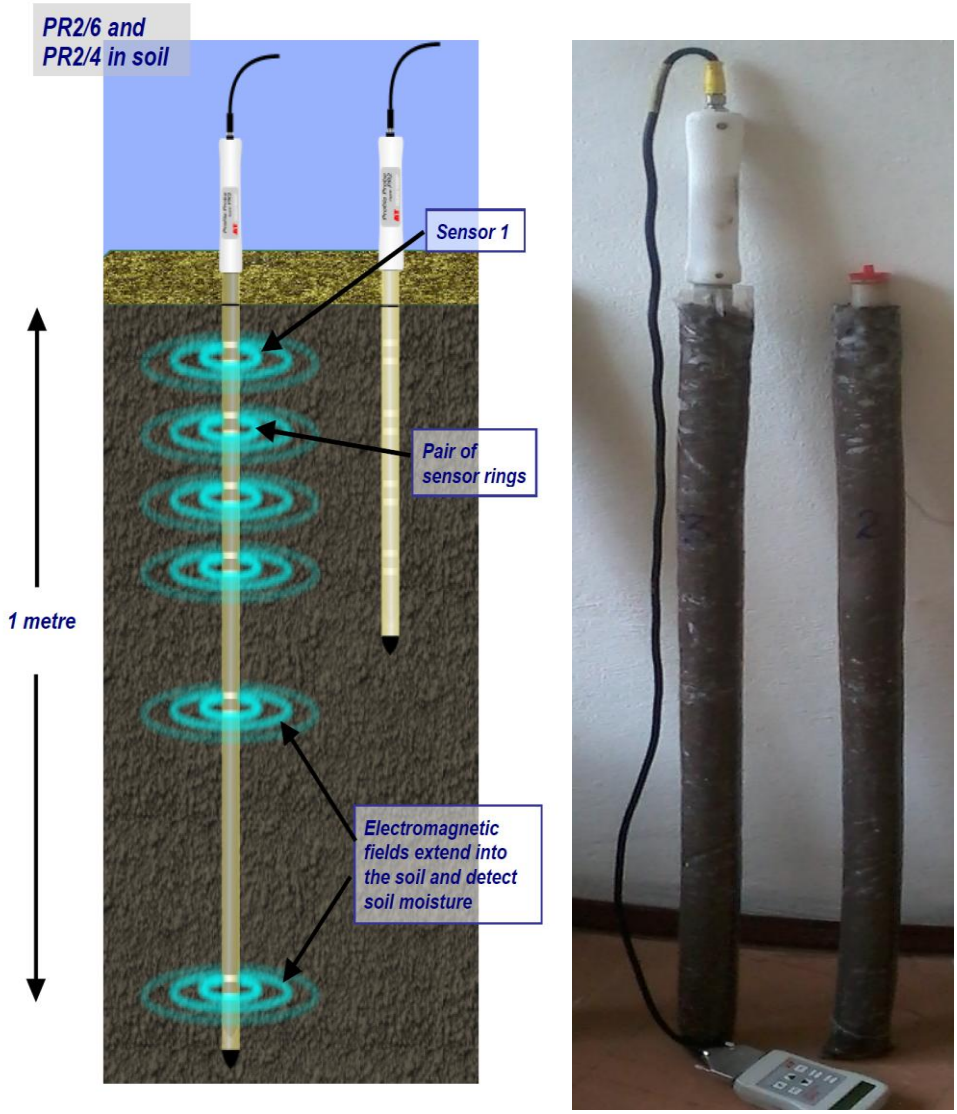

Figure 3.5: PR2/6 and PR2/4 soil moisture profile probe and working principle; Source: User Manual, Delta-T Devices, 2004 (left), PR2/6 calibration process under controlled soil moisture content (right)

The PR2/6 sensor calibration was done on a controlled soil filled plastic tubes. After immediate readings with the PR2/6 sensor, soil samples for gravimetric measurement were taken near the sensing environments of the sensor (electromagnetic fields). About 80 readings were taken and their gravimetric water content was measure. These values were used to calibrate the instrument.

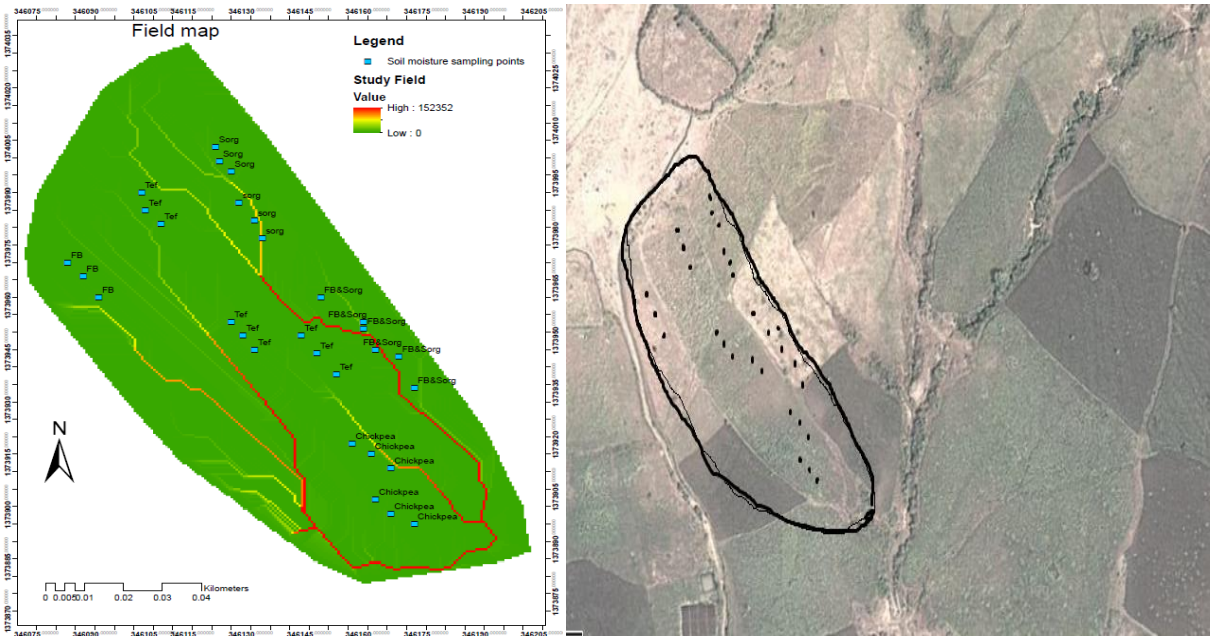

Figure 3.6: Distribution of sampled points with ArcGis10.2 map result (left) and study field as shown from satellite image (right)

Figure 3.7: PR2/6 soil moisture reading device in *tef* (*eragrostis Tef*)

The Profile probes (PR2/6) record a milli-voltage (mV), which is converted to volumetric soil moisture (m^3/m^3) by means of a calibration equation. To obtain this calibration equation than using the manufacturer calibration equation, a relationship between the equipment output and the gravimetric soil moisture results a egression line was fitted. The working principle oof this equipment is similar to FDR sensors that respond to soil

dielectric property as changed with the amount of water in the soil. This generalized equation is specified with;

$$\sqrt{\varepsilon} = a\theta + b \tag{7}$$

Where a and b are calibration parameters, which are soil specific

As a result, the respective values of a and b were found to be 1.62 and 11.53; then by converting all the voltage readings in the instrument to their respective dielectric permittivity with the following equation;

$$\varepsilon = 1.125 - 5.53V + 67.17V^2 - 234.42V^3 + 413.56V^4 - 356.68V^5 + 121.53V^6 \tag{8}$$

Volumetric soil water content, θ, is then calculated from the linear relationship between the square root of the dielectric constant and the soil water content.

This dielectric permitivity was further fitted to the observed volumetric water content and the following was obtained.

$$\theta = \frac{\left(1.07 + 6.4V - 6.4V^2 + 4.7V^3\right) - a_0}{a_1} \tag{9}$$

Where a_0 and a_1 are coefficients

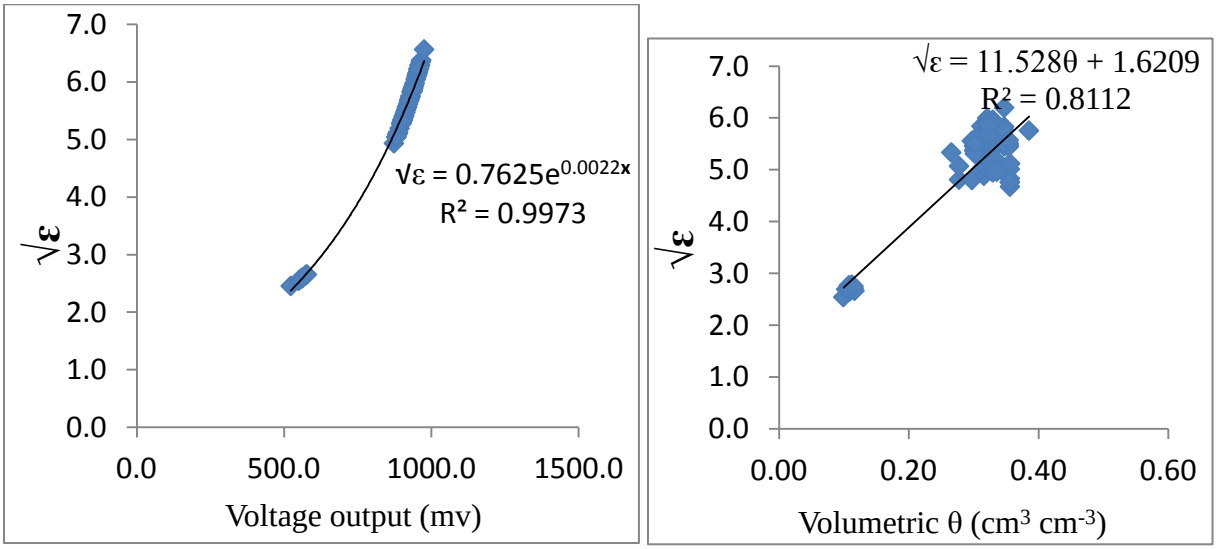

Figure 3.8. A fitting curve relating instrumental voltage output and dielectric permitivity (left); calibration curve of gravimetric moisture content versus dielectric permittivity (right)

3.3. Measurement of soil moisture controlling factors

3.3.1. Weather

Daily rainfall was collected using non-recording type of rain gauge situated 60m away from the center of the soil moisture sampling field starting from 13 June 2013 to 10th October 2013.

The model input climate parameters are collected from the local area using automatic weather station which is found 3.5km away from the study area.

The following are list of input climate, crop and soil parameters to run the model.

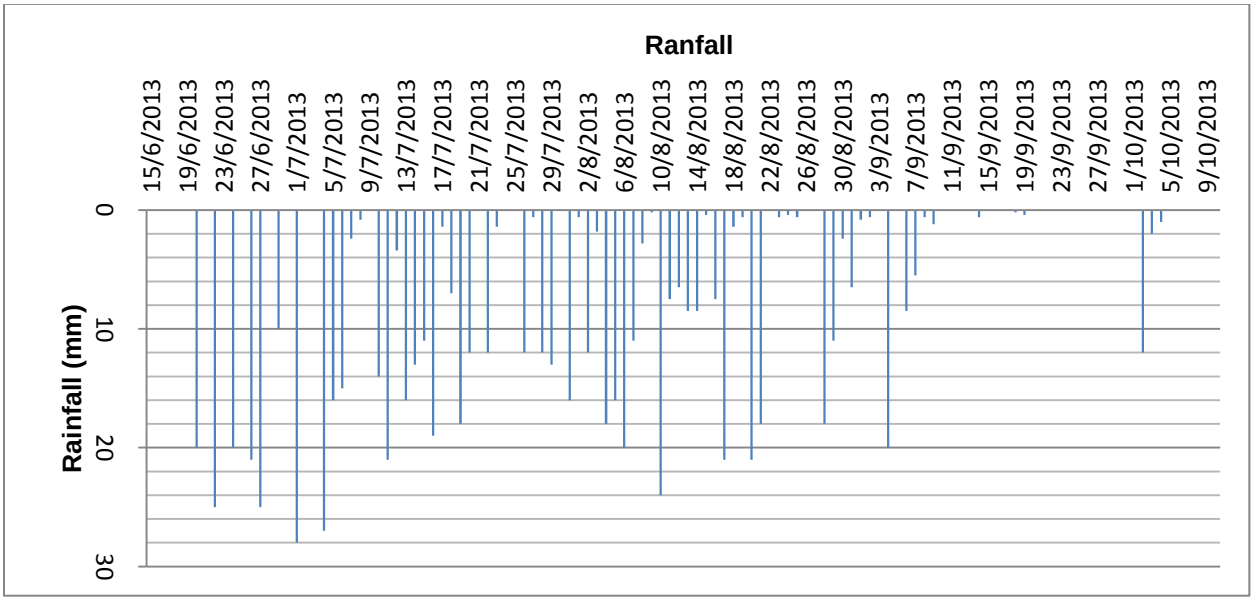

Figure 3.9. Daily rainfall (mm) of the the study fieldbetween the dates of (13rd of June 2013 to 10th of october 2013)

Daily maximum and minimum temprature(°c), relative humidity (%), Solar radation(MW/m^2) wind speed (m/s) were available from automatic weather station installed 3.5km away from the experimental field.

Only Daily maximum and minimum temprature values and estimated Penma values were used as an input data for SPAW simulation. As it is already described in the model

(Saxon, 2006), evaporation and air temprature are less sensitive, hence it is reasonable to use these data from 3.5km away from the expermental field.

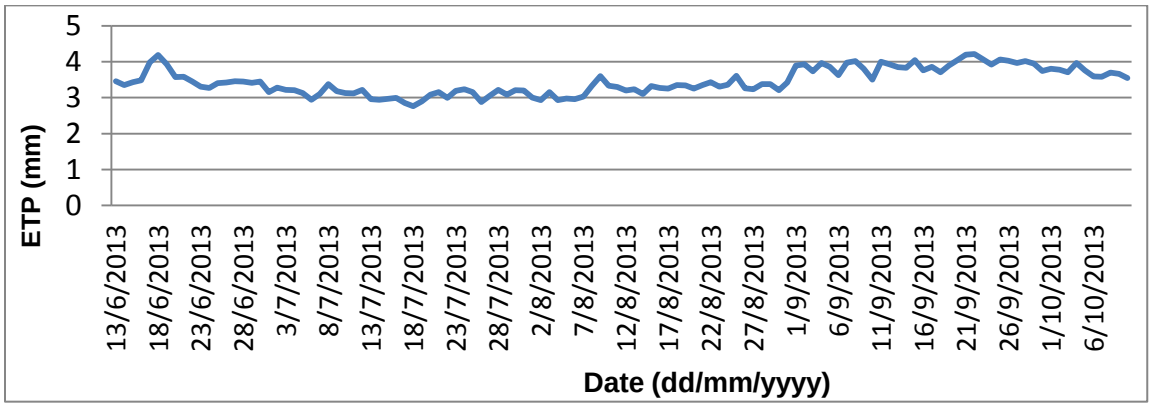

Figure 4. Daily potential evapotranspiration in and around the study area

The above figure 4 shows a list of data potential evapotranspiration estimated from Penman Montheith equation using the CROPWAT model. These data are very basic for the estimation of soil moisture in the upper soil surface. Input parameters were used 3.5 away from the study are to estimate those values.

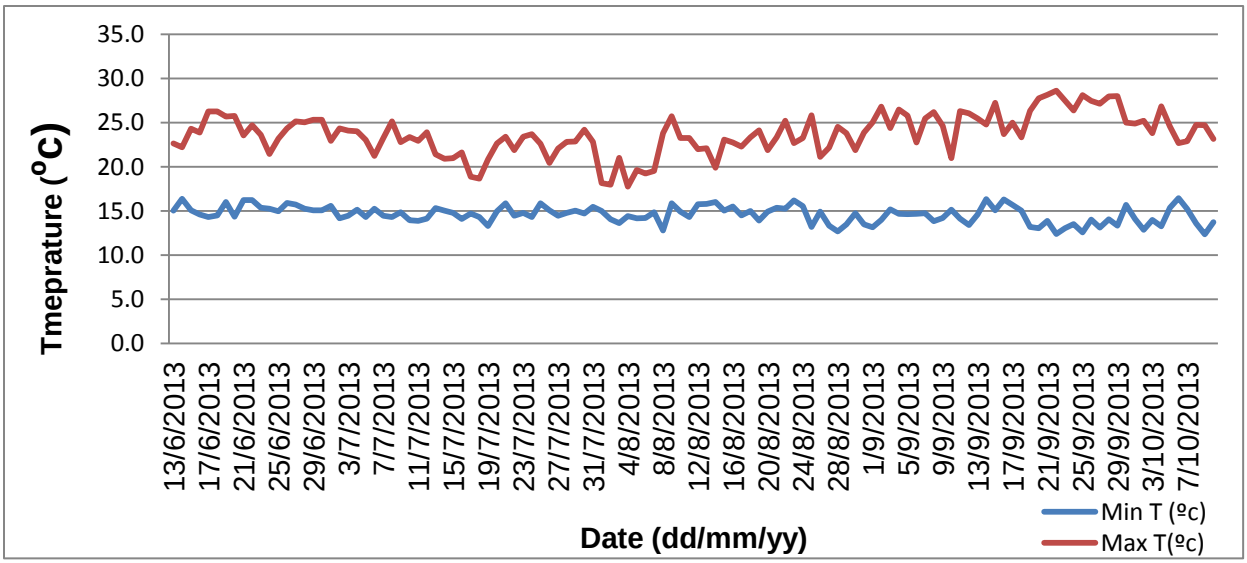

Figure 4.1: Daily maximum and minimum temprature (ºc) between the dates of (13rd June, 2013 to 10th October 2013)

Figure 4.1 is about the temperature values which are measured 3.5km away from the study area. On summer season, this study area has comparatively low values of daily

maximum temperature. These values are crucial as they influence the evapotranspiration rate of the above soil water environment.

3.3.2. Topography

In order to characterize the topographic nature of the study field, one geographic coordinate per 5meter by 5meter grid was surveyed with the help of Garmin etrex GPS and water level instrument. This was done by extending the takeoff or reference point to x and y coordinates and recording relative elevation or z values in each 5 meter interval. It continued until the surveyor gets the dividing line separating surface overland flow to different outlet points.

The coordinate points were analyzed for continuous surface topographic information with the help of ArcGIS 10.2 ESRI 2013.

Further analysis of soil moisture relationship with other topographic indices i.e, curvature, aspect, was not done because main part of the field faces to the same direction and no significant curvature was observed.

In order to derive the slope distribution in the field, some procedures were followed in the ArcGIS. Initially, topographic coordinates i.e. Eastings, Northings and Elevation were entered to an excel sheet. Next, the default Excel file format was changed to CSV file formats. This file is then put in to a folder. The folder is connected to ArcGIS program and the file is opened in this program. The input coordinates i.e. Eastings, Northings and Elevation points are then transformed to X, Y and Z values respectively hence further spatially referenced to WGS_1984_UTM_Zone_37North.

In the 3D analysis tool of the ArcGIS, the coordinates are changed to TIN. This continuous vector structure (TIN) is then converted to the raster form. Slope class was finally done using the surface analysis in spatial analyst tool.

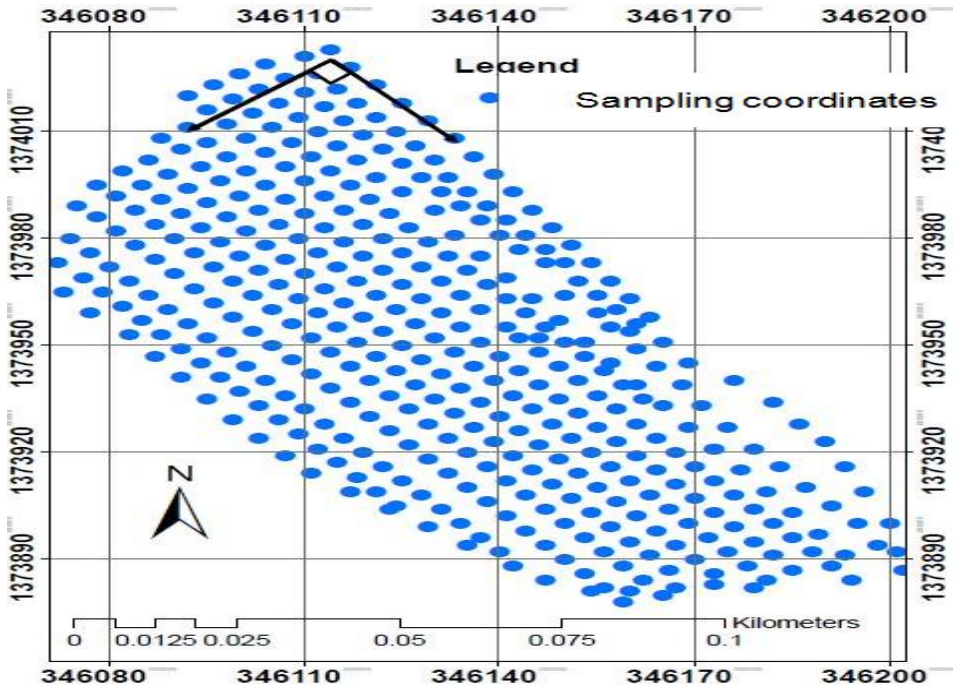

Figure 4.2: Coordinate points that were used for topographic (slope) analysis

3.3.3. Soil characteristics

Soil depth of the field is greater than 1meter and soil data was taken for textural analysis that represents each group of samples except for one group which had different soil type within the group. Eleven soil samples were analyzed for their texture in the whole field. Sampling for soil texture analysis was taken from two depths i.e. 0-30cm and 30-100cm near the soil moisture sampling points. Accordingly, the field has three soil classes in soil depth range of 30-100cm i.e. clay loam, loam and sandy clay soil while loam soil with different textural composition dominates in this layer, according to the USDA soil textural classification.

As per the textural result, higher clay content is situated in the lower part of the field while sand soil is distributed in the mid and upper part of the field. Soil texture in the soil depth range of 0 to 30cm have the same soil class which is loam soil. For both soil layers, their respective textural composition values in percentage were added to the model.

As is specified in the literature review part of this study, detailed survey of soil characteristics improve the prediction of soil moisture in a given environment.

In order to assess the amount of water available for dynamic processes such as evapo-transpiration and deep drainage to bedrock fractures, it was necessary to account for the water retention properties of the different soils in the study area. Hence, soil retention properties of the soil textural proportions (%) found in the study was mapped using Van Genutchten parameters. These values were selected from all soil textural classes available in the sampled soils.

The retention curve was derived from the measured soil textural classes using van Genuchten method. First, Van Genuchten parameters were derived using RETC version 6.02 developed by Van Genuchten, M. Th., Simunek F. J. L, and Sejna M., (2009). These parameters are fitted to Van Genuchten soil moatric potential and soil water content relationship curve was developed.

Table 3.2. Soil textural values (%) using hydrometer method in soil profile depth range of (0-30)cm and (30-100)cm.

Sampling code	Soil depth Range (cm)	Sand (%)	Clay (%)	Soil texture name
Tef1, Tef2, Tef3	0-30	42	24	loam
Tef4, Tef5, Tef6	0-30	39	25	loam
Tef7, Tef8, Tef9	0-30	41	27	loam
Sorg1, Sorg2, Sorg3	0-30	36	26	loam
Sorg4, Sor5, Sorg6	0-30	36	26	loam
FB&Sorg1, FB&Sorg2, FB&Sorg3	0-30	47	26	loam
FB&Sorg4, FB&Sorg5, FB&Sorg6	0-30	39	23	loam
FB1	0-30	35	27	loam
FB2, FB3	0-30	47	35	loam
Chickpea1, Chickpea2, Chickpea3	0-30	41	23	loam
Tef1, Tef2, Tef3	30-100	43	26	loam
Tef4, Tef5, Tef6	30-100	45	26	loam
Tef7, Tef8, Tef9	30-100	45	28	Sandy clay
Sorg1, Sorg2, Sorg3	30-100	49	22	loam

Sorg4, Sor5, Sorg6	30-100	49	22	loam
FB&Sorg1, FB&Sorg2, FB&Sorg3	30-100	45	26	loam
FB&Sorg4, FB&Sorg5, FB&Sorg6	30-100	37	28	Clay loam
FB1	30-100	29	38	Clay loam
FB2, FB3	30-100	47	22	Loam
Chickpea1, Chickpea2, Chickpea3	30-100	39	28	Clay loam

Soil bulk density, soil organic matter content and gravel content were also determined for the top soil layer from previous watershed characterization inclosing this field held in 2010.

A map showing the distribution of soil texture within the field in the soil depth range of 30 to 100cm is shown below.

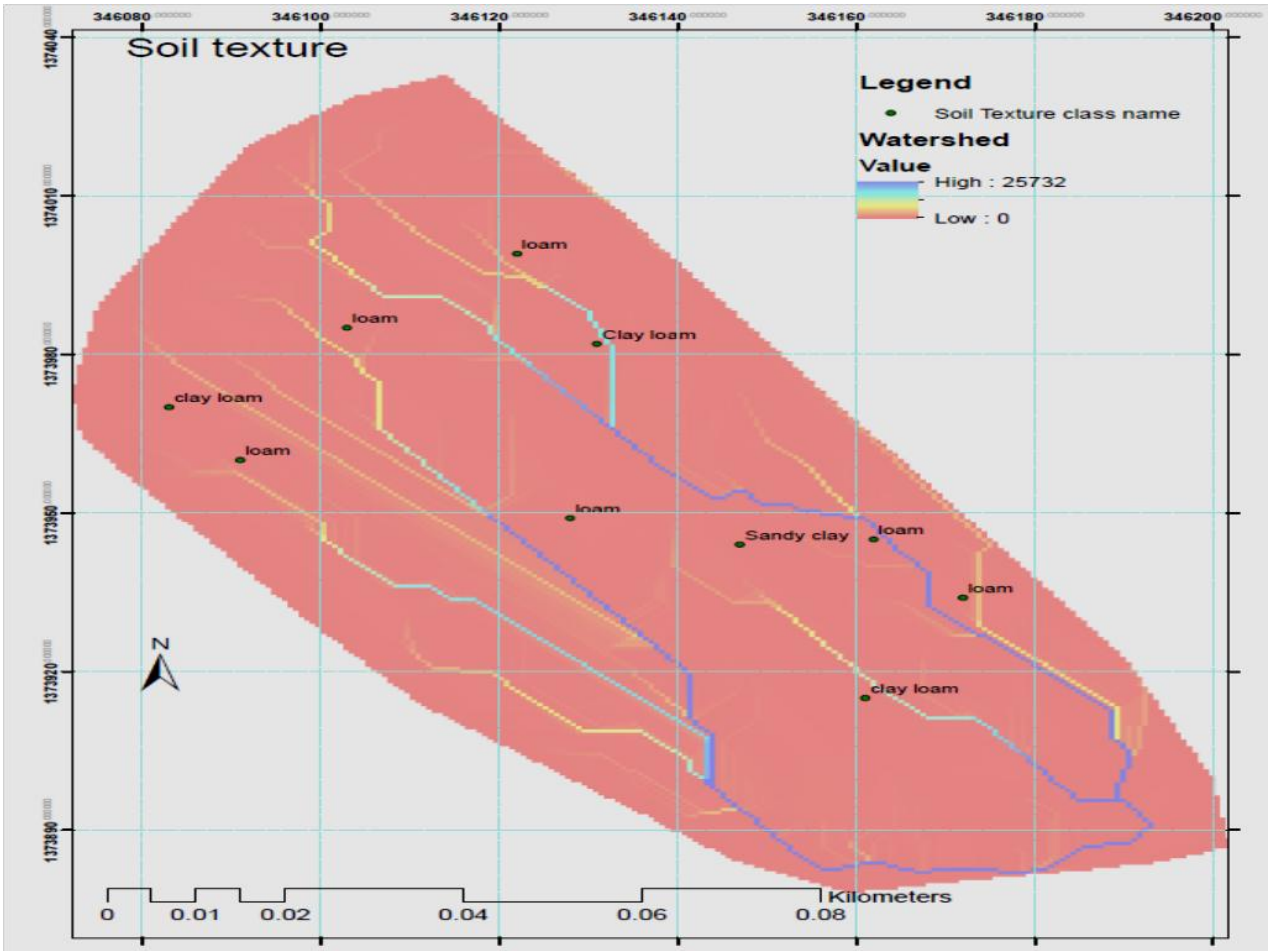

Figure 4.3: Spatial distribution of soil texture classes in the study field between soil profile depth ranges of (30-100) cm

3.3.4. Crop type and vegetative cover

The important crop parameters required to simulate soil moisture in SWAP model are; crop root depth (cm), crop greenness (%), canopy cover (%) and yield susceptibility. These parameters are noted with time in the crop growth period.

The field was covered with different crops owned by different farmers. Sowing for each crop was done at different days. They are field and cereal crops dominantly grown in and around the study field. But the growth performance of these crops was poor except faba bean with area coverage of Hence, these parameters were determined with the help of photos from growth time series.

Tef *(eragrostis Tef)* was the dominant crop in terms of coverage, while the other crops; sorghum, mixed cropping of faba bean and sorghum, as well as chickpea have proportional coverage among them. But, chickpea was planted later than all crops, because it grows with residual moisture. This is in the lower part of the field where the proportion of clay is higher relative to the other parts. As a result, the portion of field covered with chickpea lately was covered with other different scattered weeds.

As per the canopy cover, faba bean had higher coverage in most part of the soil moisture on the sampling moments. Conversely, the canopy cover of mixed crops of sorghum and faba bean was less, because of the weak growth performance. Chickpea had less canopy cover due to its leave nature and late plantation.

To identify the percentage of crop canopy cover in time series, a photo was taken using digital camera due to the subjective nature of human visual observation in cover estimation. Photo image was measured on 3 days; 30th July, 2013; 20th August, 2013 and 3rd September, 2013 near to the soil moisture sampling points. The peak canopy coverage was on the last canopy cover measurement date.

Since the field was cropped with four different crops, the model was run for each crop and soil type in order to get reasonable predicted values. Greenness of all crops other than sorghum was set to 100% starting from the date leave emergency to the crop maturity level, since newly emerged root has full greenness.

Root depth/length of tef (*eragrostis Tef*) is mostly less than 1meter, according to Mulu et al., (2001). Generally, maximum root depth values specified in the literature part of this study were used as an input for SPAW model.

Though different literatures recommended different maximum root depth and greenness of sorghum according the environment it grows, proportional values to the default values in the model was entered.

3.4. SPAW model input variables and calibration process

In order to run the model, data from an observation in the field, estimated values from local data, and cited information from the region was used. Besides, basic assumptions, as the model developer recommendation, were considered. Observed data like soil moisture, weather data, soil characteristics i.e. texture, bulk density, organic carbon content and gravel content, crop data like canopy cover and growth period were collected in and near the study field. Estimated values of evapo-transpiration values from penman-monteith equation were obtained. Catchment runoff characteristics, both qualitative and quantitative indicators were entered according to the field characteristics.

A basic assumption was taken as ground water does not contribute to the soil moisture distribution in the study field hence set to be deeper than 12meter.

As there are not measured evaporation values from pan or other direct measurement techniques and also not easy to differentiate between evaporation and transpiration from the evapo-transpiration estimates in our case, monthly inputs were cited. Evaporation defaults were entered by compromising past studies conducted in Ziway and Tana Lakes.

Equation (10) was applied to estimate evapotranspiration values as an input data for SPAW model.

$$ET_0 = \frac{0.408\Delta(R_n - G) + \gamma 900/(T + 273)U_2(e_s - e_a)}{\Delta + \gamma(1 + 0.34U_2)} \quad (10)$$

Where
ETo = Refernce evapotranspiration (mm/day)

R_n = Net radation at the crop surface (MJ/m^2day)
G = Soil heat flux density (MJ/m^2day)
T = Air temperature at 2 m height (m/s)
U_2 = Wind speed at 2 m height (m/s)
e_s = Saturation vapour pressure (Kpa)
e_a = Actual vapour pressure (Kpa)
e_s-e_a = saturation vapour pressure curve (Kpa /Co)
γ = Psychrometric constant (Kpa/ Co)

The Penman monthith method was run in a CROPWAT model to generate daily PET values with inputs of locally measured parameters and list of outputs are described in figure 4 and *Appendix vi*.

Table 3.3. Lake (open water) evaporation of Lake Ziway, Ethiopia, (Assefa and Melesse et al., 2009)

Month	Solar Radiation	Simple Method Lake Evaporation K = 0.53	Coulomb C.V et al.			Aycnew T.		
			Energy	Penman	CRLE	Penman	Radiation	Pan
	W/M^2	mm	mm	mm	mm	mm	mm	mm
January	246	142	143	154	132	150	135	159
February	250	131	149	162	135	128	120	144
March	249	144	152	166	149	148	142	192
April	252	141	156	166	155	188	138	142
May	259	150	163	170	160	188	138	156
June	243	136	147	168	155	135	107	137
July	208	121	128	136	146	139	115	126
August	219	127	136	137	136	135	115	123
September	226	126	141	136	137	164	124	112
October	260	151	159	162	141	200	151	170
November	263	147	160	161	144	223	157	178
December	249	145	143	157	139	225	157	130
Total		**1662**	**1777**	**1875**	**1728**	**2023**	**1599**	**1769**

Simple method, which mainly uses solar radiation data, in table 3.3 is defined with the following equation;

$$ET = K_1 \frac{Rs}{\lambda} \quad (11)$$

Where ET is daily evapotranspiration from wetland or shallow open water (mm d-1), Rs is solar radiation (MJ m-2 d-1), λ is latent heat of vaporization (MJ kg-1), and K1 is a coefficient (0.53).

The term energy is to mean;

$$E = \frac{Rs + N}{\lambda(1+\beta)} \quad (12)$$

Where β the Bowen ratio and N is *is* change in the energy storage in the water

The “pan” values in table 3.4 were measured with a pan that has wide use around the world called US Class A pan.

CRLE model was developed by Morton, (1986), computes evaporation for deep lakes

Penman combines the mass transfer and energy budget approaches and eliminates the requirement for surface temperature to obtain its expression for the evaporation in mm per day from open water:

$$E = \frac{\Delta R'_n}{\Delta + \gamma} + \frac{\gamma f(u)(e^*_a - e)}{\Delta + \gamma} \quad (13)$$

Model results of monthly evaporation, as monthly mean value in the years of (1960-1992), from Lake Tana showed in the range of 100mm to 150mm, Kebede et al., (2006) in the respective months of our study.

Location climate is the same to the specified climatic values; therefore, no constants were added.

Soil hydrological group was chosen to be, hydrological group “B”. The field capacity percentage of image layer before downward drainage is imagined to be 100%. Downward soil water drainage is therefore takes place after the soil in the image layer is above field capacity.

Other boundary conditions like; maximum image layer flow rate was limited to 2.54cm/day while the soil water conductivity in percent was set to 5%.

The model (SPAW) was run for total of 10 clusters, each cluster belonging its soil texture information. Soil moisture (v/v) for model calibration was entered to the model averaging each cluster’s value.

Figure 3.1 shows a general flow chart on how water from precipitation is distributed throughout and above the soil surface. Both evaporation and transpiration are employed in removal of water from the soil surface. The potential evapotranspiration demand is met based on the quantity of water in the soil. Soil water status at field capacity and above tends to meet these demands.

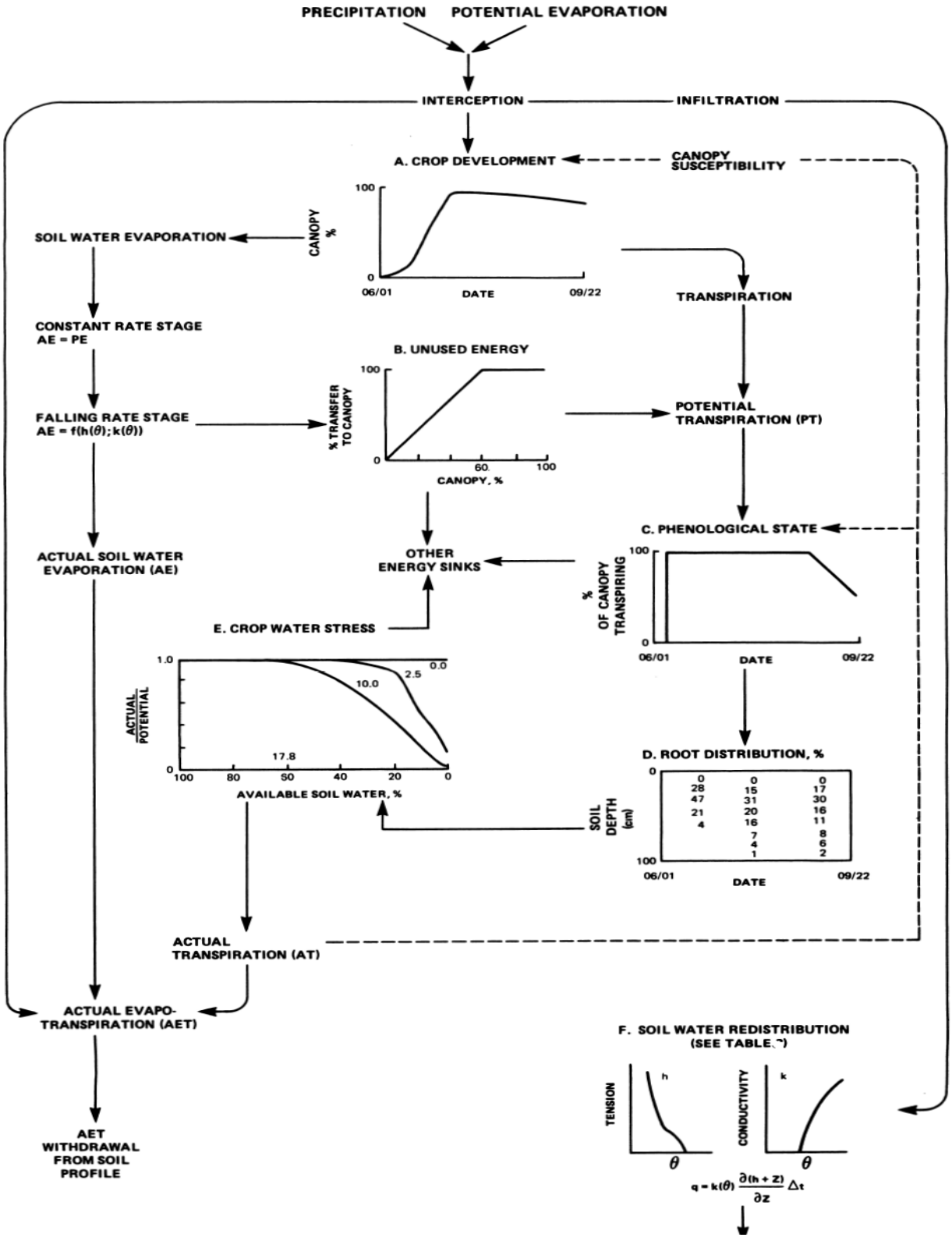

Figure 4.4: Flow chart for the SPAW model (Hayhoe and De Jong)

Initial soil moisture conditions were specified with the first 5 successive observed soil moisture data. These values are used for calibration of SPAW by adjusting the uncertain input parameters.

3.5. Spatial soil moisture distribution using Gesostatistical analysis (Co-kriging)

Correlation analysis was done for some topographic indices like; curvature, slope and relative elevation with instrumental measured profile soil water storage (mm/m) and water content (v/v). After significant correlation was found with one of these indices, slope, spatial soil moisture distribution was mapped. The slope classes of the field were set to 5 with the highest slope range of (33-62) in degree, which are steep depressions and a minimum slope range of 0.4 to 7 degree. The same procedure was followed for the SPAW model predicted outputs of profile soil moisture (mm/m) and volumetric water content (v/v) for the specified slope values.

To map both the instrumental output and SPAW model predicted soil moisture distribution in the field, Geostatistical analyst tool in ArcGIS 10.2, ESRI was used. An estimate of cross validation to the sampling points for their residual error, sum of squared error and root mean squared error was done following the output of this geostatistical too.

Since soil moisture reading was taken once a week and this does not much with the rainfall that rains in the afternoon, error is expected as far as analysis was done for all days.

4. Result and Discussion

4.1. Results of measured and estimated soil moisture controlling factors

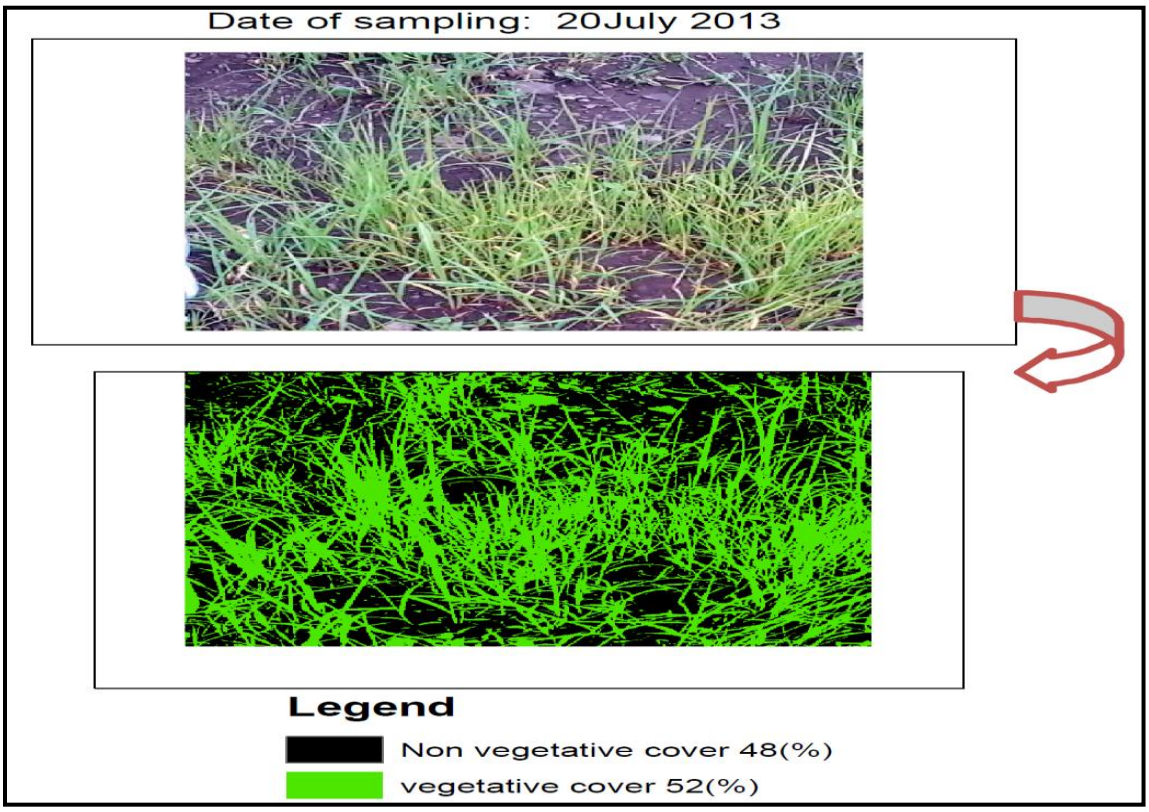

Figure 4.5. Canopy cover estimated using Iso Cluster Unsupervised Image Classification in ArcGis10.2, ESRI 2013.

Table 3.4. Measured canopy cover (%) and leaf greenness (%) of crops on measurement dates

Crop Name	Planting date (dd.mm.yy)	30-July-2013		20-Auguest-2013		03-September-2013	
		Greenness (%)	Canopy cover(%)	Greenness (%)	Canopy cover(%)	Greenness (%)	Canopy cover(%)
Teff	22.07.13	100	15	100	68	100	80
Sorghum	12.06.13	100	50	100	75	100	75
Faba bean	27.06.13	100	75	100	85		90
Chickpea	27.08.13	100	15	0	0	80	35
FB& Sorg	12.06.13	80	67	80	85	100	85

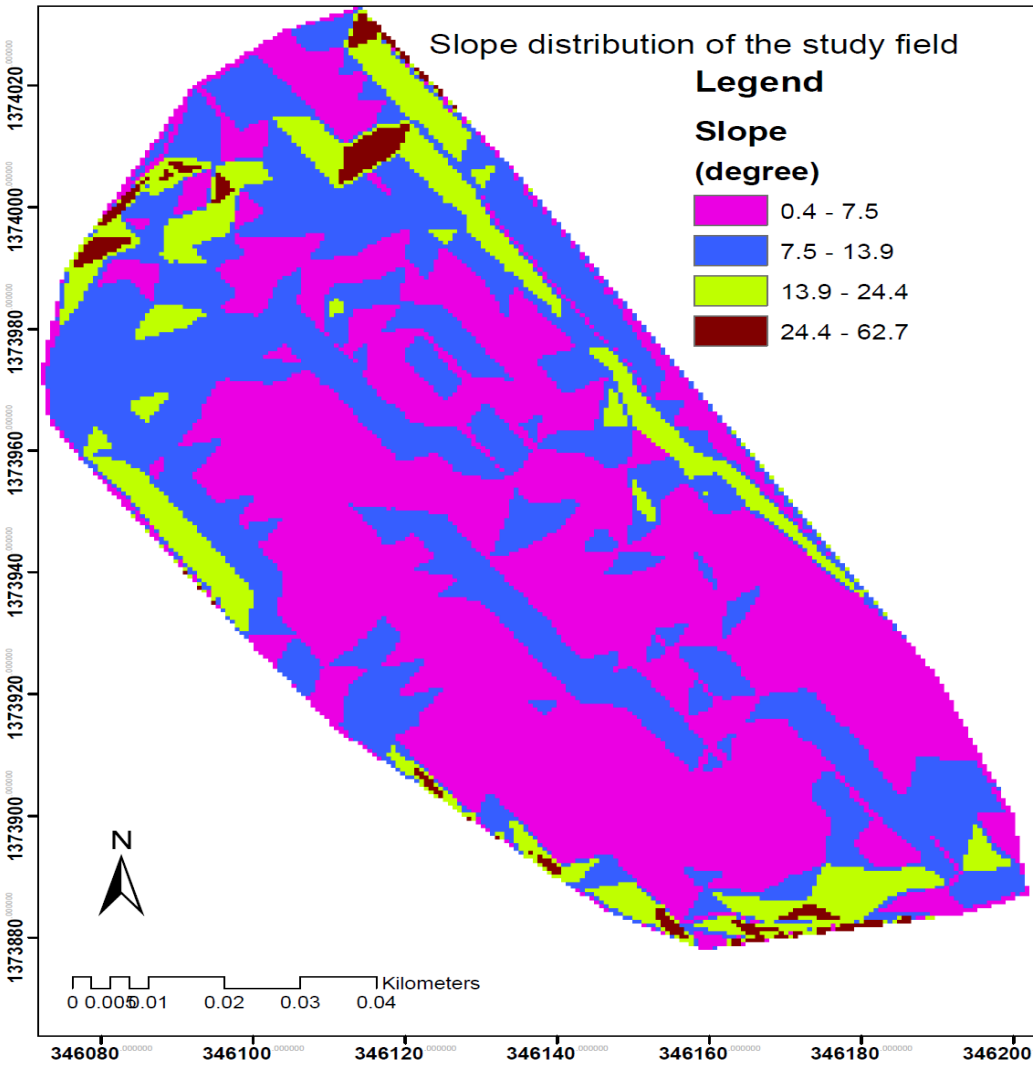

Figure 4.6: Slope distribution of the study agricultural field

In figure 4.5, vegetative cover was resulted from the analysis of crop cover using iso-clustering technique which is unsupervised classification.

Slope in degree in figure 4.6 was characterized in the field and the range of minimum values was from 0.4degree to 7degree and maximum values from 34degree to 62degree after classification has been made in to four classes. But, most of the slope coverage was in the lower range. The objective of this detail topographic survey was to find detailed slope which is important indicator of soil moisture distribution in the soil surface. Topographic aspect has not mining in this field; because surface of the field faces to the same direction.

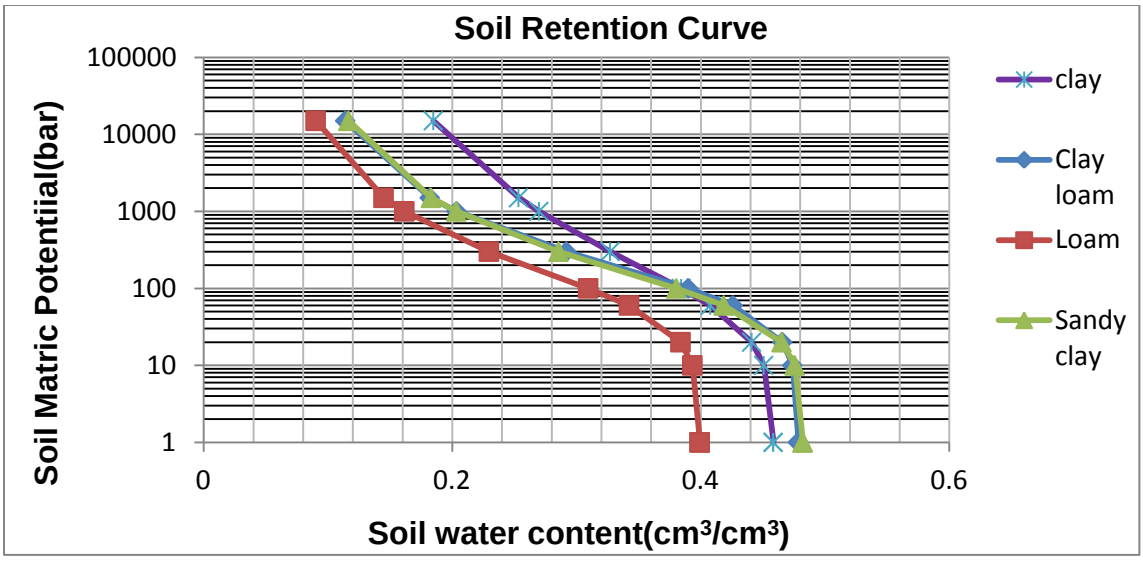

Figure 4.7: Soil water retention characteristics curve of selected soil texture classes in the field, according to Van Genutchten parameters

Infiltration rate of three crops was resulted by graphing the infiltration rate (mm/h) to the time (minutes) along which measurement was done. It was done in locations specified as; location1, location2 and location3.

Though the soil textural class in the profile depth, 0 -30cm, is uniform for all the locations where the infiltration rate was measured, there is still difference in textural fractions. Location1, which is covered with sorghum and whose sand to clay ratio is 1.4, has an infiltration rate of 50mm/h and attained its steady state at around 1 hour. This may be strange as compared with results from Lili et al. (2008) who concluded that it ranges from 2 to 7 hours. For location2, covered with mixed crops of faba bean and sorghum and whose sand to clay ratio is 1.8, has an infiltration rate of 85.1mm/h. it attained its steady infiltration state at nearly 2hours. Location 3 covered with tef (*eragrostis Tef*) and with sand to clay ratio of 1.5, had an infiltration rate of 34.6mm/h. This has attained at its steady infiltration rate to about 110minutes.

From this result, It can be inferred as soil infiltration rate does not only depend on soil texture, but also on other soil characteristics like; soil structure, compaction level, bulk density, organic carbon content, and soil chemical properties etc.

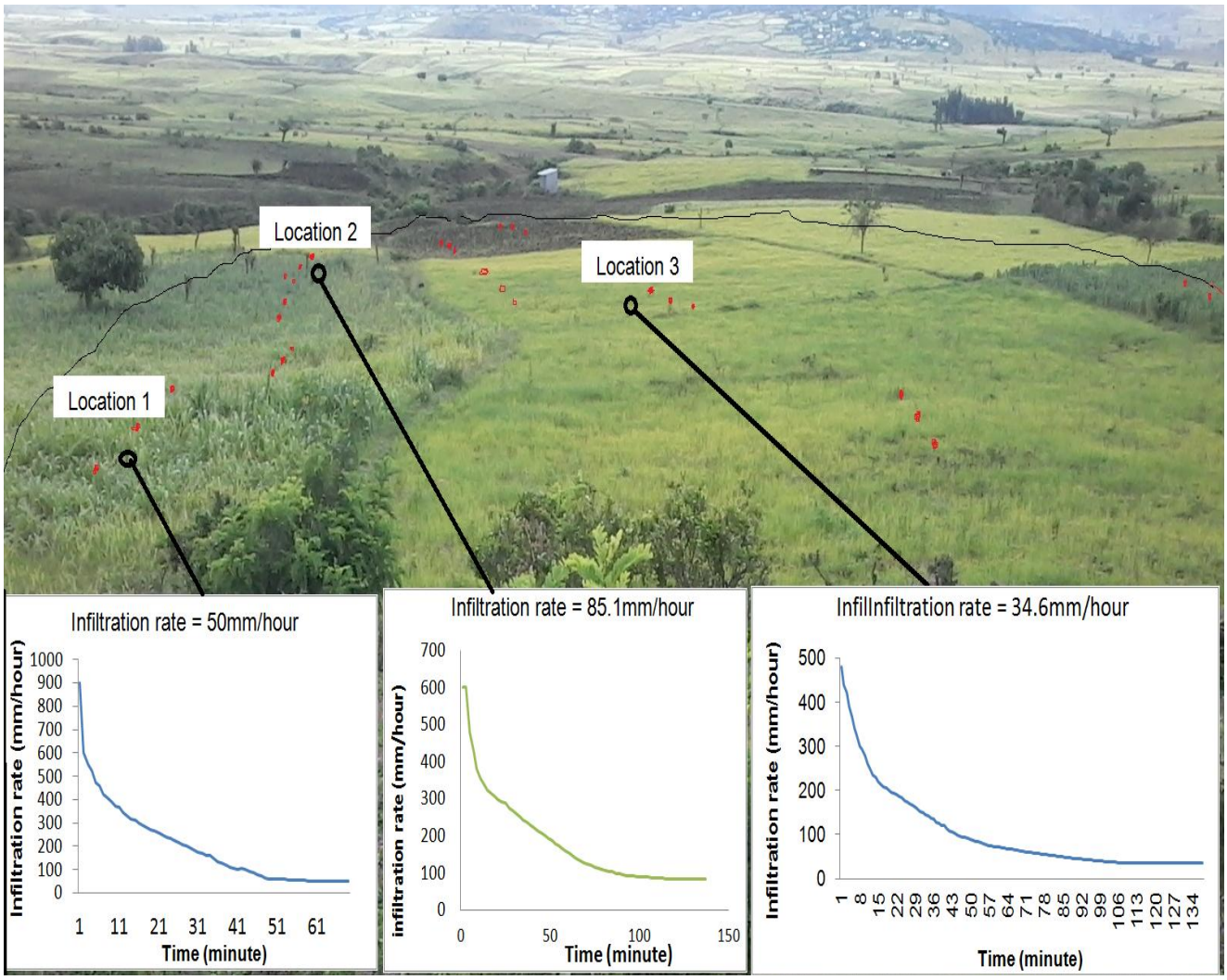

Figure 4.8: Infiltration rate (mm/hour) of soils as measured on the date of 24 September, 2013.

4.2. Measured SM data

4.2.1. Soil moisture content

In order to assess the consistency of soil moisture values in all the 6 soil moisture points down 1meter soil profile of 11 sampling days distributed in 30 points throughout the field collected with the instrument, analysis was done with the help of excel sheet mostly displayed as graphs.

The scatter plots of soil moisture in the next figures are partitioned in to two parts whose values are going to be applied for calibration and validation of the SPAW model.

Besides the above crop information, slope distribution and soil informations, estimated climatic information are already in the Appendix part of this study.

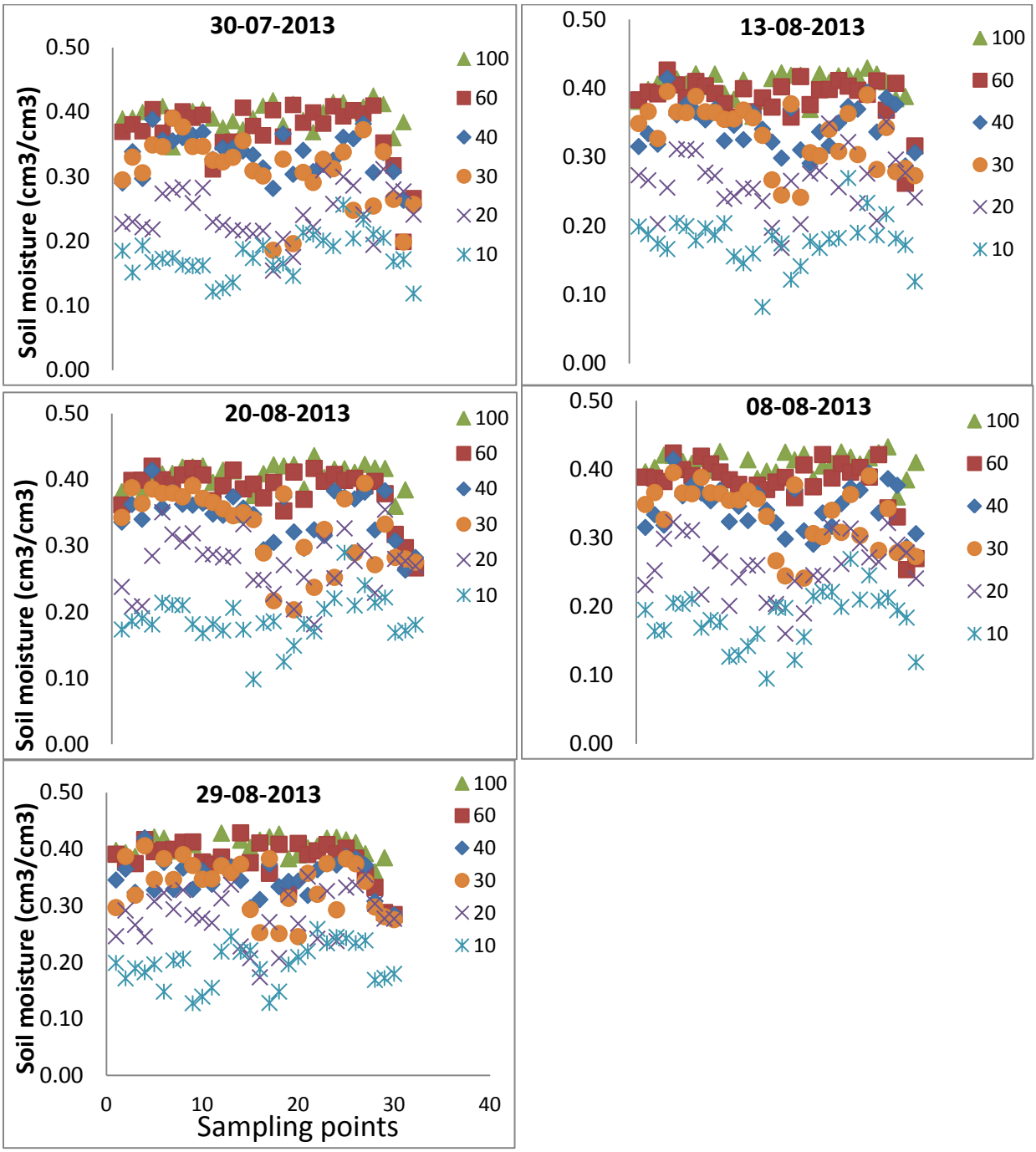

Figure 4.9: Time series soil moisture distribution in 1meter soil profile (will be applied for SPAW calibration or initial conditions).

As shown in figure 4.9 and figure 5, more scattered observation points are displayed in the top 10 cm soil profile. Savva (2013), showed in his/her result that soil microclimate characteristics, evapotranspiration as its commulative effect, had a stronger influence at the upper 10cm depth than at the 20cm depth, and pointed out that frequent measurement have to be done in the top soil surface than in the lower for soil moisture temporal dynamic analysis.

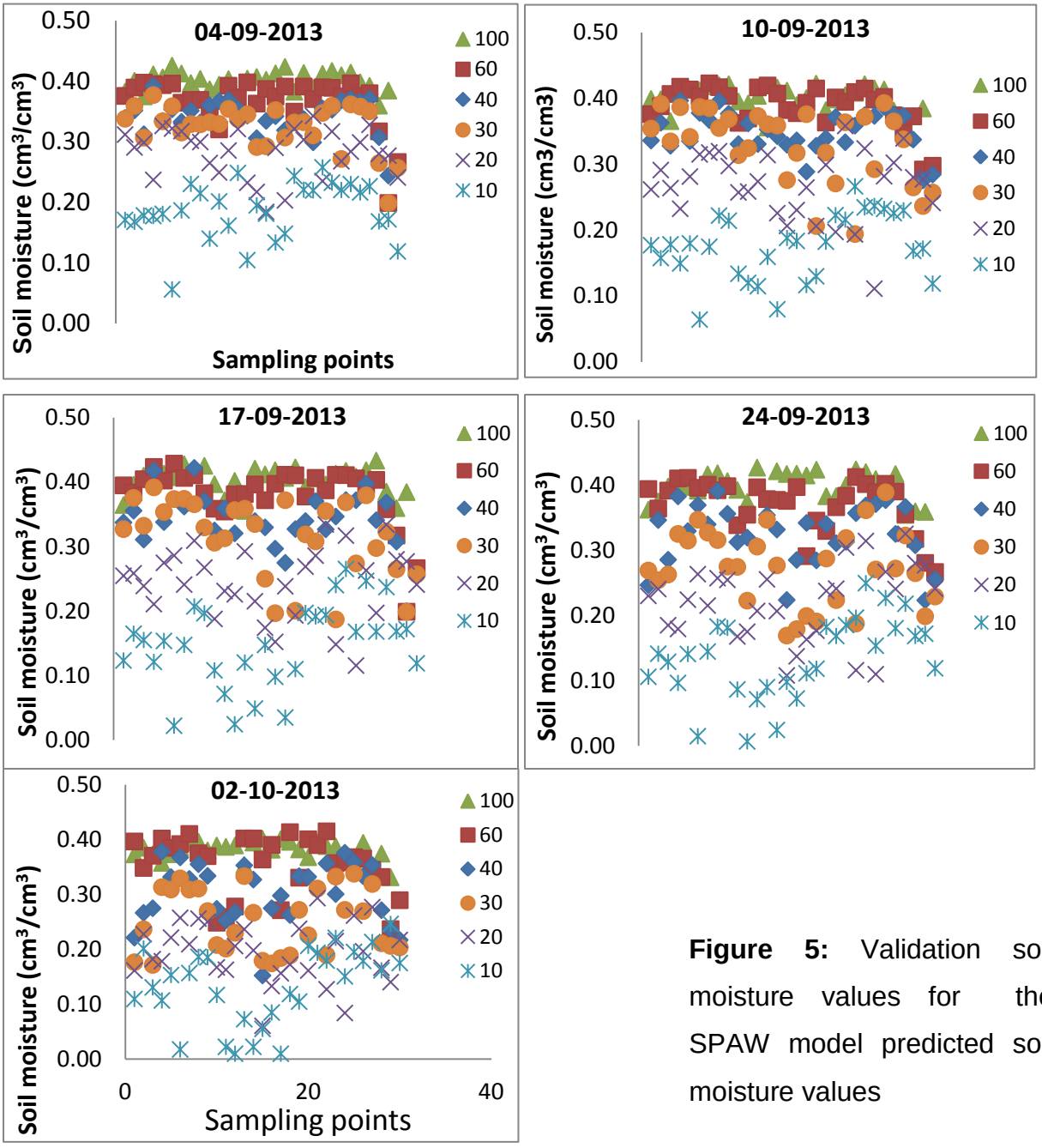

Figure 5: Validation soil moisture values for the SPAW model predicted soil moisture values

Though some researchers, Chow (2009), as an example has found that field soil moisture point measuring sensor that works with dielectric method found to be better with comparisons to other types of field sensors, it was found in our case to underestimate soil moisture values at the top 10 to 20cm while it over showed the bottom near 1meter values.

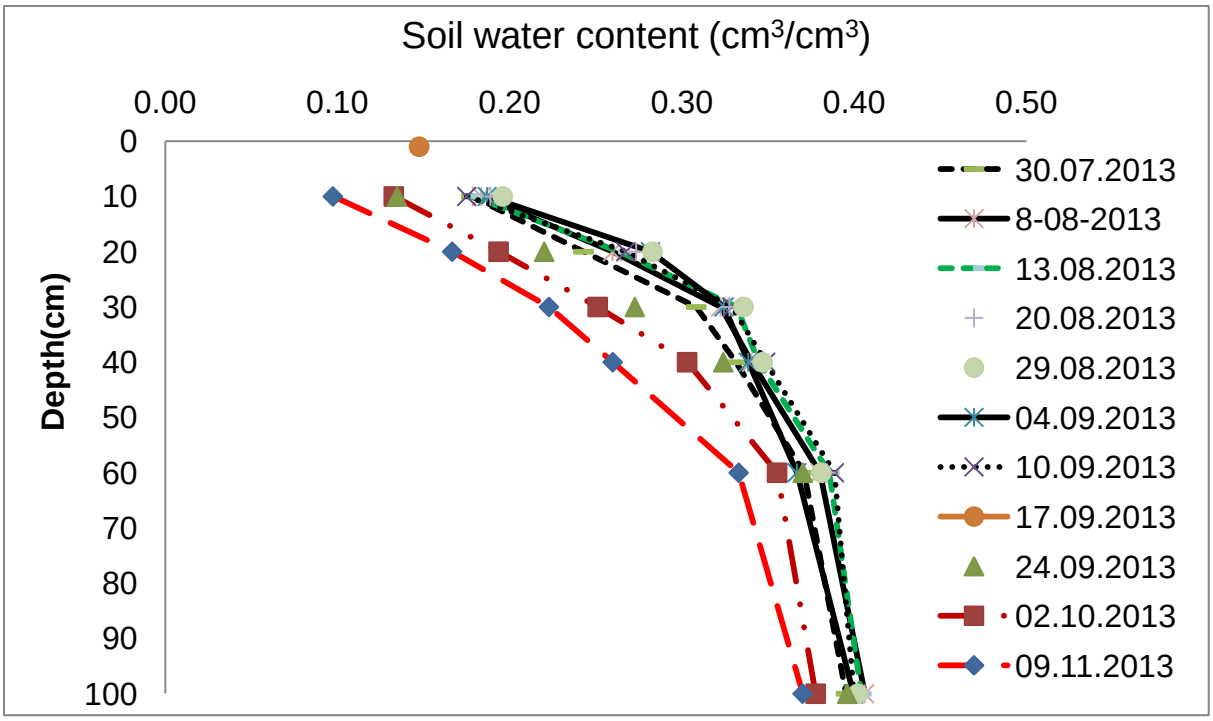

Figure 5.1: Soil moisture variation with soil depth along time

As shown in figure 5.1, soil moisture is higher in the lower soil depth while it is low in the top layer. Comparatively, it decreases in latter days i.e. day 9th of November and 9th of September because of the decrease in rainfall on or before these days. The last rain for the study time range was occurred on 2nd of October, in the same date but some hours after soil moisture sampling was done. Figure 5.9 and figure 6.3 explained more about sum of antecedent rainfall and potential evapo-transpiration (ETP) impact on the 1 meter profile soil moisture variation.

It is also observed that difference in soil moisture of the successive sampling dates is higher in the dry period. In the soil profile range of 60cm to 100cm, soil moisture variation is low. This is, may be, due to the fact that once the soil wetted, it is not easy

to deplete the water in the soil through evaporation as it is comparatively far away from the soil-atmosphere boundary. Localized surface runoff can affect the soil moisture profile at smaller scale especially in the top soil surface; hence this condition can be resulted.

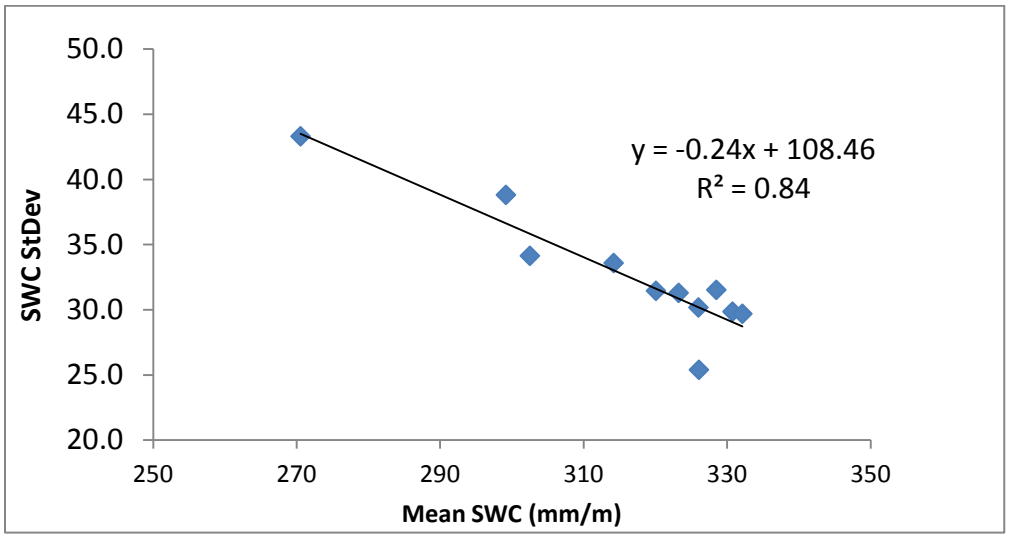

Figure 5.2: Regression between mean profile soil water and soil water standard deviation

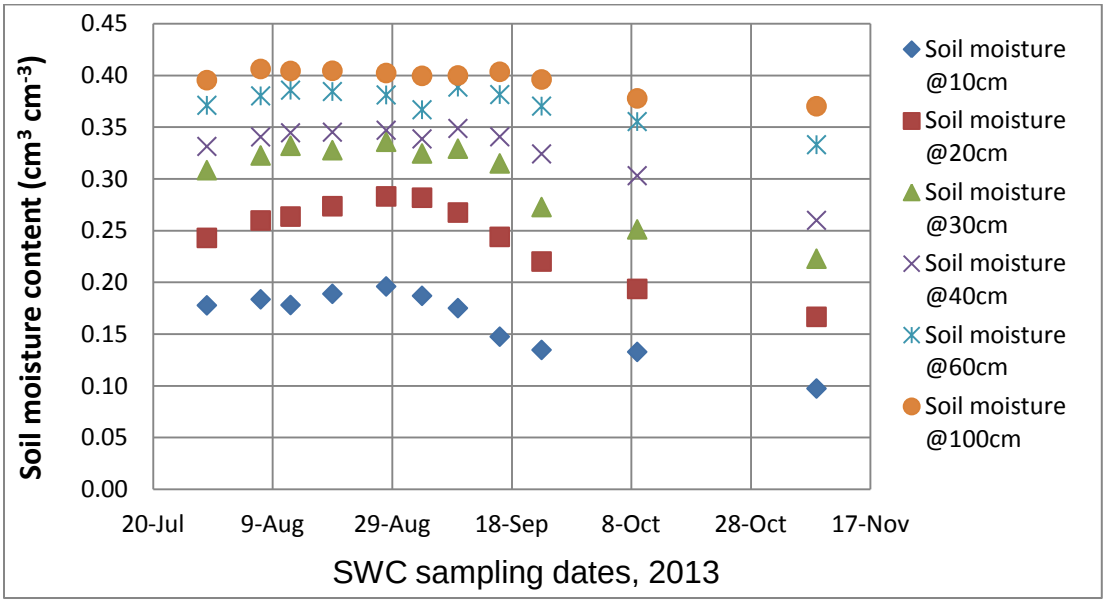

Figure 5.3: Soil water temporal distribution in soil profile and a long time

Figure 5.3, shows soil moisture range of mean values between 271 mm/m to 330 mm/m. soil moisture deviation is high in the lower mean values and low in the higher

means of values. Maximum deviation is an absolute value of 43 mm/m and a minimum deviation of 25 mm/m. It is possible to conclude that most values are on the side of the higher soil moisture record values.

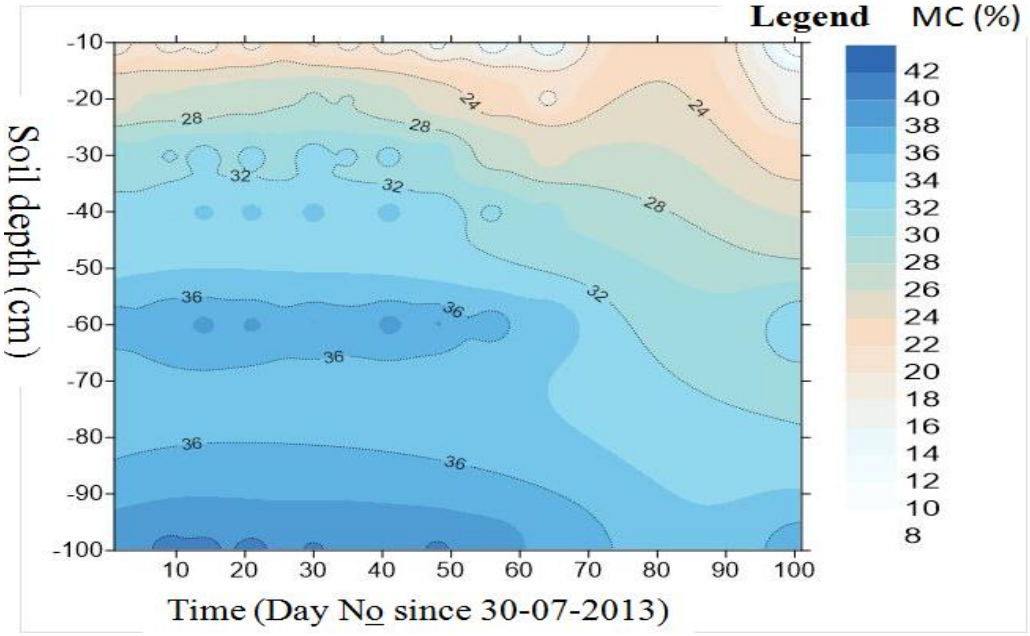

Figure 5.4: Overall field mean soil moisture content distributed with in soil profile depth along time

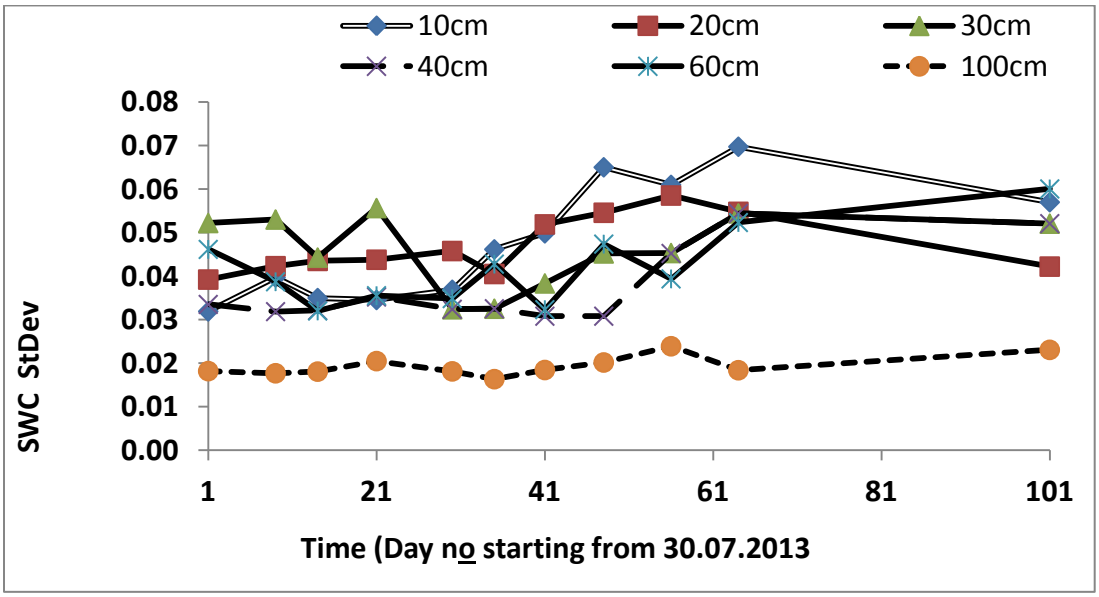

Figure 5.5: Standard deviation of soil water content on soil profile depth as goes to dry period.

Figure 5.5, shows high resolution of soil moisture deviation in each soil sampling depth with its mean values. It does not show clearly but a trend of increasing variability as soil gets dry but again decreased when drying process continues in all sampling depths other than 100cm. It may be, as soil gets more dry, moisture status of the soil comes into similarity. The same figure also shows standard deviation is higher during drying than in the wet period, reaches a maximum value at specific day, and then decreases during further drying.

As shown in the above figure 5.4, there is a variation in soil moisture distribution with time. The contours in this figure show distribution of soil moisture along time in all depths. Interpolation of soil moisture (v/v) between profile depths of 60cm and 100cm undermines the values.

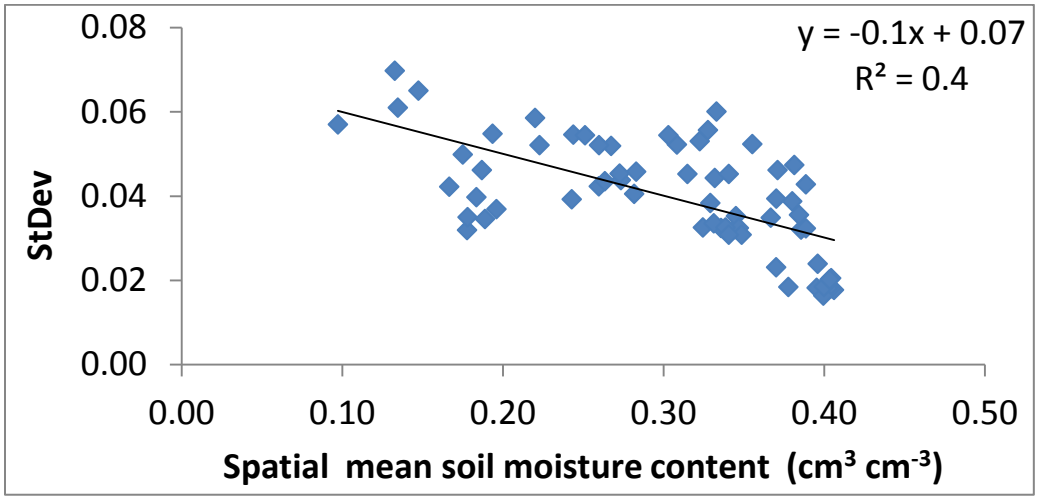

Figure 5.6: Standard deviation and spatial mean soil moisture distribution

Figure 5.6, is about the standard deviation of soil moisture (cm^3 cm^{-3}), in each soil profile moisture recording of each sampling points. With total observations of 66, high deviation is shown clearly in the low soil moisture level (cm^3 cm^{-3}) values. But, the strength of the fitting equation is strong enough to conclude that soil moisture deviation is high in the lower soil moisture records. As shown from this figure, the coefficient of determination is low which is below 0.5. The outliers shown on both sides, resulted from uncertainty of the measuring equipment, may be the reason for the stated fitting equation with low accuracy.

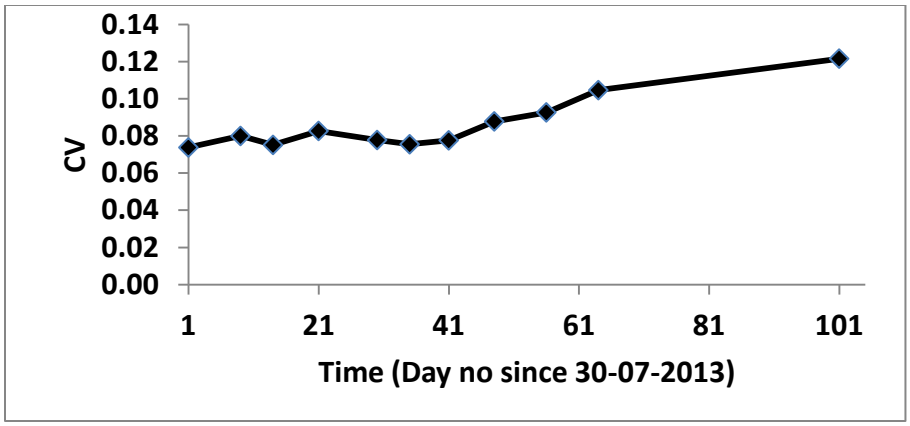

Figure 5.7: Coefficient of Variation (CV) of soil moisture (SM) along time

The result in figure 5.7 shows soil moisture coefficient of variation increased as the soil gets dry. The same work of *Yang et al.,* (*2001)*; showed the same result indicating soil moisture variability was higher on the dry period than in the wet period.

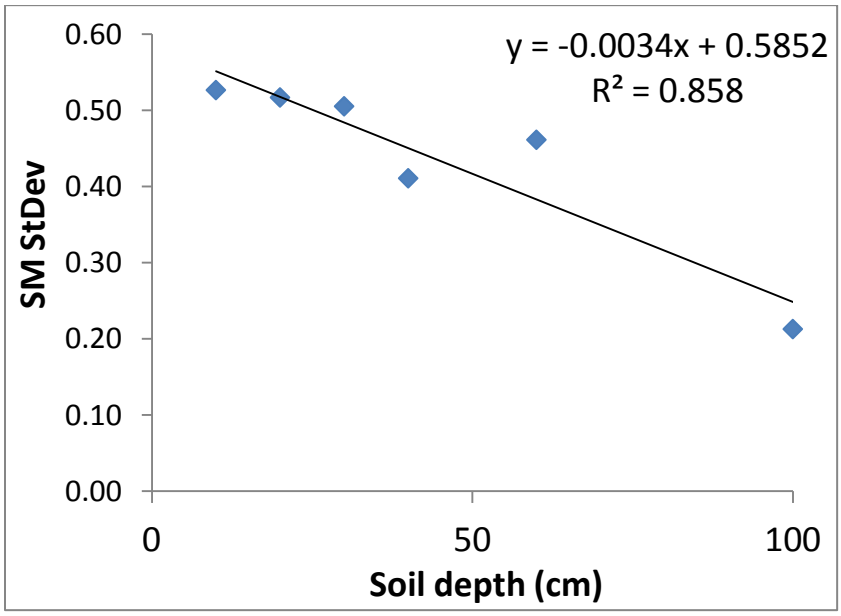

Figure 5.8: Standard deviation (StDev) of soil moisture (SM) with soil depth

Figure 5.8 shows that soil moisture values are comparatively dispersed in the top soil than as approach near to 1meter depth. This may be due to the fact that soil moisture dynamics is higher in the top soil, the soil water exchanging medium between atmosphere and the soil, that simply loss water to the atmosphere and receive

precipitation, rainfall in this case. Besides, the variability of soil texture where coarse soil texture releases water easily than fine textures in the field is the possible reason.

But, as soil profile gets deeper or gets far away from the soil-atmosphere boundary, soil moisture showed less variability, because it is not easy to meet the atmospheric water demand (ETP) from this layer. This result opposes to a similar study done by Yang et al., (2001). However, the possibility that water moves vertically or laterally, when soil water content is near or below its field capacity, is low. As a result, there is an indication of time invariability soil moisture in the lower part of the sampled soil profile.

Figure 5.9, shows how much the spatially averaged soil moisture content varies in the drying process (after rainfall recession). As was described on this figure, soil moisture variability was low where antecdent rainfall was greater or propertional to the atmospheric water demand, named as potential evapotranspiration (ETP).

4.2.2. **Profile soil water storage**

Measured volumetric water content and soil depth were used to calculate the total water stored in the 1 meter profile. This stored water can be defined as water depth.
The descriptive statistics such as mean, standard deviation, coefficient of variation and others of the point soil moisture samples used in this study is given in Table 3.5. From the perusal of this table, it is evident that there is a trend with low mean soil moisture (mm/m) values observed during the drying periods from September to early of December of the same study year.

Table 3.5: Summary of statistical index of Soil moisture in space of 1hectare cultivable field along time (2013)

Date Statistics	**30/07**	**08/08**	**13/08**	**20/08**	**29/08**	**04/09**	**10/09**	**17/09**	**24/09**	**02/10**	**09/11**
Mean (mm/m)	322	331	333	334	337	329	333	324	308	292	266
Median (mm/m)	327	335	336	334	343	333	336	329	309	298	275
CV (%)	7	8	8	8	8	8	8	9	9	10	12
Skewness (-)	-1.32	-1.52	-1.71	-1.41	-1.84	-2.22	-1.70	-0.91	-0.26	-0.63	-0.95
StDev (mm/m)	24	26	25	28	26	25	26	28	29	31	32
Kurtosis (-)	2.33	3.15	5.06	3.22	5.28	5.75	5.14	1.63	-0.03	-0.95	-0.21
inter.quar (mm/m)	311	318	321	319	325	324	323	309	289	277	247
Lower bound (mm/m)	272	273	280	263	285	296	289	259	232	219	176
Upper bound (mm/m)	376	392	390	413	392	371	380	392	385	373	366
Minimum (mm/m)	250	245	242	241	241	240	240	240	242	232	190
Maximum (mm/m)	358	365	370	372	370	357	370	371	365	332	299

In table 3.5, it is evident that there is a seasonal trend of soil moisture decrease in the late sampling dates i.e. 17th of September to 9th of November. All spatially averaged profile soil water storage values are negatively skewed, indicating there are fewer records whose soil water storage values are greater than their respective mean in all the sampling points. These values are also more skewed as time gets approach to dry period. The range of soil water storage values, between maximum and minimum), do not show any trend along time.

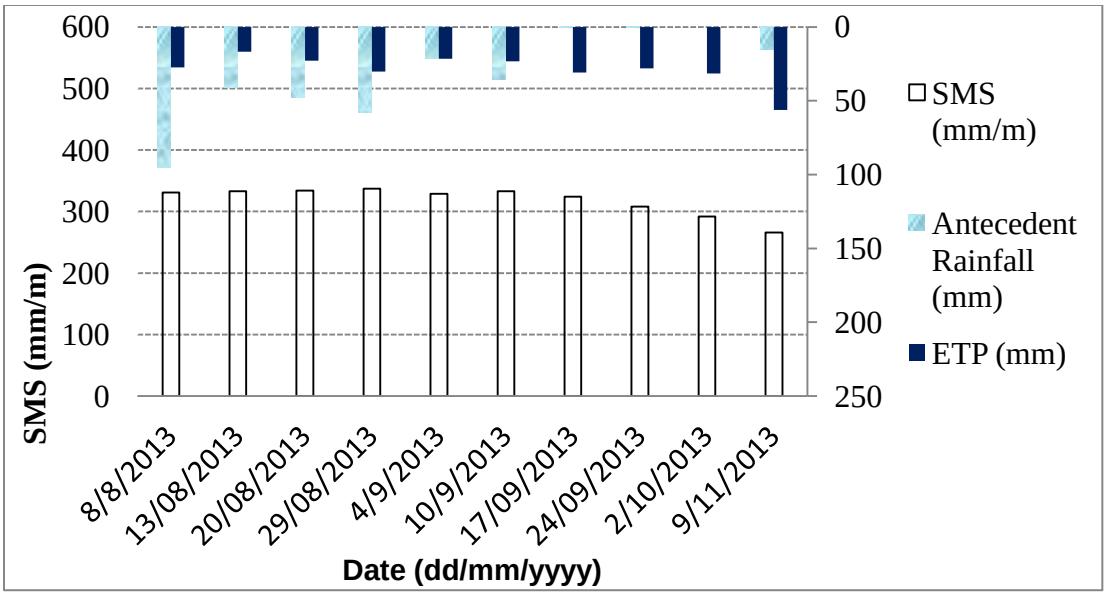

Figure 5.9: SMS (mm/m) on sampling dates with their respective antecedent soil rainfall (mm/m) and commulative ETP (mm).

Antecedent rainfall in this case is sum of rainfall occurred in the last days that varies between 5 and 22 days.

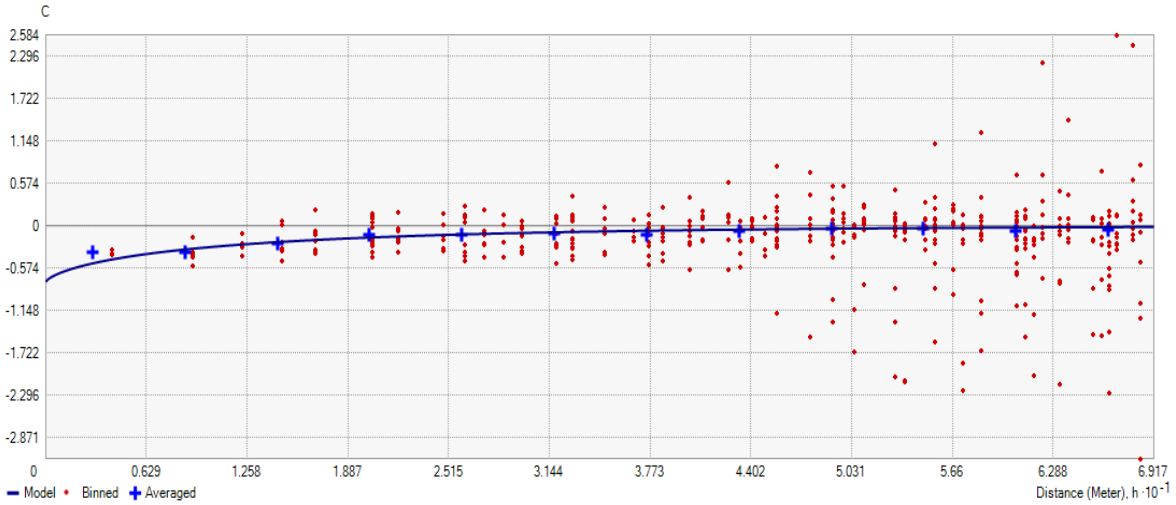

Figure 6: Covariance of soil moisture and slope steepness(degree).

Stating figure 6, in order to map the soil moisture distribution in the field considering slope distribution as a covariate, the covariance of soil moisture with slope was tested and the result is shown in *Appendix iii*.

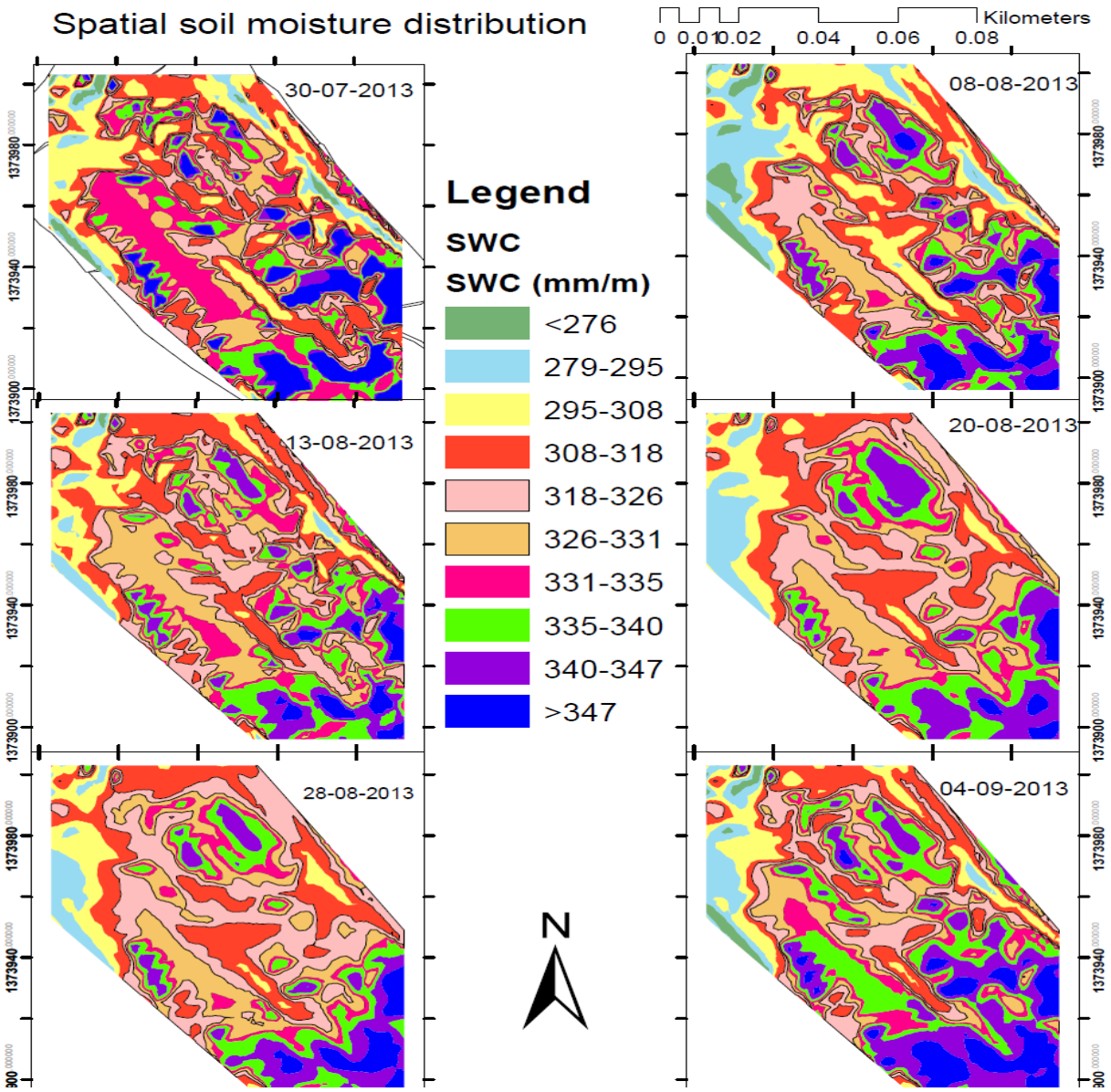

Figure 6.1: Spatial soil moisture distribution along sampling period

The map shown in figure 6.1, was developed with Geostatistical Analyst available in ArcGIS 10.2 package. With relative higher profile soil moisture values in the darker blue color, their distribution is denser in the bottom part of the sampling field, where there is higher relative clay content (%) and flat topography (< 7 degree).

The coefficients of correlation (*r*) were used to determine the relationship between soil moisture content and quantitative some controlling variables.

Table 3.6: Correlation coefficients of some soil moisture controlling factors to soil water storage (mm/m) and soil water content (v/v), (soil texture and SWC (%) are only for the top 30cm soil profile.

	SWS (mm/m)	*SWC (v/v)*	*Cover (%)*	*Sand (%)*	*Clay (%)*	*Silt (%)*	*Slope (degree)*
SWS (mm/m)	1						
SWC (v/v)	0.68	1					
Cover (%)	-0.44	-0.07	1				
Sand (%)	-0.31	-0.25	0.11	1			
Clay (%)	0.50	0.60	-0.17	-0.35	1		
Silt (%)	0.10	-0.02	-0.03	-0.90	-0.10	1	
Slope (degree)	-0.52	-0.25	0.23	-0.03	0.06	0.00	1

It can be argued from table 3.6, that both slope and soil texture shows some correlation with SWS (mm/m) and SWC (v/v). Slope (%) correlates with clay content (%) with a factor of -0.52, which indicates as slope steepness increases, profile water content decreases. But, SWS was negatively affected than SMC with the increase of slope steepness. Similar study by Lang et al., (2012), showed a clear impact of topography on soil moisture spatial distribution.

Clay content (%) positively correlates with SWS (mm/m). This is resulted from the fact that clay soils have higher water holding capacity than silt and sandy soils. But, sand (%) and silt (%) negatively correlated with both SWC (%) in the top 30cm soil profile and SWS (mm/m).

It was investigated from the negative correlation between the moisture indicator i.e. SWC (v/v) and SWS (mm/m), that higher values of these indicators were in the bottom of the research field where soil cover was less or near to zero resulting from late chickpea planting. Therefore, this correlation coefficient is not convincing because of this justification behind. More investigation after chickpea plantation and full canopy cover was not possible due to time boundary beyond the stay of the researcher on the country where research was done.

The small sample size spatially distributed soil moisture observations throughout the study field may cause the less accuracy of the prediction.

Yaclin E., 2005 described that as the accuracy of an estimate from co-kriging depends on the size of the samples and found decreased variance as the sample size increase using covariance.

4.3. Temporal predicted (SPAW model output) soil moisture

Allowing the model (SPAW) to run for 10 points as averaged SWS (mm/m) of the clustered points whose their soil texture is similar, the following regression equations relating observed and model predicted SWS output are displayed. Statistically, the coefficient of determination is above 0.5, which is good, but it can be observed simply that the residual error is too high in all observation points. One of the main reason may be the time invariant of soil moisture change in the soil profile near to one meter. This is clearly shown in figure 5.1 that the soil moisture content at 60 and 100cm soil profile depths are similar throughout the drying period. Variation is always expected due to variation in input variables.

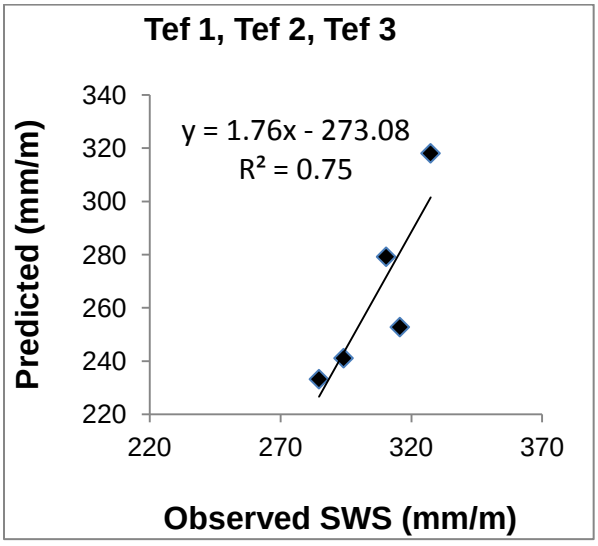

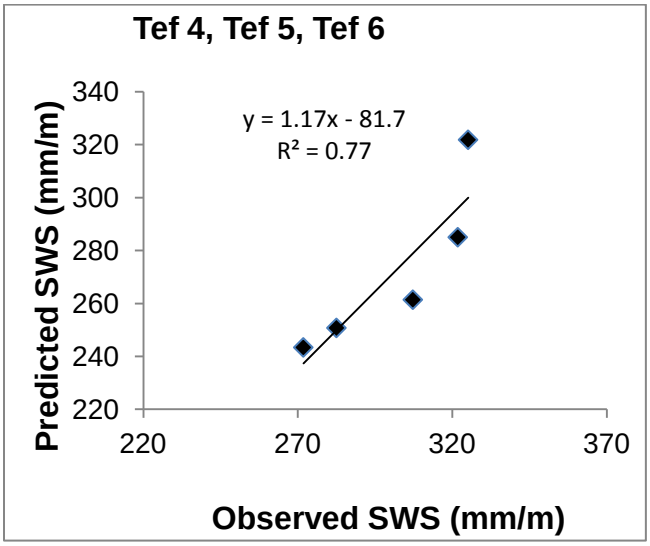

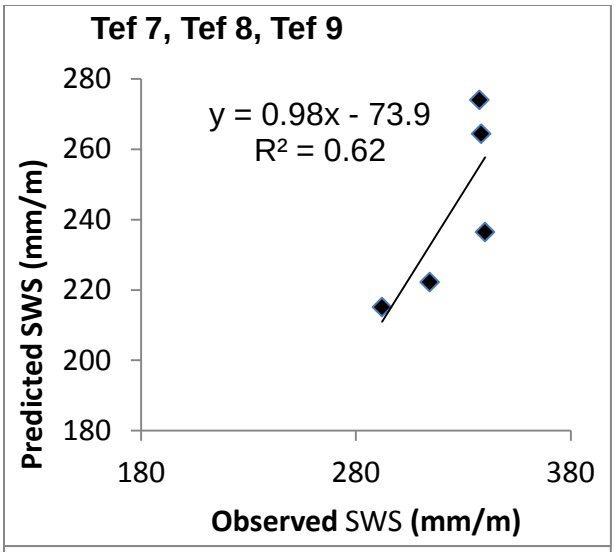
Tef 7, Tef 8, Tef 9
y = 0.98x - 73.9
R² = 0.62
Predicted SWS (mm/m)
Observed SWS (mm/m)
280
260
240
220
200
180
180
280
380

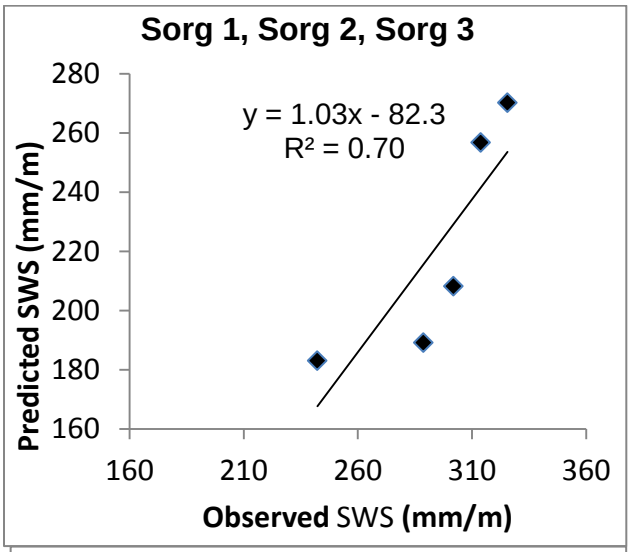
Sorg 1, Sorg 2, Sorg 3
y = 1.03x - 82.3
R² = 0.70
Predicted SWS (mm/m)
Observed SWS (mm/m)
280
260
240
220
200
180
160
160
210
260
310
360

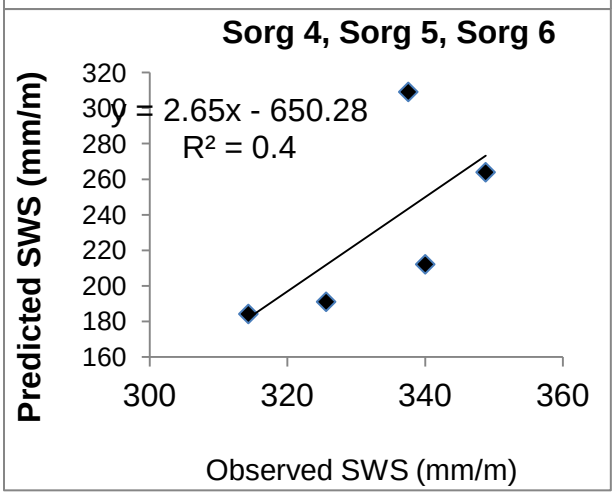
Sorg 4, Sorg 5, Sorg 6
y = 2.65x - 650.28
R² = 0.4
Predicted SWS (mm/m)
Observed SWS (mm/m)
320
300
280
260
240
220
200
180
160
300
320
340
360

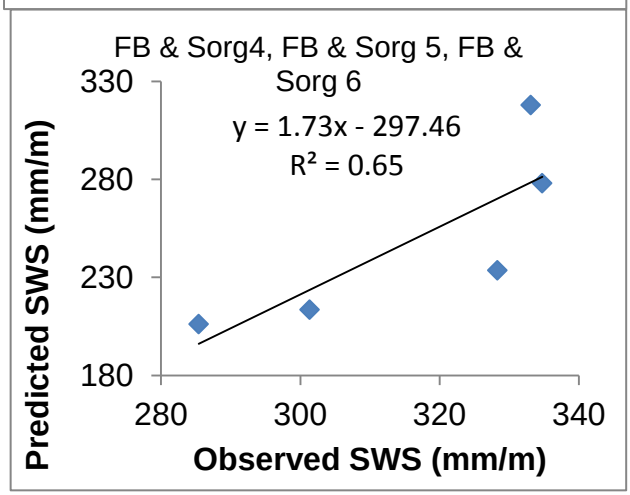
FB & Sorg4, FB & Sorg 5, FB & Sorg 6
y = 1.73x - 297.46
R² = 0.65
Predicted SWS (mm/m)
Observed SWS (mm/m)
330
280
230
180
280
300
320
340

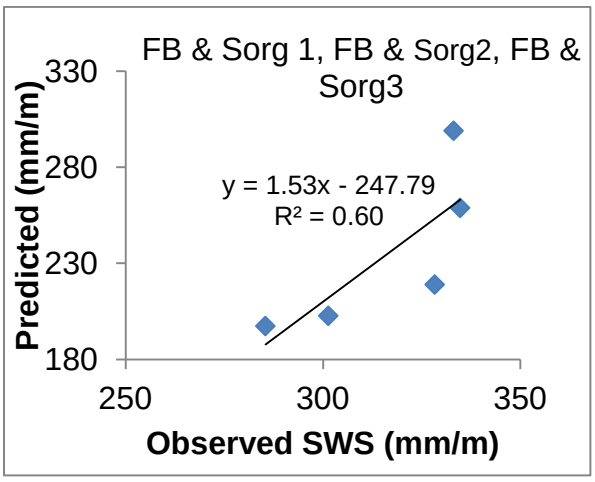
FB & Sorg 1, FB & Sorg2, FB & Sorg3
y = 1.53x - 247.79
R² = 0.60
Predicted (mm/m)
Observed SWS (mm/m)
330
280
230
180
250
300
350

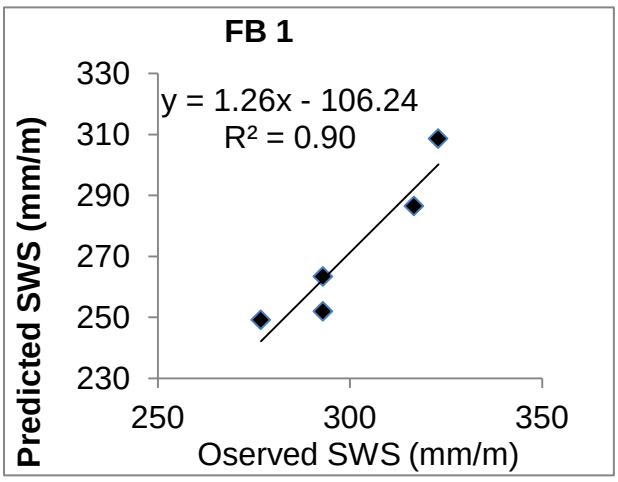
FB 1
y = 1.26x - 106.24
R² = 0.90
Predicted SWS (mm/m)
Oserved SWS (mm/m)
330
310
290
270
250
230
250
300
350

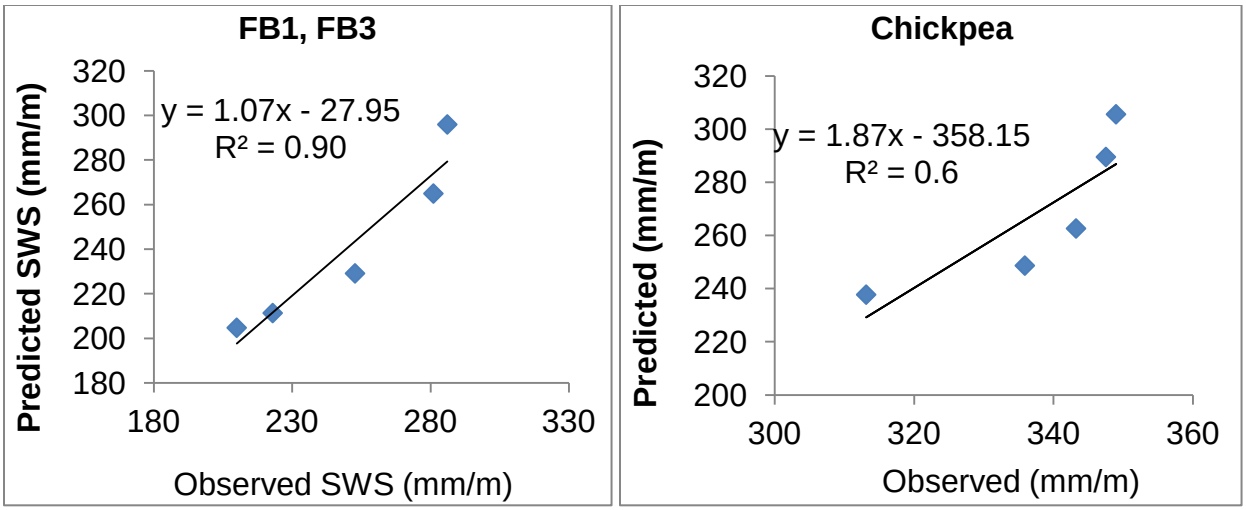

Figure 6.2: Linear regression between observed and SPAW model predicted SWS (mm/m) on each clusters.

The above figure 6.2 indicates regression lines with different slopes and intercepts. Some soil moisture measurement points, clusters in this case, did not show strong relations though both observed and predicted are still go in the same direction. Regression equation in cluster of (Sorg 4, Sorg 5, Sorg 6) shows an impact of leverage point.

Understanding the Variation between each sampling clusters and variations between the observed and model predicted soil moisture storage is important.

Besides to the error that comes after the use of data away of the study field, errors from measurement could be a source of the deviation i.e. high residual error. The calibration soil moisture measuring equipment is not an appreciable to indicate there is a perfect relationship between the gravimetric and instrumental output soil moisture values. Therefore, it seems justifiable to describe as the instrumental shares part of the errors. Obvious causes of the instrumental output error was also understood from the field observation that there were frequent soil cracking in the top 10cm soil profile especially in soils where clay texture composition is high. This reason can minimize the doubt that the model over/under predict the soil moisture values in 1meter soil profile.

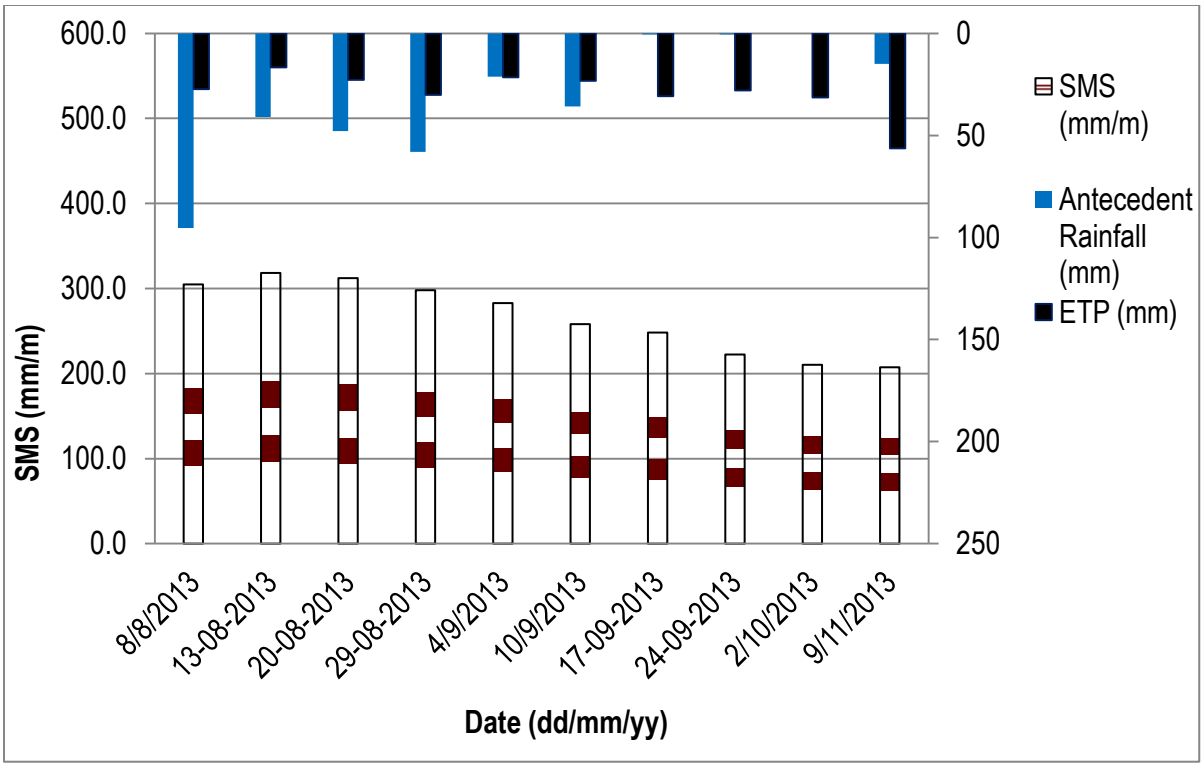

Figure 6.3: Relationship among profile soil moisture, antecedent soil moisture and potential evapo-transpiration, considering soil moisture at the date of 30-07-2013 as offset value for the antecedent soil rainfall estimation.

As shown in Figure 5.9, and figure 6.3, the antecedent rainfall, input for soil moisture, and cumulative ETP, a reason for soil moisture to be depleted in the soil, are equivalent in the time range between 13th and 29th of August. It was produced from the mean values of SPAW model output of all sampling clusters. Hence variation in profile soil moisture was observed as is displayed in this figure.

The gradual decrease of soil moisture from 10th of September onwards is reasonable because of rainfall reduction/ nonoccurrence of rainfall near or on these soil moisture sampling dates.

Generally, if comparison is done between Figure 6.1 and figure 6.5, under similar boundary conditions, the SPAW predicted SWS (mm/m) values are different from the instrumental measured. These values are underestimated at depths of 60 to 100cm and overestimated at the upper 10cm.

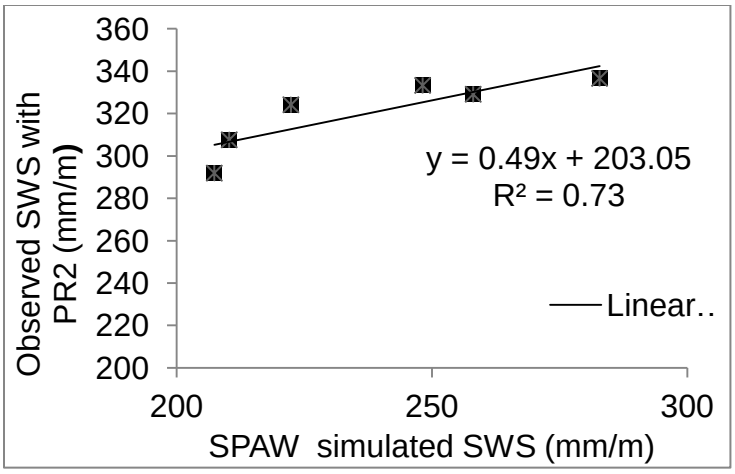

Figure 6.4: SPAW model output of SMS (mm/m) as calibrated with measured spatial average SMS

4.3. Spatial predicted (interpolated) soil moisture

ArcGIS 10.2 was applied for the geo-statistical analysis of soil moisture in the field where temporal prediction of soil moisture has been done using SPAW model. These results are displayed in the following figure where prediction was done for five successive days. It was evident to observe decreasing soil moisture distribution along time in the drying period. This idea can be confirmed by detail investigation of the antecedent rainfall and cumulative ETP displayed in figure 5.9 and figure 6.3.

Based on the co-kriging analysis, the two-dimensional kriged maps of soil moisture predicted from the SPAW model were generated in the field plot (figure 6.5).

The distribution maps revealed moderate positional similarity of the soil moisture in the five sampling times, with complex positional effects in the plot's interior. The spatial distribution of soil moisture was characterized by a significant difference between the dry and rainy seasons in the agricultural field.

In general, the study demonstrated that the variability of surface soil moisture was higher in the dry season with lower mean soil moisture, yet with lower variability during the rainy season with higher mean soil moisture in the bottom part of the field where clay content is relatively higher. The rainfall, evapotranspiratipn, topography and texture had an important impact on the variability and patterns of surface soil moisture. Soil

texture, especially clay content, was found to be the main explanatory variable for the temporal stability of soil moisture.

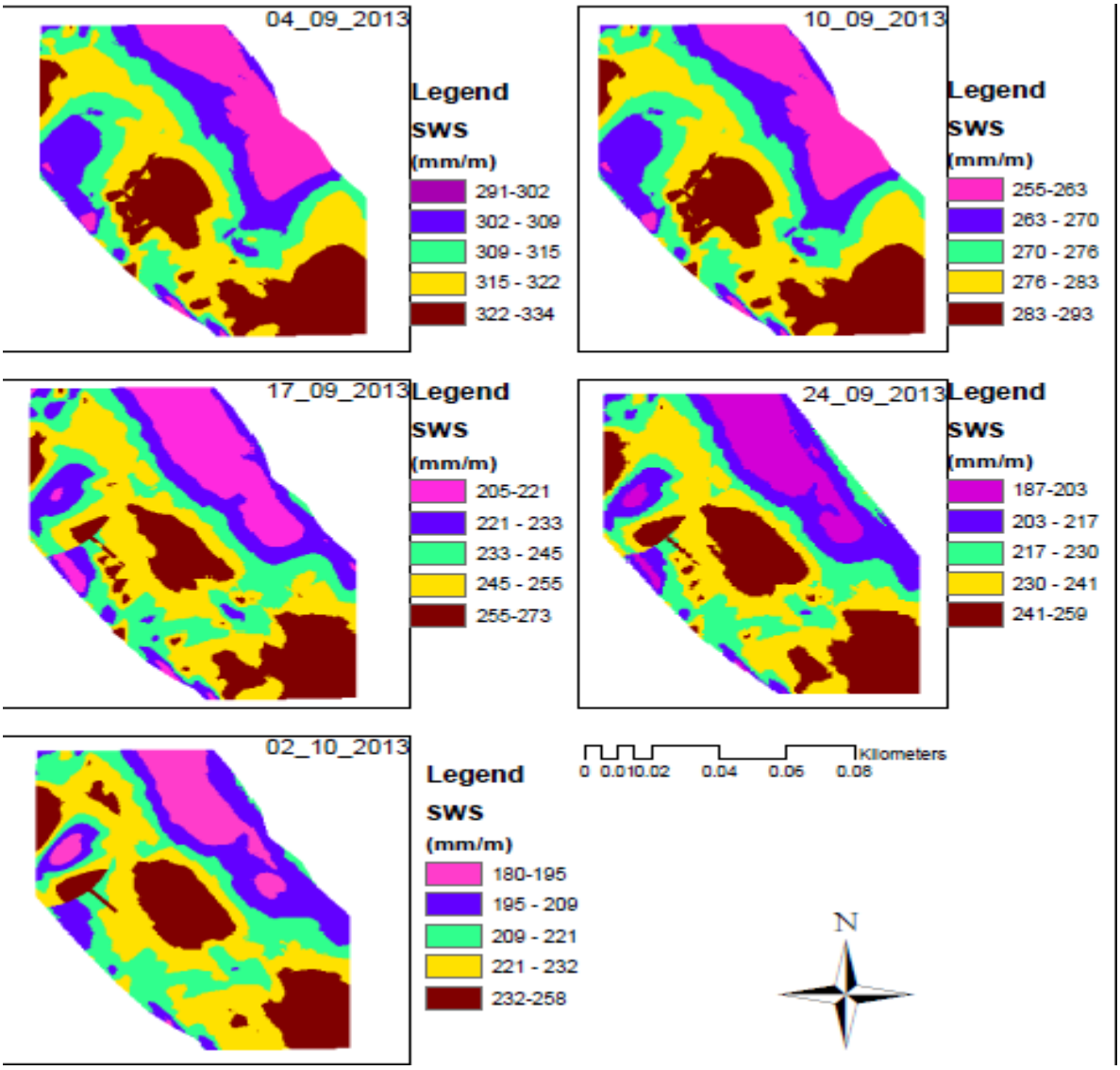

Figure 6.5: Predicted spatial soil moisture distribution on the drying process

The co-kriged values were cross-validated and compared to the SPAW model predicted values in each sampling date on the drying period. Sum of squared error (*SSE*), Mean squared error (*MSE*), Root mean squared error (RMSE), Nash Suitcliff Efficiency (NSE) Coefficient of determination (R^2), have been applied to determine goodness of fit between model prediction and measured values. They are defined as;

$$SSE = \sum_{i=1}^{N} (O_i - P_i)^2 \quad (14)$$

$$MSE = 1/N \left(\sum_{i=1}^{N} (O_i - P_i)^2 \right) \quad (15)$$

$$RMSE = \sqrt{\left(1/N \left(\sum_{i=1}^{N} (O_i - P_i) \right)^2 \right)} \quad (16)$$

$$NSE = \frac{\sum_{i=1}^{N} (O_i - P_i)^2}{\sum_{i=1}^{N} (O_i - \overline{O})^2} \quad (17)$$

$$R^2 = \left\{ \frac{\sum_{i=1}^{N} (O_i - \overline{O})(P_i - \overline{P})}{\left[\sum_{i=1}^{N} (O_i - \overline{O})^2 \right]^{0.5} \left[\sum_{i=1}^{N} (P_i - \overline{P})^2 \right]^{0.5}} \right\}^2 \quad (18)$$

Hence, we applied the above equation for each sampling dates in the drying period for which geostatistical analysis have been done. Table 4.1 shows these evaluating parameters.

Table 3.7: Analysis of spatially distributed soil moisture predicted with geostatistics using measures of goodness of fitting

Date (dd-mm-yyyy)	SSE	MSE	RMSE	NSE	R^2
04-Sep-2013	957	32	5.6	0.72	0.76
10-Sep-2013	1180	39	6	0.74	0.75
17-Sep-2013	2944	98	10	0.77	0.78
24-Sep-2013	4458	149	12	0.73	0.75
02-Oct-2013	5969	199	14	0.60	0.66

Table 3.7 indicates the various measures of goodness for the fitting curves that relate SPAW predicted versus spatially predicted with geostatistical method (co-kriging). From these results, it is clear to understand that soil moisture variability increased as time gets far away wet period. MSE with a value of 32 on 4th of September indicates a mean variation (error) of 32mm/m between the SPAW predicted soil moisture and Co-kriged (spatially predicted soil moisture). But, from 2nd of October onwards, it showed higher variation (error). These results correspond to the instrumental measured soil moisture values which showed higher variation on the drying period than in the wet period.

The coefficient of determination (R^2) for the model, that determines strength of relationship between the SPAW simulated and co-kriged values, in all dates where prediction was done shows above 66 to 78, which is fair. But, better than those values would be expected since it is clear for everyone that soil moisture decrease on moments where rainfall stops in rainfed agriculture condition. Indeed, lowest value of (R^2) is in the very driest period i.e. on the 2nd October of 2013 corresponding to the highest sum of squared error (SSE).

Using the combined information of topography and soil characteristics, soil moisture variation can be improved. Zhu and Lin (2009, 2011) pointed out that when available auxiliary variables were sufficient, prediction of soil moisture was significantly improved in an agricultural site in central Pennsylvania, USA.

5. **Conclusion and Summary**

Generally, the study which is based on soil moisture prediction both in terms of time and space was applied on an agricultural field covered with seasonal crops. The general intention of this study is to have basic knowledge on how to answer questions related to soil moisture content of a given agricultural area on specific moment. Specifically, it was aimed to predict soil moisture that tends from wet season to a dry season (on the drying process) both in the spatial and temporal scale of interests.

The study was conducted in 1ha of agricultural field circumscribed within Gumara Maksegnit watershed found in North Gondar zone, Amhara Regional State, Ethiopia. Taken place on the summer season, July to November of 2013, temporal prediction was done on five specific days each apart with minimum of 6days. Statistical analysis was done for the measured soil moisture and profile stored soil water content. The Soil Plant Atmosphere Water (SPAW) was applied to predict soil moisture on the rainfall recession period keeping main input variables like; climatic and meteorological variables, soil characteristics and vegetation cover. Then, Geostatistical analysis, co-kriging method, was applied in order to get distributed soil moisture using these temporally predicted values and additional topographic (slope in degree) information. As a result, the next lists of conclusions are described followed by summarized information.

- The instrumental measured soil moisture data were analysed for variability among eachother with similar SM controlling factors and still high variability was observed both along time and across locations.
- Result indicated that with increasing soil depth, the mean soil moisture content increases significantly, but tends to be constant as it gets approach to 1m deep.
- Coefficient of variation for the spatial averaged SMS was higher on the dry period than in the wet period.
- The influence of topography (slope) on soil moisture was uncovered, larger in the 1m soil profile than in the top 30cm.
- Locations with relatively higher clay content (%) showed higher profile soil moisture.
- There was not obvious relationship between soil moisture and crop cover in the instrumental measured soil moisture. It was also shown that profile soil moisture

status has followed the rainfall pattern along the sampling period and impact of soil texture was evident.

- Instrumental measured soil moisture contents (v/v) at all sampling dates were highly correlated to each other.
- Soil moisture down near to 1m depth remained unchanged at many sampling points.
- Soil moisture at the upper top soil was very dynamic while at 1m was stable across sampling points and through the sampling time.
- Soil moisture variance increased through time during the drying down or cease of the seasonal rainfall.
- The SPAW model results of soil moisture values were shown to be under-predicted at higher moisture levels
- Though the followed procedure, prediction of spatially distributie soil moisture, seems to work well, there is some doubt that depression areas with steep slope might be under predicted, while they are wetter than others whose slope is equal with these stated one.
- Both soil texture and topographic indices (slope) have an impact on soil moisture variation, while vegetation cover was not due to coverage dissimilarity within the clustered soil moisture sampling points.
- Results indicated that with increasing soil depth, the mean soil moisture content increases significantly for five layers and the coefficients of variation (CV) also increases with depth from 10–100cm down.
- Teporal prediction of soil moisture using SPAW model and the spatial distribution using geostatistical method is promising, but this does not consider the influence of lateral flow both in the surface and subsurface. However, the correlation between soil moisture and slope distribution tends to minimize such gaps.
- Uncertainties of model results were relatively higher on dry days than on the wet days.

Though higher uncertainties were observed in the temporal prediction of soil moisture using SPAW model including measurement errors produced with the PR2/6 instrument,

there are still good indicators that enable to predict soil moisture temporally. Spatial soil moisture prediction with geostatistics (co-kriging) showed good results; hence, this technique is recommended for up scaling soil moisture information of specific agricultural areas keeping topographic information, especially slope distribution, is available. In an agricultural field of various soil characteristics and crop coverage, soil spatial moisture prediction with the integration of the SPAW model and Co-kriging method potentially makes it better. Similar future works with detailed and intensive soil moisture observation would improve uncertainties and errors produced from the model.

6. **References**

Alexandratos, N. and J. Bruinsma (2012). World agriculture towards 2030/2050: the 2012 revision. ESA Working paper No. 12-03. Rome, FAO.

Allen, R. G, Pereira LS, Raes D, Smith M (1998). Crop evapotranspiration. Guidelines for computing crop water requirements. FAO irrigation and drainage paper 56. Food and Agriculture Organizationn of the United Nations (FAO), Rome, Italy

Anderson, W. B., B. F. Zaitchik, C. R. Hain, M. C. Anderson, M. T. Yilmaz, J. Mecikalski, and L. Schultz., (2012). Towards an integrated soil moisture drought monitor for East Africa, *Hydrol. Earth Syst. Sci., 16, 2893–2913*

Assefa, M. Melesse, Wossenu Abtew and Tibebe Dessalegne, (2009). Evaporation Estimation of Rift Valley Lakes: Comparison of Models, *sensors, ISSN 1424-8220*.

Ayenew, T., (2003). Evapotranspiration Using Thematic Mapper Spectral Satellite Data in the Ethiopian Rift and Adjacent Highlands. *J. Hydrol., 279, 83-93.*

Basara, J. B., (2001). Soil Moisture Observation for Flash Flood Research and Prediction, NATO Science Series Volume 77, pp 231-241.

Bronstert, A., B. Creutzfeldt , T. Graeff , I. Hajnsek , M. Heistermann, S. Itzerott, T. Jagdhuber , D.Kneis, E. Lu¨ck • D. Reusser , E. Zehe., *(2012)*. Potentials and constraints of different types of soil moisture observations for flood simulations in head water catchments; *Nat Hazards 60:879–914.*

Buol, S.W., Hole, F.D. and R.J. Mc Cracken. (1989). *Soil Genesis and Classification.* 3rd ed. Iowa State University Press, Ames.

Calanca, P., D. Bolius, A. P. Weigel, and M. A. Liniger (2011), Application of long-range weather forecasts to agricultural decision problems in Europe, Journal of Agricultural Science, 149, 15–22.

Casey, H. E., (1972). Sanitary problems in Arid Lands Irrigation, A literature Review and Selected Bibliography; Office of Arid Lands Studies, University of Arizona, USA.

Chow, L., (2009). Field Performance of Nine Soil Water Content Sensors on a Sandy Loam Soil in New Brunswick, Maritime Region, Canada. *Sensors (Basel). 9(11): 9398-9413*

Conacher, A.J. and J.B. Dalrymple. (1977). The nine unit landscape model: an approach to pedogeomorphic research. *Geoderma* 18: 1-154.

Conil, S., Douville, H., Tyteca, S., (2008). Contribution of Realistic Soil Moisture Initial Conditions to Boreal Summer Climate Predictability; Climate Dynamics;Jan2009, Vol. 32 Issue 1, p75

Coulomb, C.V.; Legesse, D.; Gass,e F.; Travi, Y.; Chernet. T., (2001). Lake Evaporation Estimates in Tropical Africa (Lake Ziway of Ethiopia*)*. *J. Hydrol*., *245*, 1-18.

Dean, T.J., J.P. Bell, and Baty J.B., (1987). Soil moisture measurement by an improved capacitance technique, Part I. Sensor design and performance. J. Hydrol. 93:67-78.

Duke J.A., 1981, Hanbook of legumes of world economic importance, plenum press, New York. P. 52-57.

Delta-T Devices, (2004). User Manual, Eijkelkamp Agrisearch Equipment, The Netherlands

Eldeiry, A. and Garcia L. A., (2010). Comparison of Regression Kriging and Cokriging Techniques to Estimate Soil Salinity Using Landsat Images, Journal of Irrigation and Drainage Engineering, Vol. 136, No. 6 : pp. 355-364

Ernest, H. (1994). Simulation Modeling Methodology: Principles and Etiology of Decision Support, PhD Dissertation Virginia Polytechnic Institute and State Blacksburg, Virginia.

Gaskin, G.J., and Miller, J.D., (1996). Measurement of soil water content using a simplified impedance measuring technique. J. Agr. Eng. Res. 63:153-160.

George, P. Petropoulos, Hywel M. Griffiths, Wouter Dorigo. Angelika Xaver, and Alexander Gruber., (2013). Surface soil moisture estimation; International Standard Book Number 13: 978-1-4665-0478-0.

Gregory, P.J., (1988). Root growth of chickpea, faba bean, lentil, and pea and effects of water and salt stresses, World crops: Cool season food legumes Volume 5, 1988, pp 857-867

Hupet, F. and Vanclooster, M., (2002). Intra-seasonal dynamics of soil moisture variability within a small agricultural maize cropped field. Journal of hydrology, 261(1-4): 86-101

Hernandez, R. P., and Stefanoni L. H., (2006). Mapping the spatial variability of plant diversity in a tropical forest: comparison of spatial interpolation methods. Environmental Monitoring and Assessment 117:307-334.

Hayhoe, H.N. and Dejong, R., (1982). Computer simulation model of soil water moement and uptake anby plants roots. Land Resource research Institute, Agriculture Canada, Ottawa, Ontario 74 pp.

IAEA, (2008). A field estimation of water content: A practical Guide to Methods, Instrumentation and Sensor, IAEA-TCS-30, IAEA , VIENNA, ISSN 1018–5518

Jennifer, M. Jacobs, Binayak P. Mohanty, En-Ching Hsu, Douglas Miller *(2004).* Field scale variability, time stability and similarity of soil moisture, *Remote Sensing of Environment 92, 436–446*

Kasteel, R., Vereecken H., Kamai T., Harter T., Hopmans J., and Vanderborght J. (2007)**.** Explaining Soil Moisture Variability as a Function of Mean Moisture Content, *Agrosphere, Geophysical Research Abstracts, VOL. 34, L22402*.

Kebedea, S., Travia Y., Alemayehub T., and Marc V., (2006). Water balance of Lake Tana and its sensitivity to fluctuations in rainfall, Blue Nile basin, Ethiopia; Journal of Hydrology 316 233–247.

Kendie Addis, H., Strohmeier, S., Srinivasan, R., Ziadat, F., Klik, A., (2013). Using SWAT Model to Evaluate the Impact of Community-based Soil and Water Conservation Interventions for an Ethiopian Watershed.

Krauer, J., (1988). Rainfall, erosivity and isoerodent map of Ethiopia. Soil Conservation Research Project, Research Report 15. University of Berne, Switzerland, p. 132.

Koster, R. D., S. P. P. Mahanama, T. J. Yamada, G. Balsamo, A. A. Berg, M. Boisserie, P. A. Dirmeyer, F. J. Doblas-Reyes, G. Drewitt, C. T. Gordon, Z. Guo, J.-H. Jeong, W.-S. Lee, Z. Li, L. Luo, S. Malyshev, W. J. Merryfield, S. I. Seneviratne, T. Stanelle, B. J. J. van den Hurk, F. Vitart, and E. F. Wood (2011). The Second Phase of the Global Land Atmosphere Coupling Experiment: Soil Moisture Contributions to Sub-seasonal Forecast Skill, J. Hydrometeorol., 12, 805–822.

Lee, H., Zehe E., and Sivapalan M., (2007). Prediction of rainfall runoff response and soil moisture dynamics in micro-catchment using CREW model; Hydrol. Earth Syst. Sci., 11, 819–849.

Lewis, M., (2010). Influence of Antecedent Soil Moisture and Rainfall Rate on the Leaching of Nitrate and Phosphate from intact Monoliths of Agricultural Soil, Master Thesis, University of Waterloo Library 200, University Avenue West, Waterloo, Ontario, Canada

Likeyelesh, G.., (2005). Biotechnological Studies in Tef (Eragostis Tef) (Zucc.) Trotter) with Reference to Embryo Rescue, Plant Regeneration, Haplodization and

Genetic Transformation. A PhD Thesis, Addis Ababa University, Addis Ababa, Ethiopia.

Lili, M., Bralts, V. F., Yinghua, P., Han, L. & Tingwu, L. (2008) Methods for measuring soil infiltration: State of the art, Int J Agric & Biol Eng. 1(1), 22-30.

Manabe, S., Delworth, T., (1990). The temporal variability of soil wetness and its impact in climate. Climatic Change 16, 185–192.

Maria, A., (1997). Introduction to modeling and simulation; Proceedings of the 1997 Winter Simulation ; State University of New York, NY 13902-6000, USA.

Mohr, K. I., J.S. Famiglietti, A. Boone, and P.J. Straks, (2000). Modeling soil moisture and surface flux variability with untuned land surface scheme. A case study from the Southern Great Plains 1997 Hydrology Experiment, J. Hydrometeorolgy., 1: 154-169.

Morton , F.I., (1986). Practical Estimates of Lake Evaporation, J. Clim. Appl. Meteorol., 25, 371-387.

Mulu Ayele, A. Blum & Henry T. Nguyen, (2001). Diversity for osmotic adjustment and root depth in TEF [*Eragrostis tef* (Zucc) Trotter]; *Euphytica* ***121:*** *237–249.*

Mutua, F. and Kuria D., (2012). A comparison of spatial rainfall estimation techniques: A case stuudy of Nyando river basin, *Jomo Kenyatta University of Agriculture and Technology,* Kenya (Republished).

Noshadi, M. and Sepaskhah, A. R., (2005). Application of Geostatistics For Potential Evapotranspiration Estimation Iranian Journal of Science & Technology, Transaction B, Engineering, Vol. 29, No. B3

Nyssen, J. H. Vandenreyken, J. Poesen, J. Moeyersons, J. Deckers, Mitiku Haile, C. Salles, G. Govers., (2004). Journal of Hydrology 311 (2005) 172–187

Robock, A., Konstantin Y. V., Govindarajalu S., Jared K. E., Steven E. H., Nina A. S., Suxia Liu, and Namkhai A., (1999).The Global Soil Moisture Data Bank, *Bulletin of the American Meteorological Society.*

Savva, Y., (2013). Spatial patterns of soil moisture under forest and grass land cover in a suburban area, in Maryland. *Geoderma*, Vol. 192, pp. 202-210.

Saxon, E., (2006). Field and Pond hydrologic Analysis with the SPAW model, American Society of Agricultural and Biological Engineers, An ASBE Meeting Presentation, Paper Number: 062108.

Sampath, S., (2001). Sampling Theory and Methods. pp 140. Department of Statistics, Looyola College, Chennai-600, India.

Senevirane, S. I. and Orth. R. K., (2012). A Revised Framework for Analyzing Soil Moisture Memory in Climate Data: Derivation and Interpretation. *J. Hydrometeor*, **13**, 404–412

Seyfried, M.S. & Wilcox, B.P. (1995). Scale and nature of spatial variability: field examples having implications for hydrologic modeling. *Water Resource Research*, **31**: 173–184.

Shao, Y. I , Leslie L. M., Munro R. K., Irannejad P., Lyons W. F., Morison R., Short D. and Wood M. S., (1996).Soil Moisture Prediction over the Australian Continent, *Meteorol. Atmos. Phys. 63, 195-215 (1997)*

Tolk, J. A., (2003). Soils' Permanent Wilting Points; United States Department of Agriculture (USDA), Bushland, Texas, U.S.A.

Van Genuchten, M. Th., Simunek, F. J. L, and Sejna, M., (2009). Code for Quantifying the Hydraulic Functions of Unsaturated Soils, www.hydrus3d.com.

Van den Hurk, B., F. Doblas-Reyes, G. Balsamo, R. D. Koster, S. I. Seneviratne, and H. Camargo, Jr., (2012). Soil moisture effects on seasonal temperature and precipitation forecast scores in Europe, Clim. Dyn., 1-2, 349–362.

Verstraeten, W. W., Veroustraete F. and Feyen J., (2008). Assessment of Evapotranspiration and Soil Moisture Content Across Different Scales of Observation; ***Sensors*** ISSN 1424-8220.

Viste, E. and Sorteberg, A., (2013). Moisture transport into the Ethiopian highlands, *Int. J. Climatol.* 33: 249–263

Walker, J., Willgoose, G., Kalma, J., 2004. In situ measurement of soil moisture: a comparison of techniques. Journal of Hydrology. 293 (1-4), 85–99.

Webster, R. and Oliver, M. A., (2001). Geostatistics for Environmental Scientists. 2th ed. John Wiley and Sons, Brisbane, Australia.

Western, A. W., (2004). Spatial correlation of soil moisture in small catchments and its relationship to dominant spatial hydrological processes, Journal of Hydrology 286: 113–134.

Western, A. and Grayson R., (2001). Soil moisture and Runoff processes at Tarrawarra Catchment; *Cambridge University Press.*

Western, A.W., Grayson, R.B., Bloschl, G., Willgoose, G.R. & McMahon, T.A. (1999). Observed spatial organization of soil moisture and its relation to terrain indices. *Water Resources Research*, **35**: 797–810.

Whalley, W.R., Dean T.J., and Izzard, P., (1992). Evaluation of the capacitance technique as amethod for dynamically measuring soil water content. J. Agric. Eng. Res. 52:147-155

Yaclin, E., (2005). Cokriging and its effect on the estimation precision , *the Journal of The South African Institute of Mining and Metallurgy* Volume 105.

Yang, L., (2010). Spatio-temporal patterns of field-scale soil moisture and their implications for *in situ* soil moisture network design, PhD dissertation, Iowa State University, Ames, Iowa

Yang Qiu, Bojie Fu, Jun Wang and Liding Chen, (2001). Spatial variability of soil moisture content and its relation to environmental indices in a semi-arid gully catchment of the Loess Plateau, China, *Journal of Arid Environments 49: 723–750*

Yeakley, J. A., Swank, W. T., Swift, L. W., Hornberger, G. M., and Shugart, H. H. (1998). Soil moisture gradients and controls on a southern Appalachian hillslope from drought through recharge, Hydrol. Earth Syst. Sci., 2 (1) 41-49.

Yenesew, M. and Tilahun K., (2009). Yield And Water Use Efficiency Of Deficit-Irrigated Maize In A Semi-Arid Region Of Ethiopia, African Journal of Food, Agriculture, Nutrition and Development, VOL. 9, NUM. 8, PP. 1635-1651

Yonas, W, Teferi A., Asmamaw, Y., Solomon, A., Hailu, K. and Ambachew, G., (2010). Socio-economic Survey of Gumara-Maksegnit Watershed, (Unpublished)

Yonghui, Y., Masataka W., Zhiping W., Yasuo S. and Changuan T., (2003). Prediction of changes in soil moisture associated with climatic changes and their implications for vegetation changes, *Climatic Change* 57**:** 163–183.

Yu-Hua, J., Ming-An S., Xia-Xu J., (2013). Spatial pattern of soil moisture and its temporal stability within profiles on a loessial slope in northwestern China, *Journal of Hydrology, 495:150–161.*

Zhang, Y., Wei H. and Nearing, M. A.., (2011). Effects of antecedent soil moisture on runoff modeling in small semiarid watersheds of southeastern Arizona Hydrol. Earth Syst. Sci., 15, 3171–3179

Zhu, Q, and Lin, H.S., (2009). Simulation and validation of concentrated subsurface lateral flow paths in an agricultural landscape. *Hydrology and Earth System Sciences 13, 1503 1518.*

Zhu, Q, and Lin H.S., (2011). Influences of soil, terrain, and crop growth on soil moisture variation from transect to farm scales. *Geoderma 163, 45 54.*

7. **Appendices**

Appendix i. Crop type and cover of the field where soil moisture prediction has been carried out in the rain recession period of 2013 summer season.

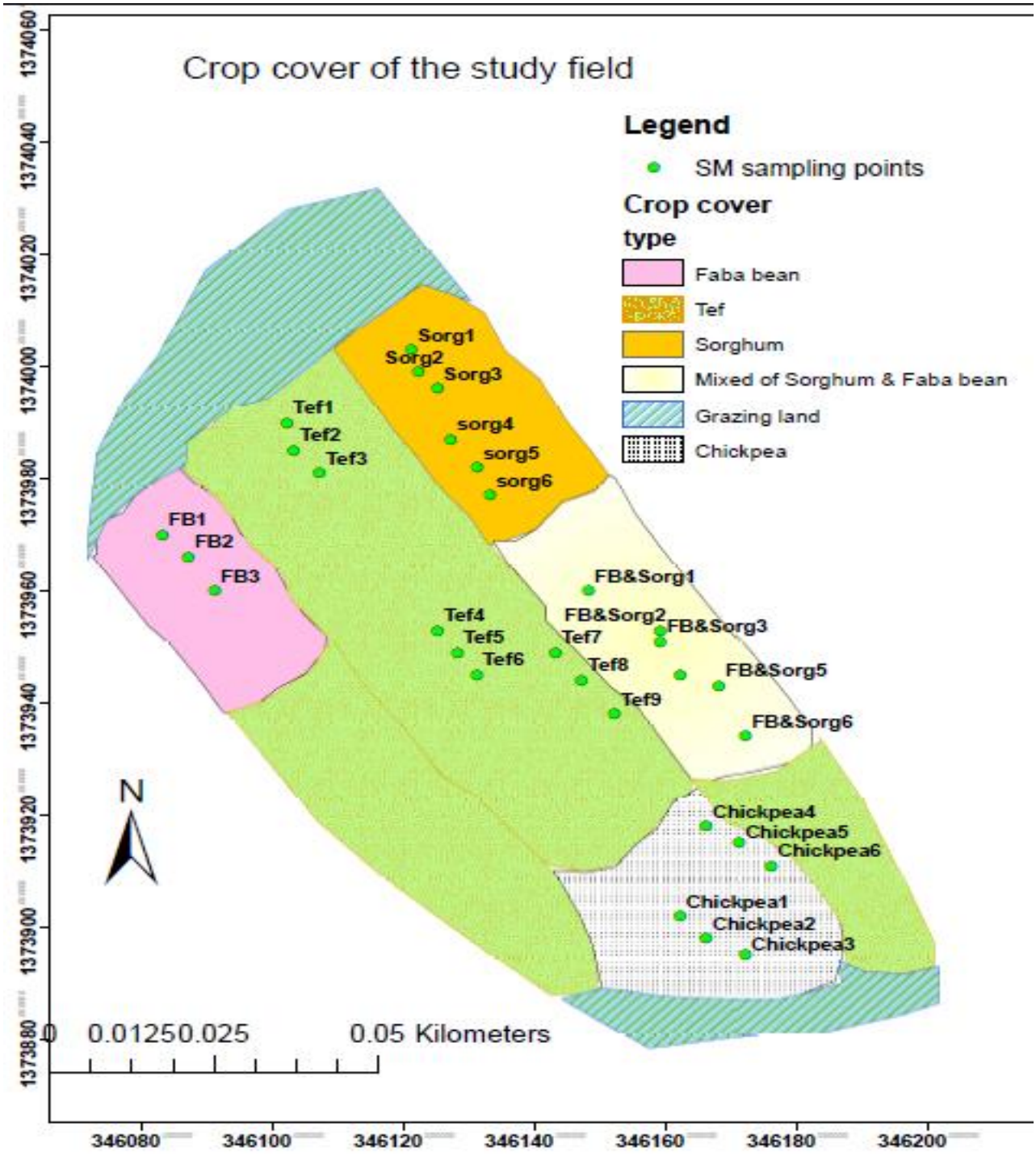

Appendix ii. List of graphs showing soil moisture (v/v) and SWS (mm/m) in each sampling clusters

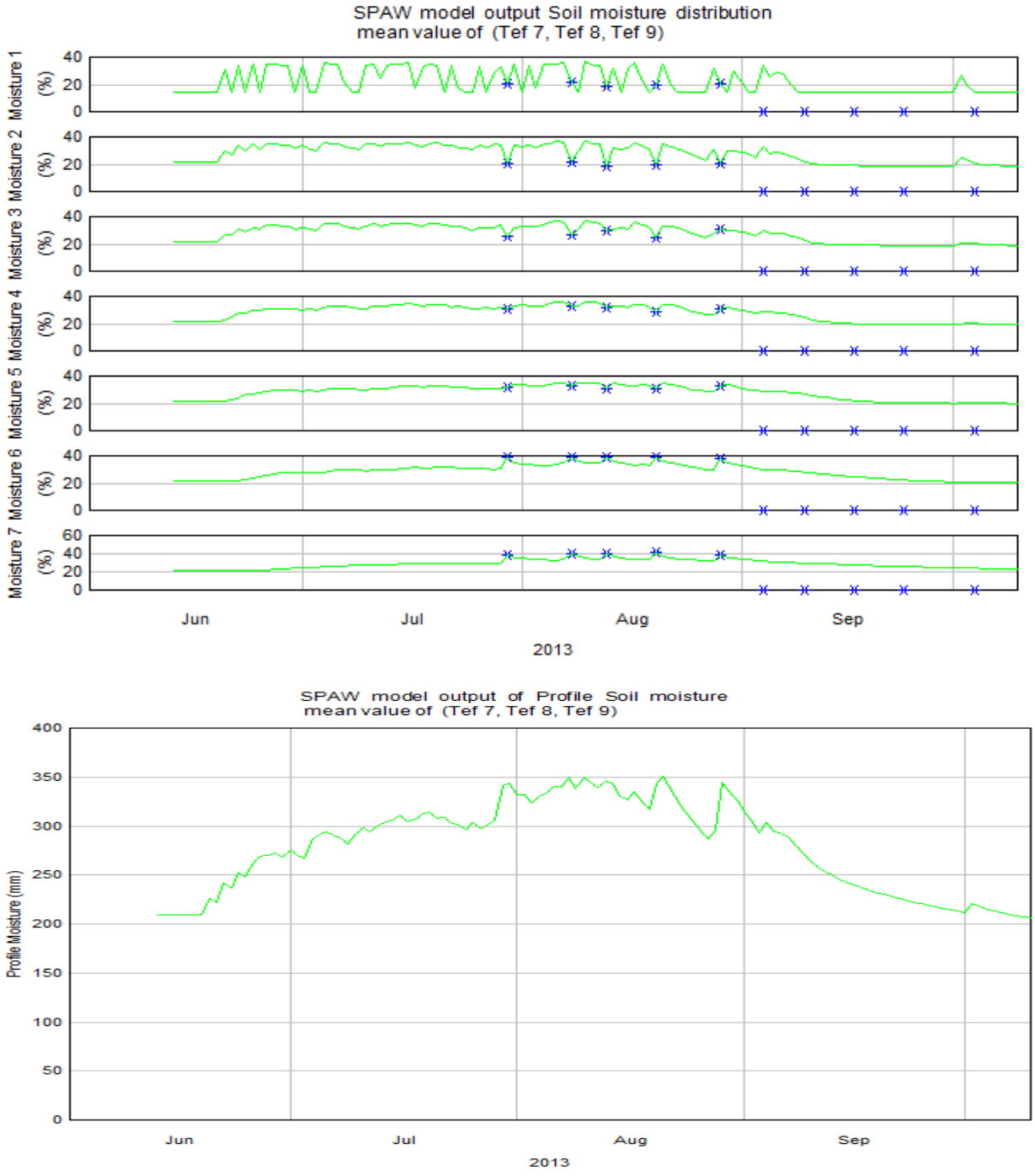

Soil moisture (v/v) and SWS (mm/m) in tef field of point tef 7, tef 8 and tef 9, along the drying period.

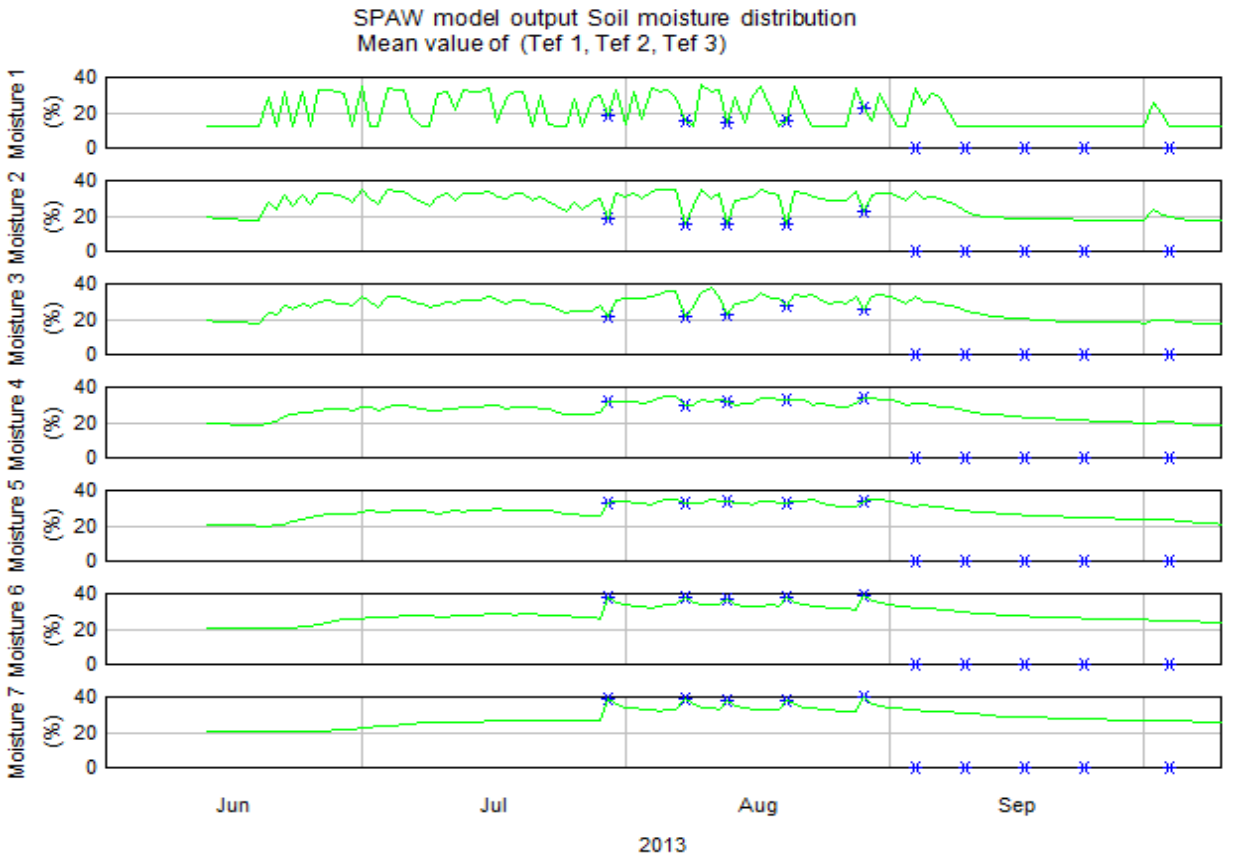

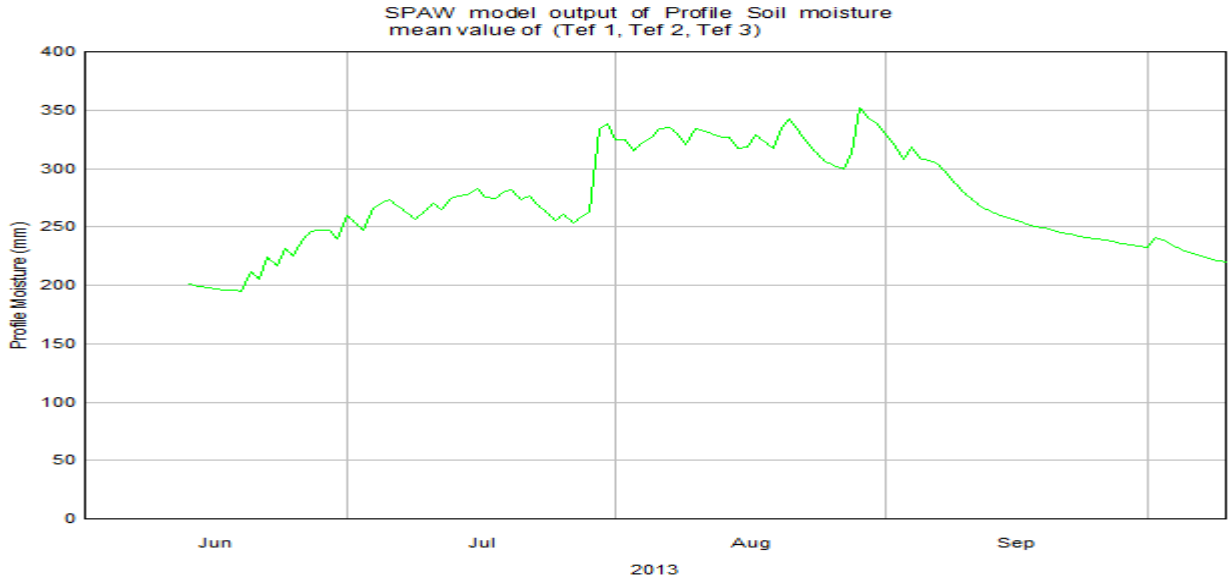

Soil moisture (v/v) and SWS (mm/m) in tef (*eragrostis Tef*) field of points (tef 1, tef 2 and tef 3).

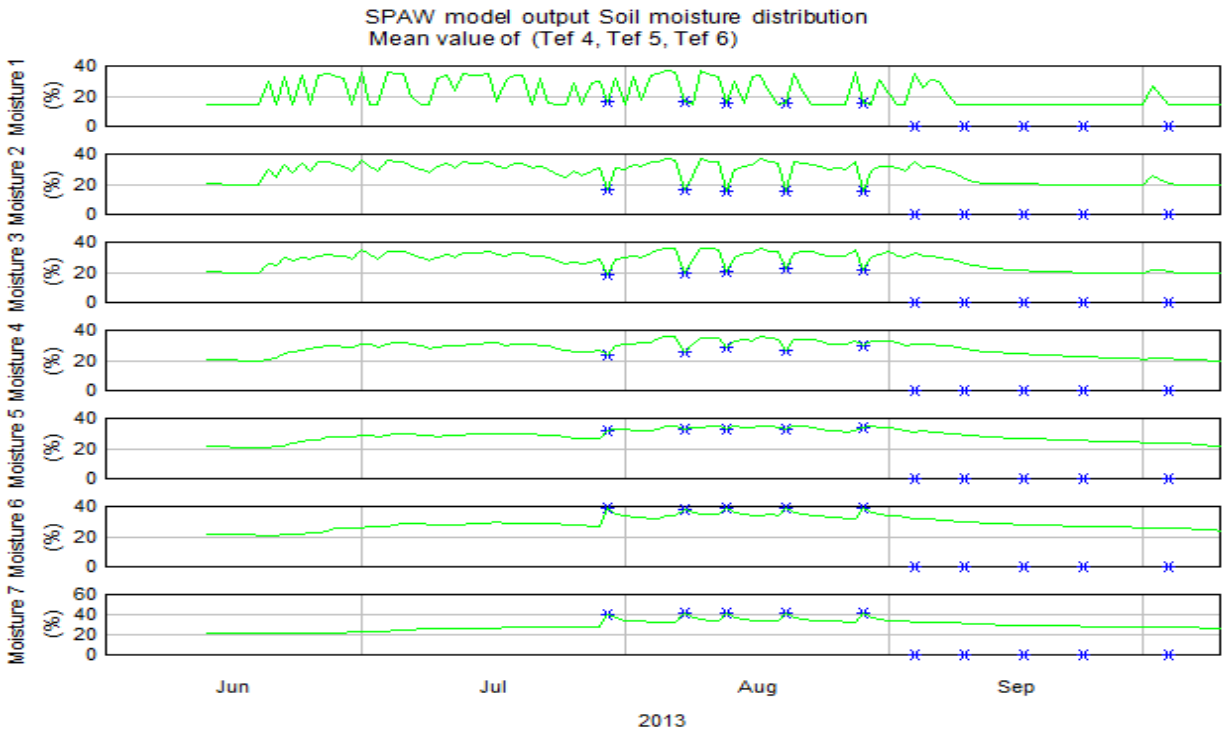

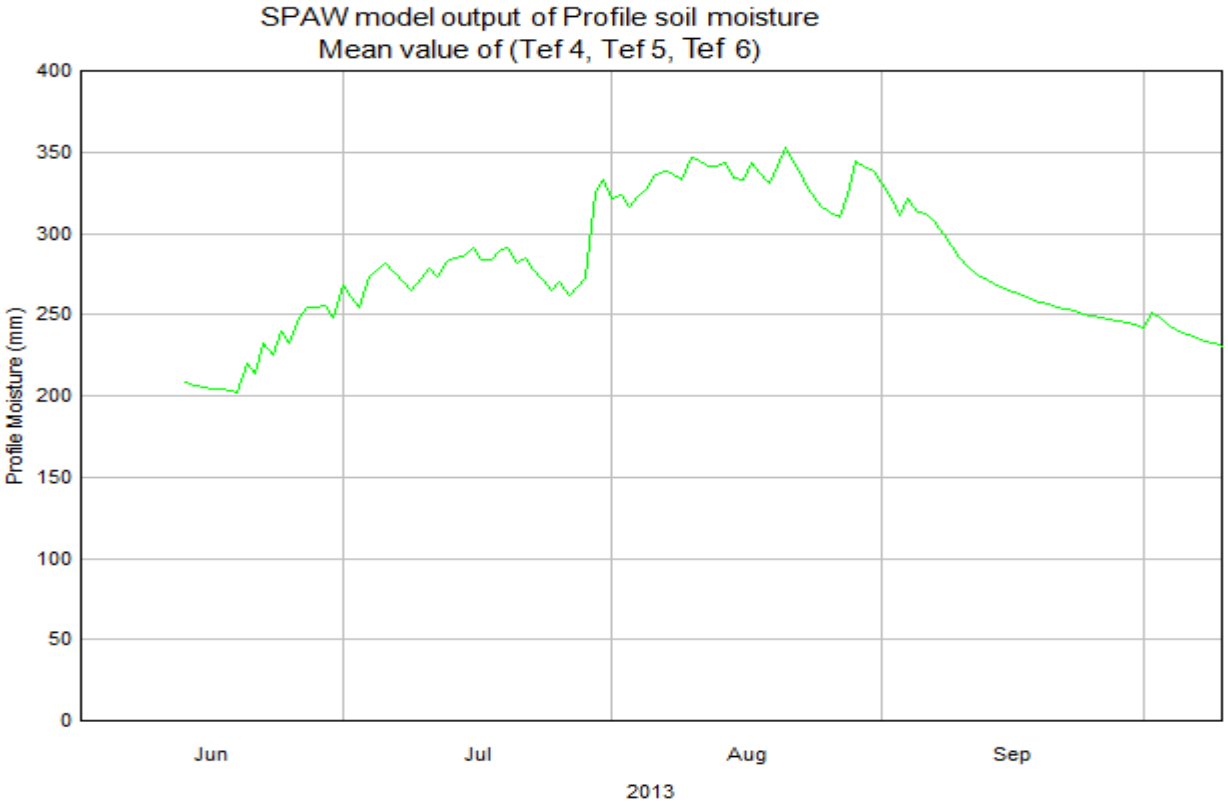

Soil moisture (v/v) and SWS (mm/m) in tef (*eragrostis Tef*) field of points (tef 4, tef 5 and tef 6)

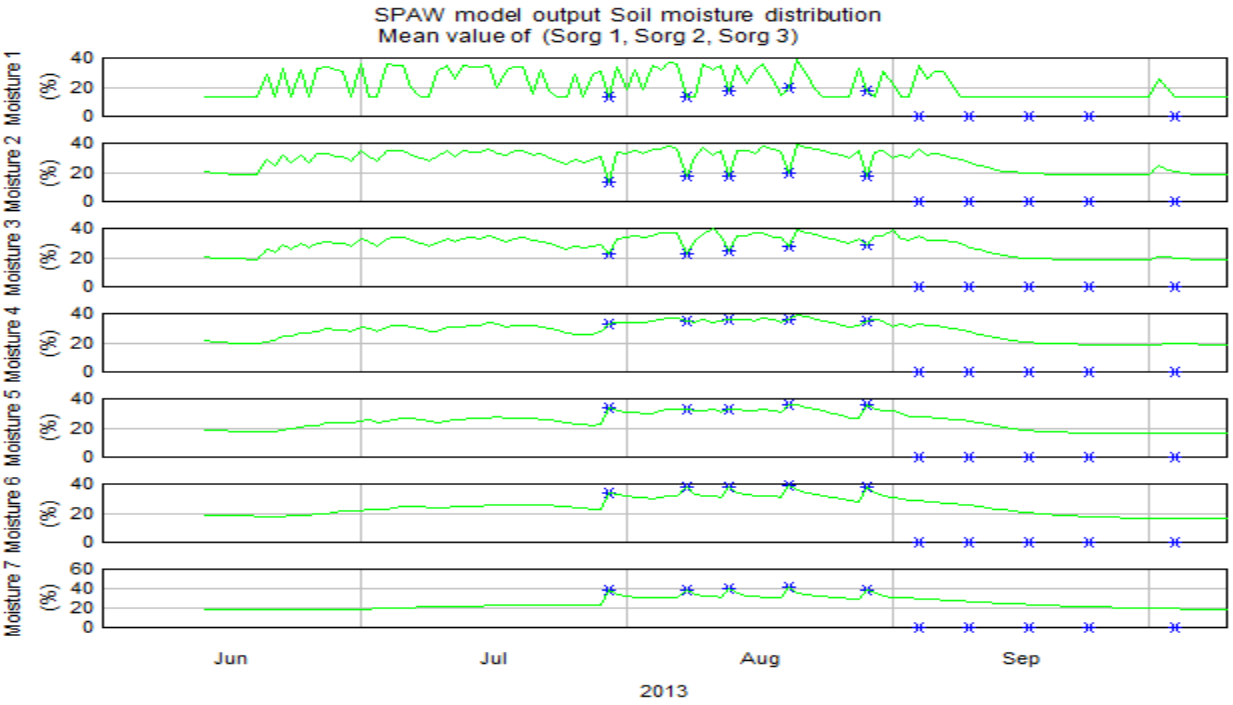

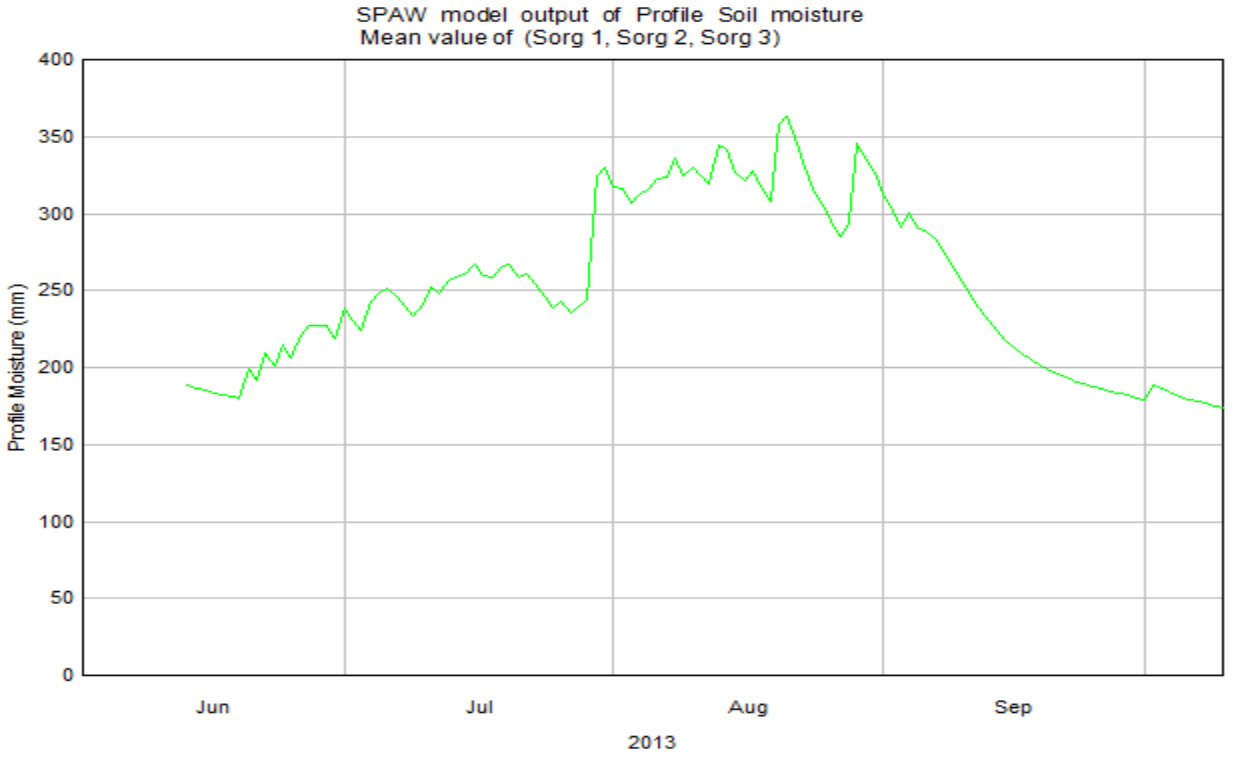

Soil moisture (v/v) and SWS (mm/m) in sorghum field of points (Sorg 1, Sorg 2, and Sorg 3).

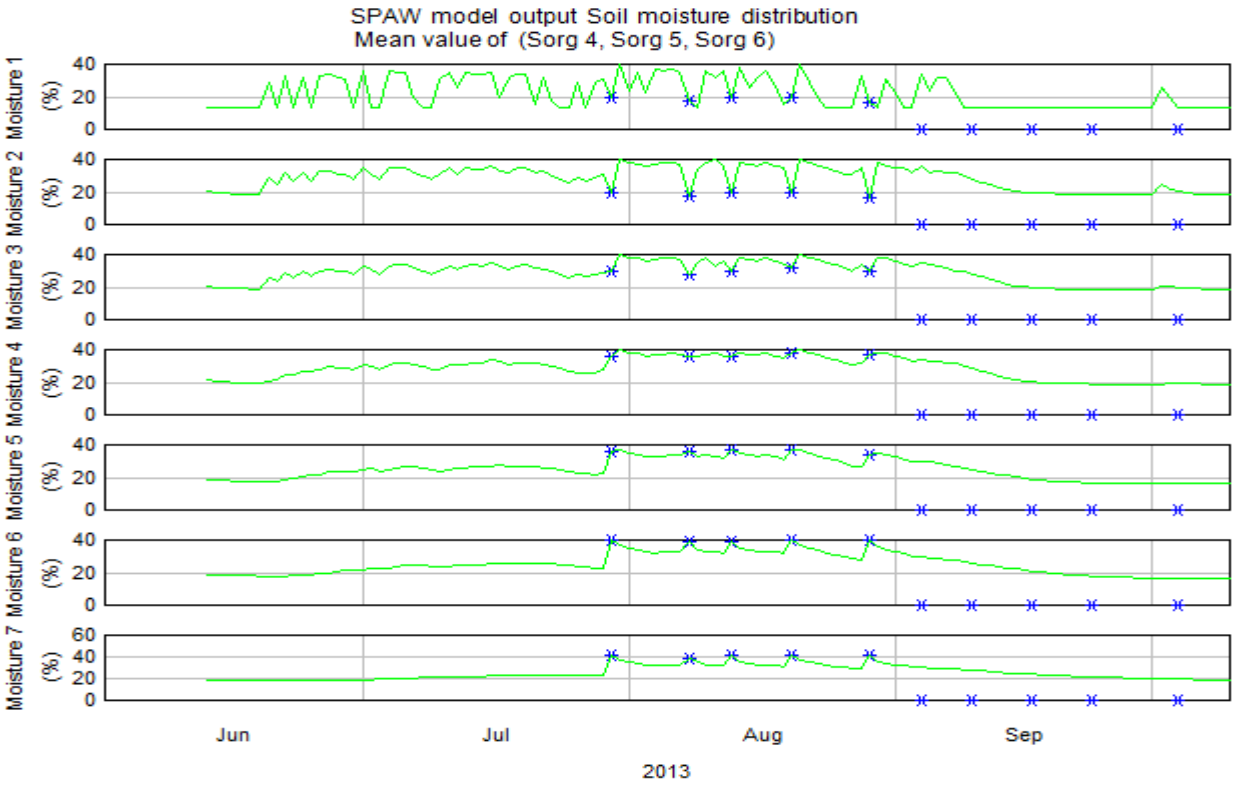

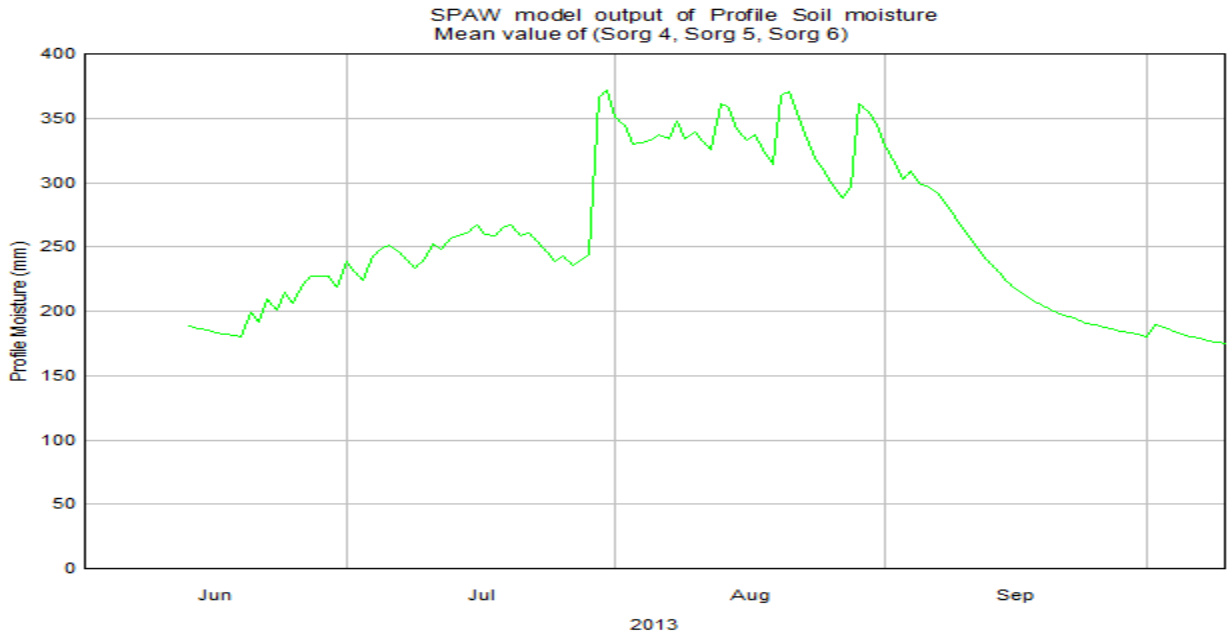

Soil moisture (v/v) and SWS (mm/m) in Sorghum field of points (Sorg 4, Sorg 5 and Sorg 6).

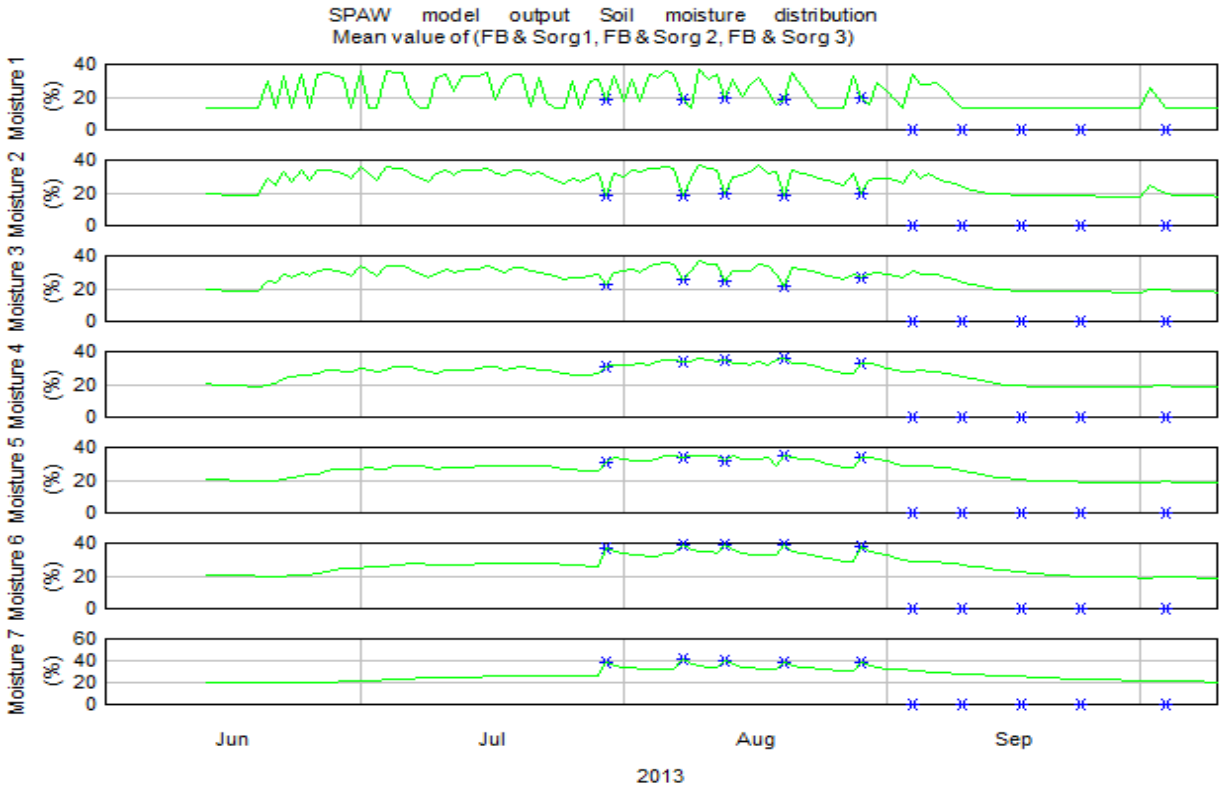

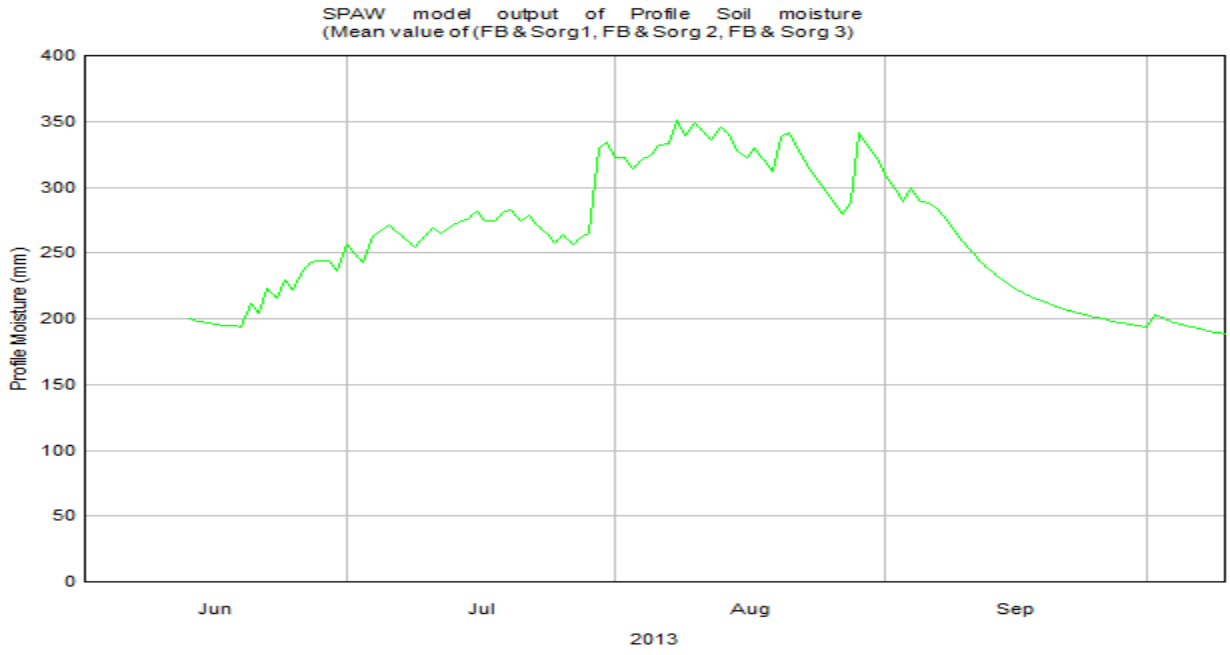

Soil moisture (v/v) and SWS (mm/m) in mixed cropped of Sorghum and faba beean field of points (FB & Sorg 1, FB & Sorg 2, FB & Sorg 3).

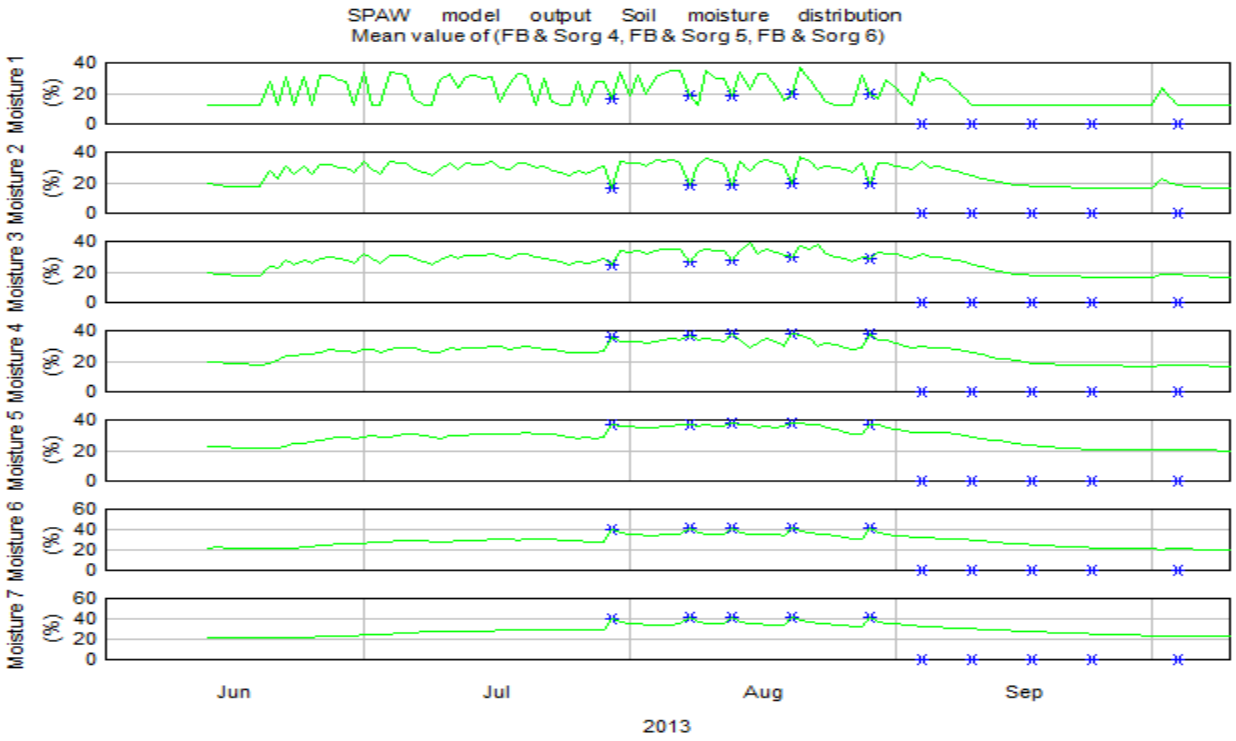

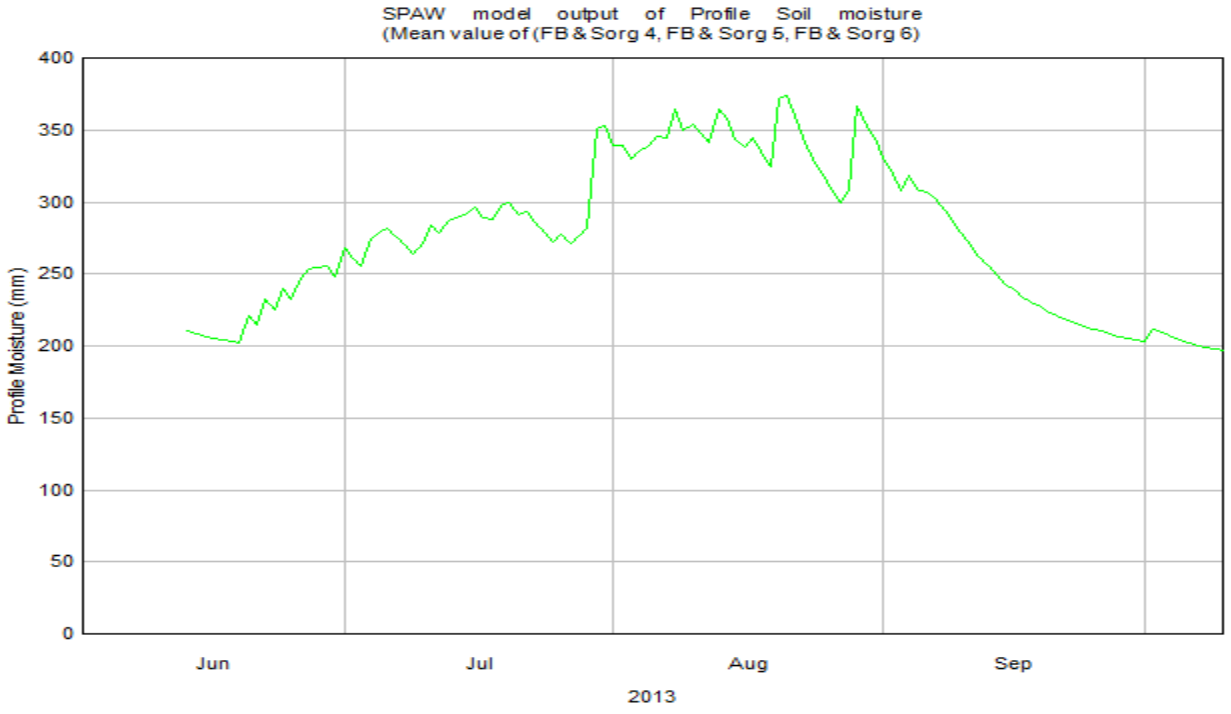

Soil moisture (v/v) and SWS (mm/m) in mixed cropped of Sorghum and faba beean field of points (FB& Sorg 4, FB& Sorg 5, (FB& Sorg 6).

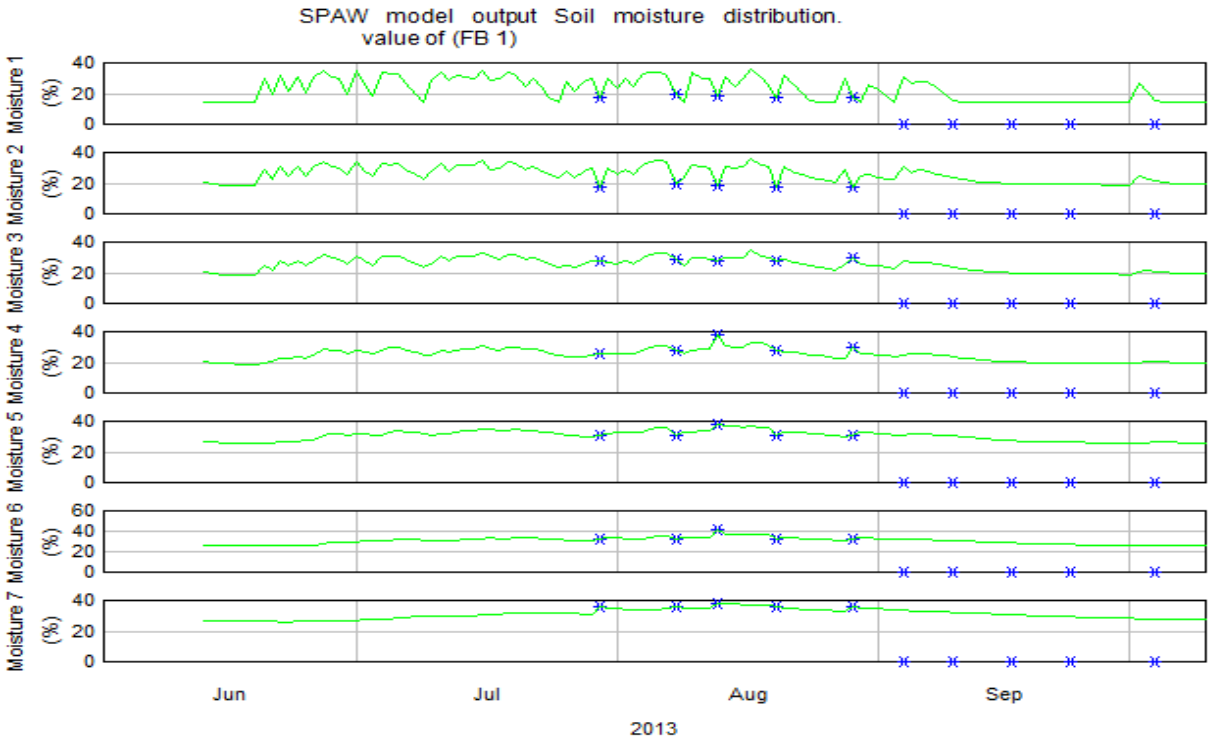

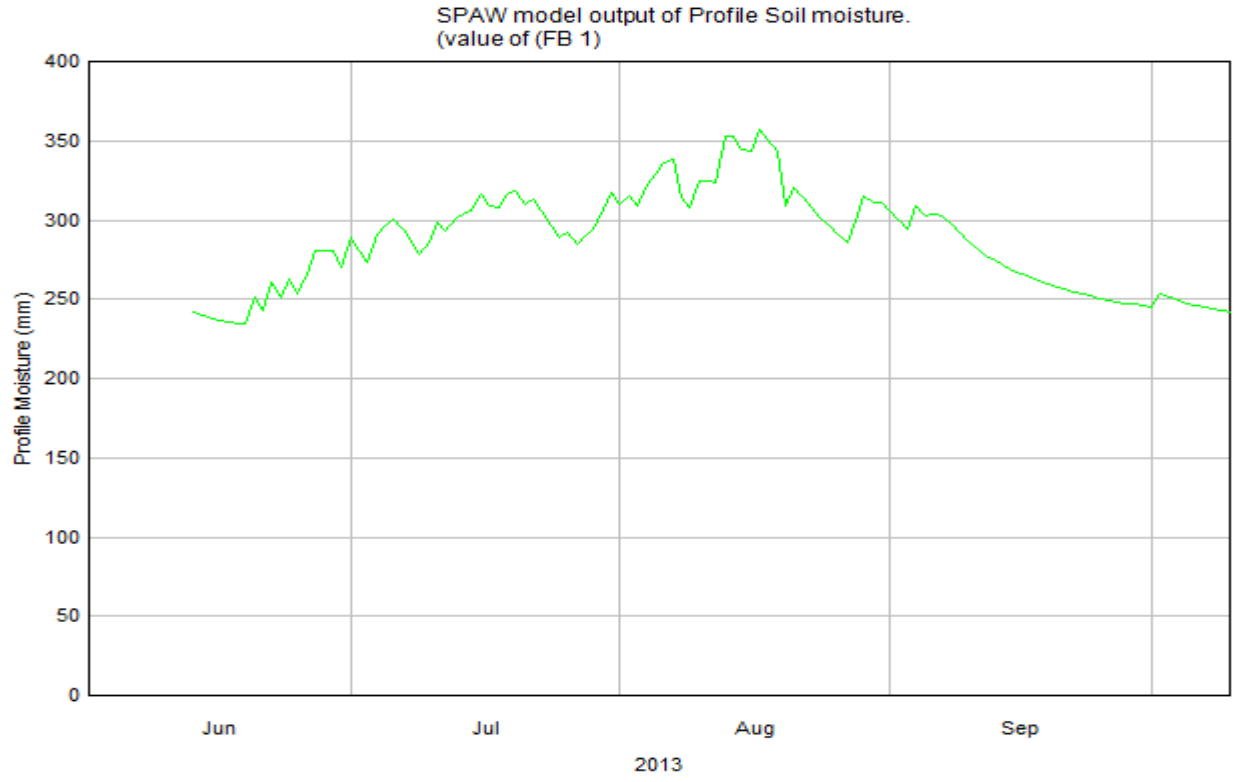

Soil moisture (v/v) and SWS (mm/m) in faba bean field of point (Faba bean 1).

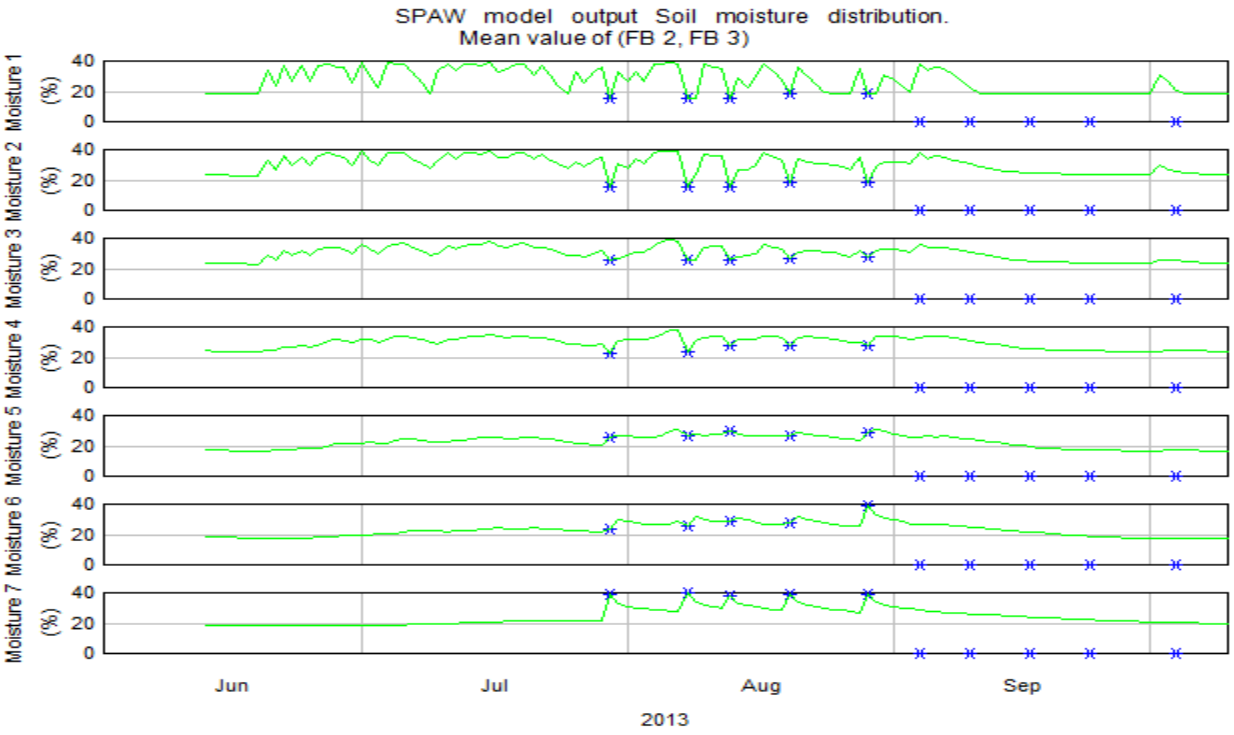

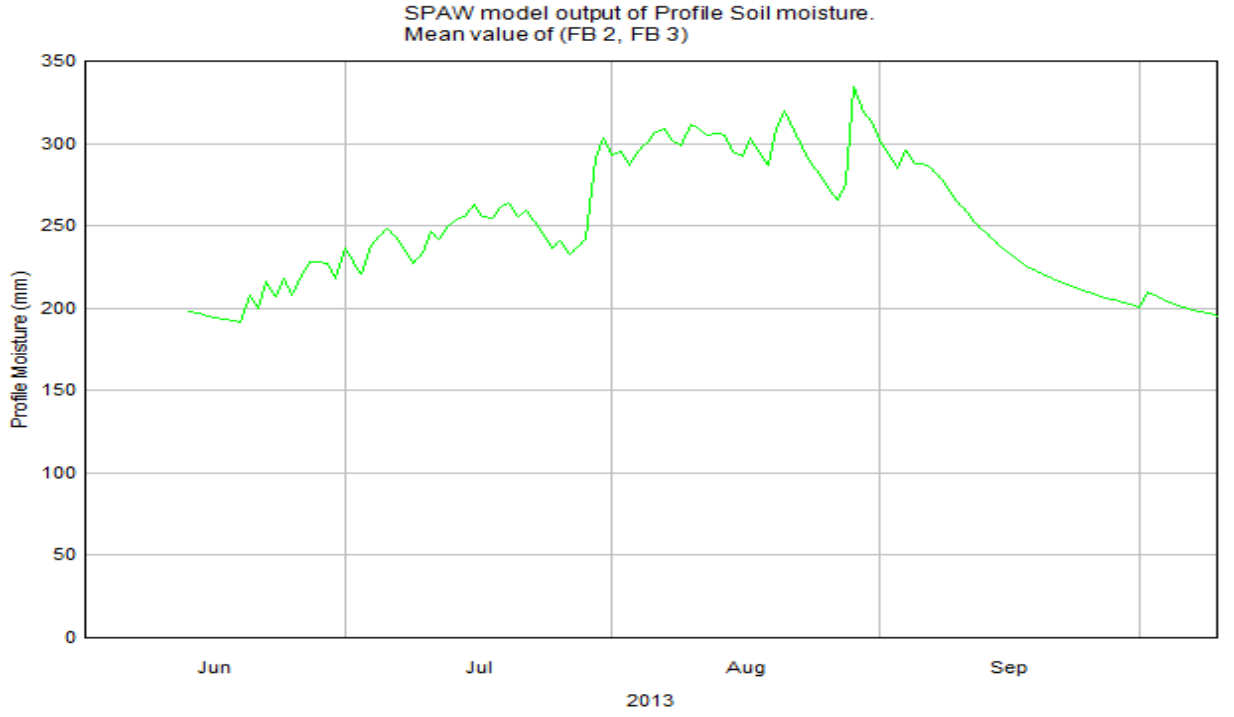

Soil moisture (v/v) and SWS (mm/m) in Faba bean field of points (FB2 and FB3)

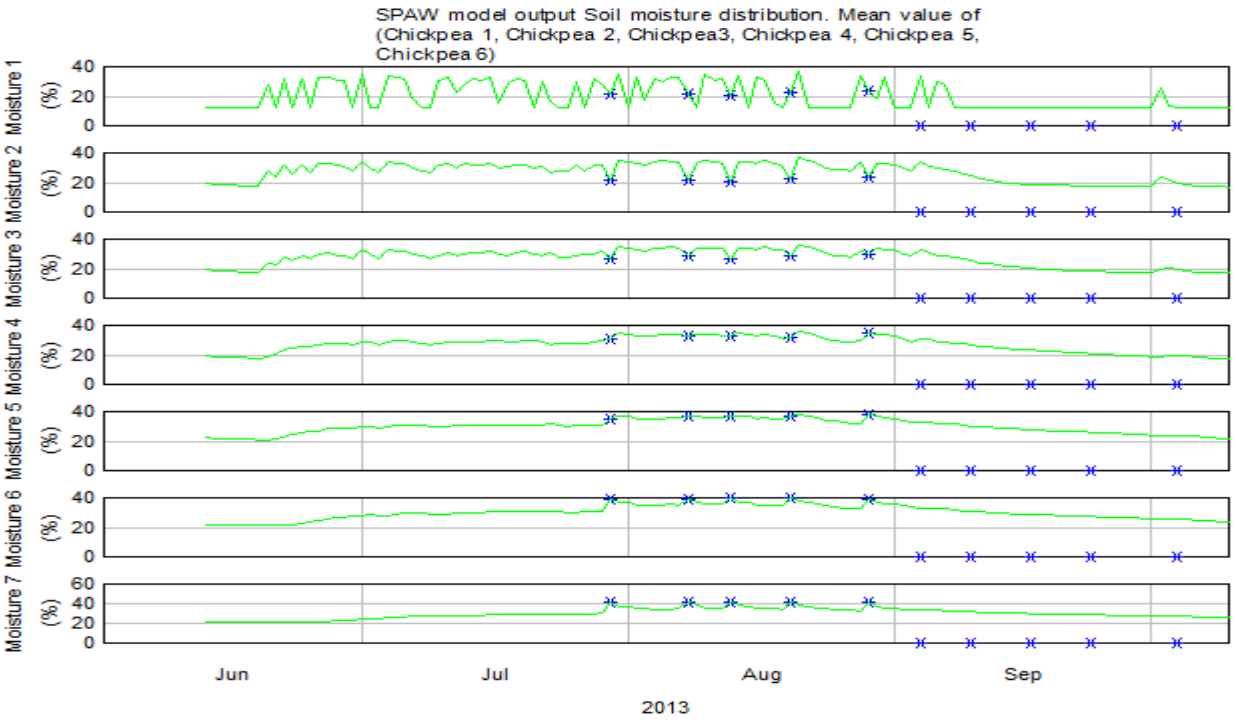

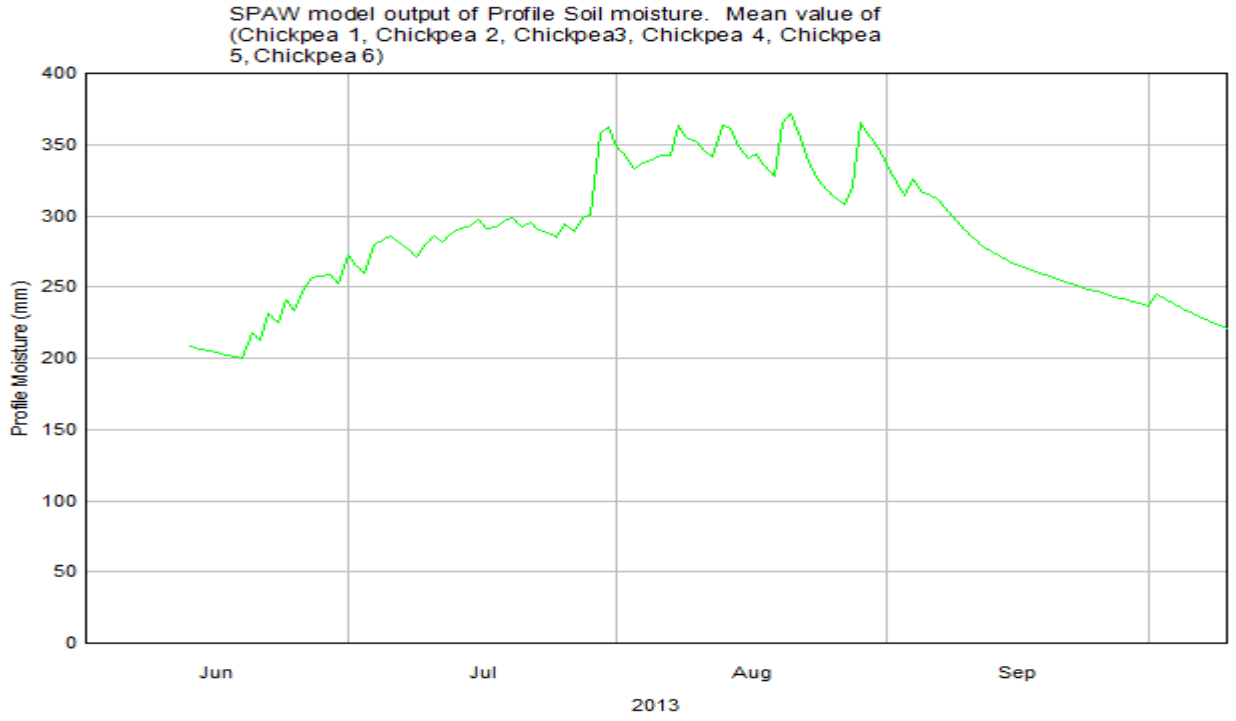

Soil moisture (v/v) and SWS (mm/m) in chickpea field of points (chickpea 1, chickpea, chickpea 2, chickpea 3, chickpea 4, chickpea 5 and chickpea 6).

Appendix iii. Graphs showing covariance of measured soil moisture, considering field slope as covariate, in agricultural field of the study area.

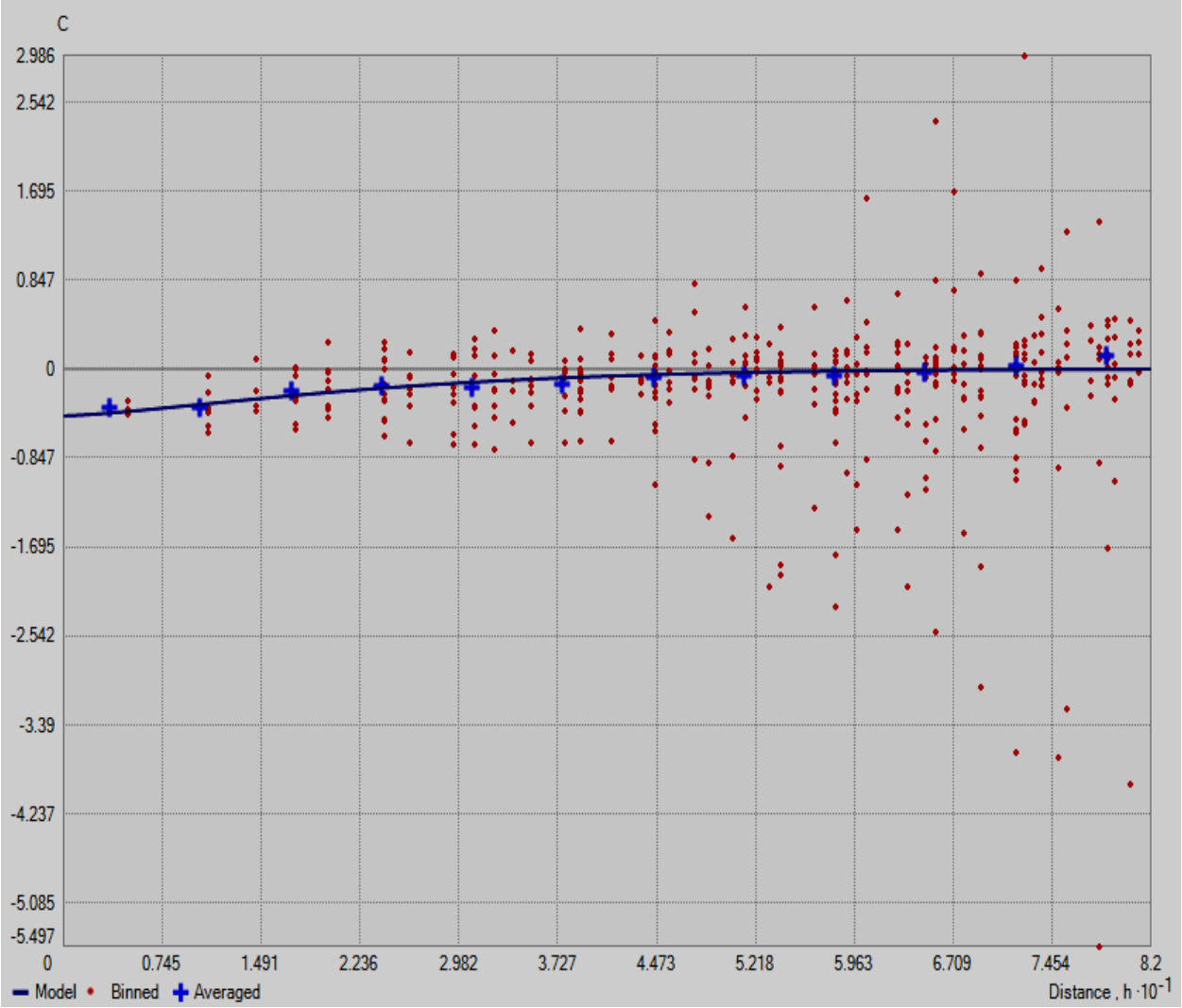

Covariance of measured soil moisture with slope distribution in agricultural field of the study area

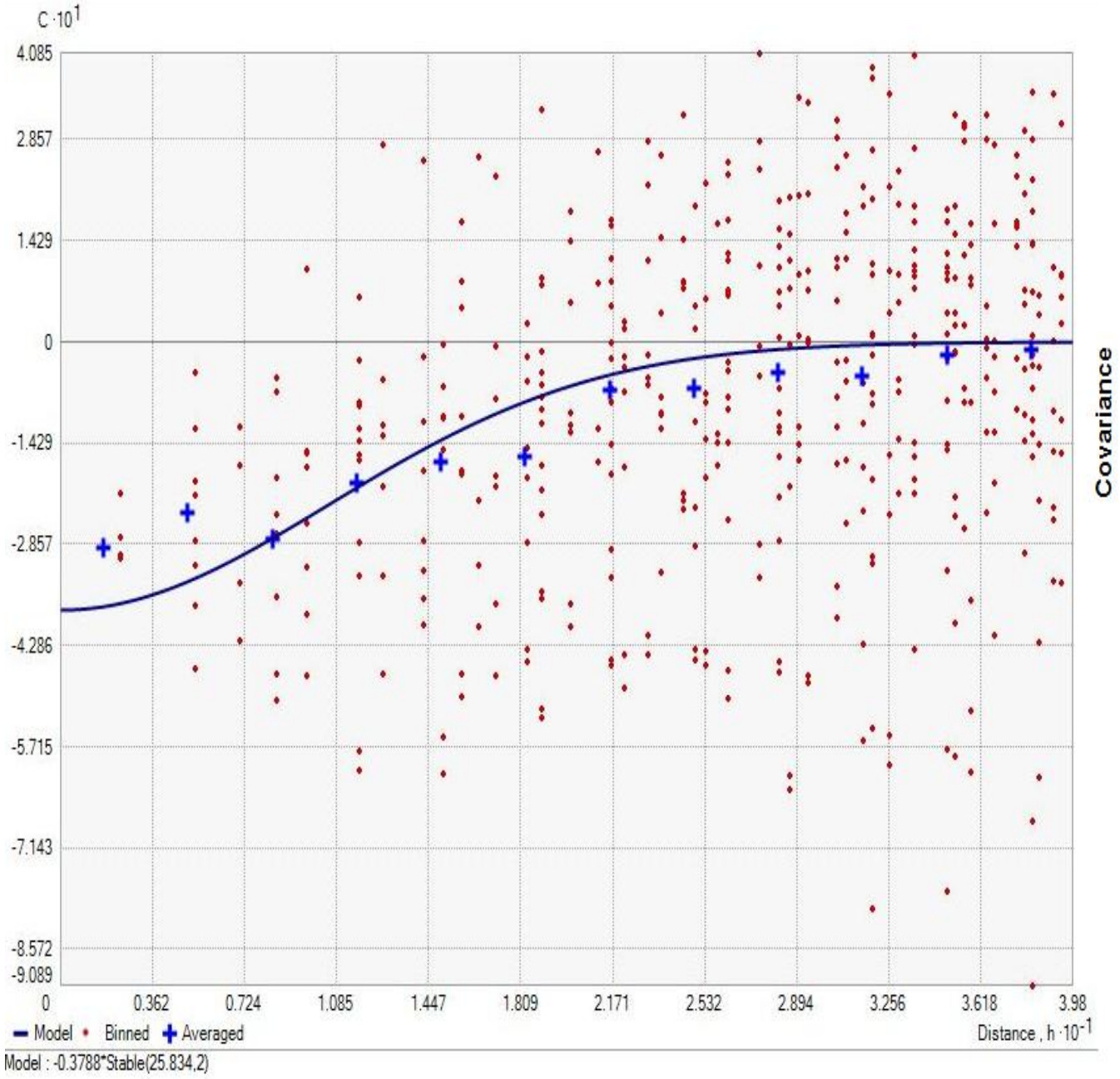

Covariance of SPAW predicted soil moisture distribution, slope of the field (degree) as covariate, on the date of (04-09-2013)

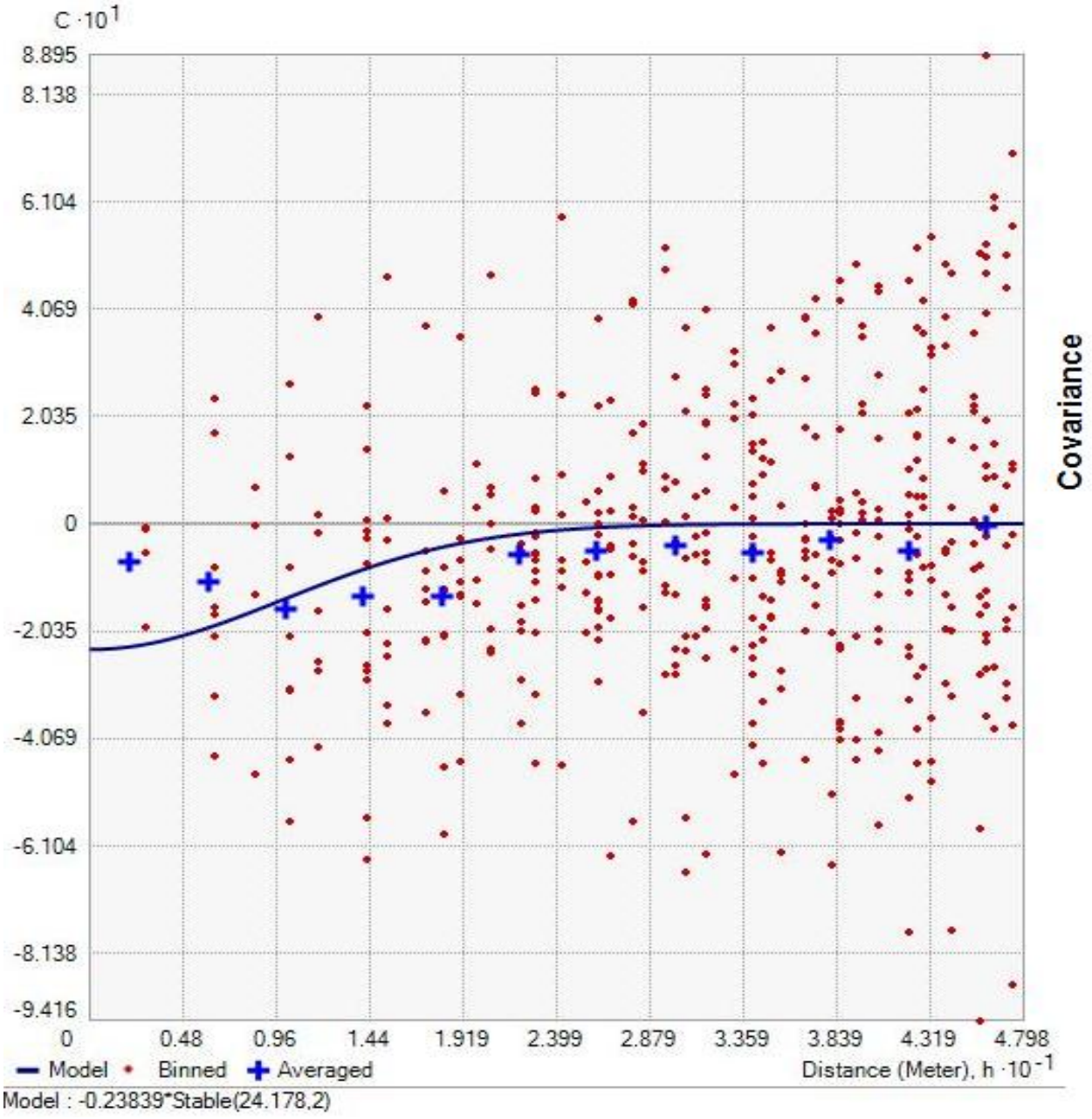

Covariance of SPAW predicted soil moisture distribution, slope of the field (degree) as covariate, on the date of (02-10-2013)

Appendix iv. SPAW predicted soil moisture versus measured spatially distributed soil moisture on dates selected for prediction

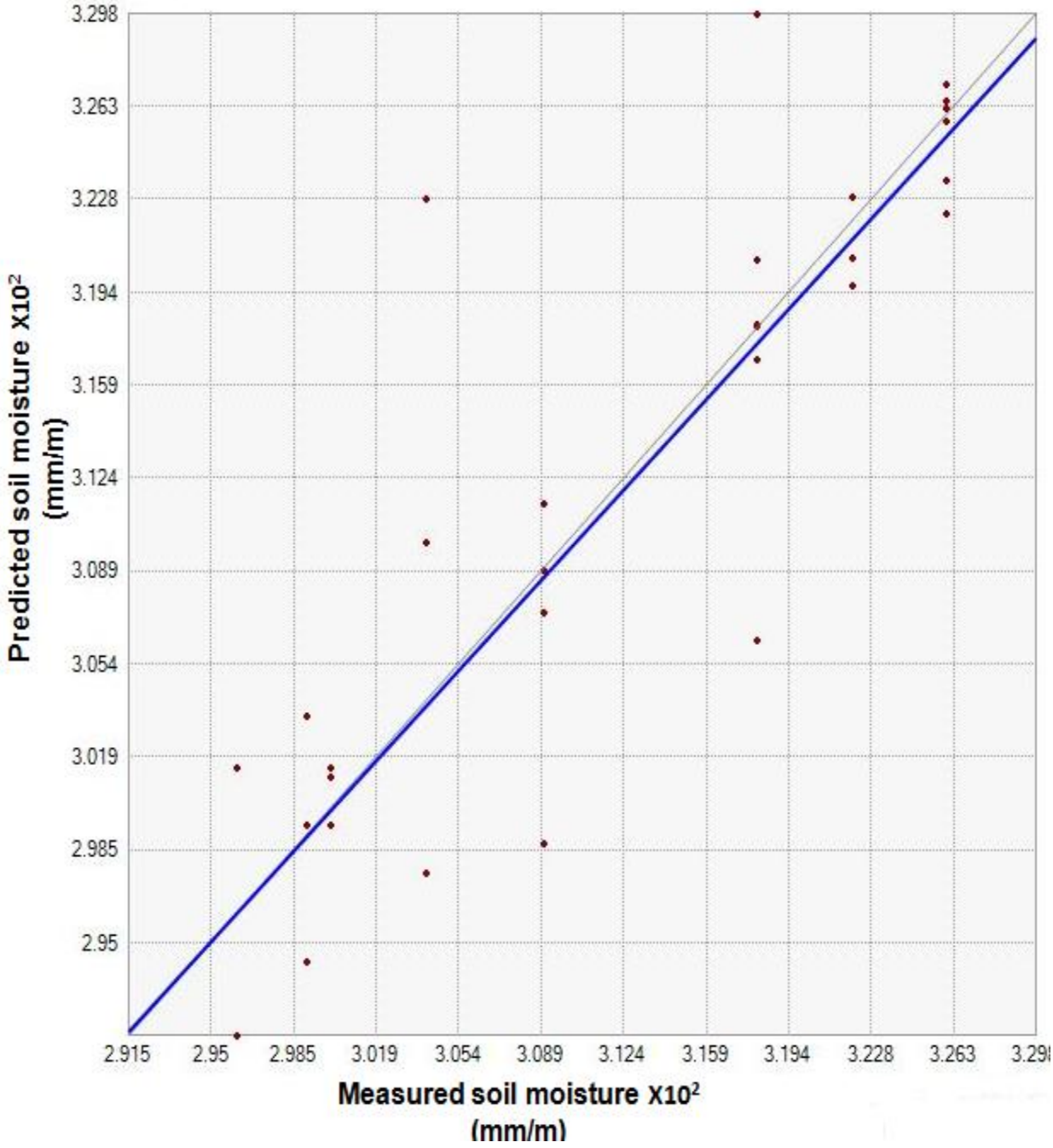

SPAW predicted soil moisture versus measured spatially distributed soil moisture on the date of (04-09-2013)

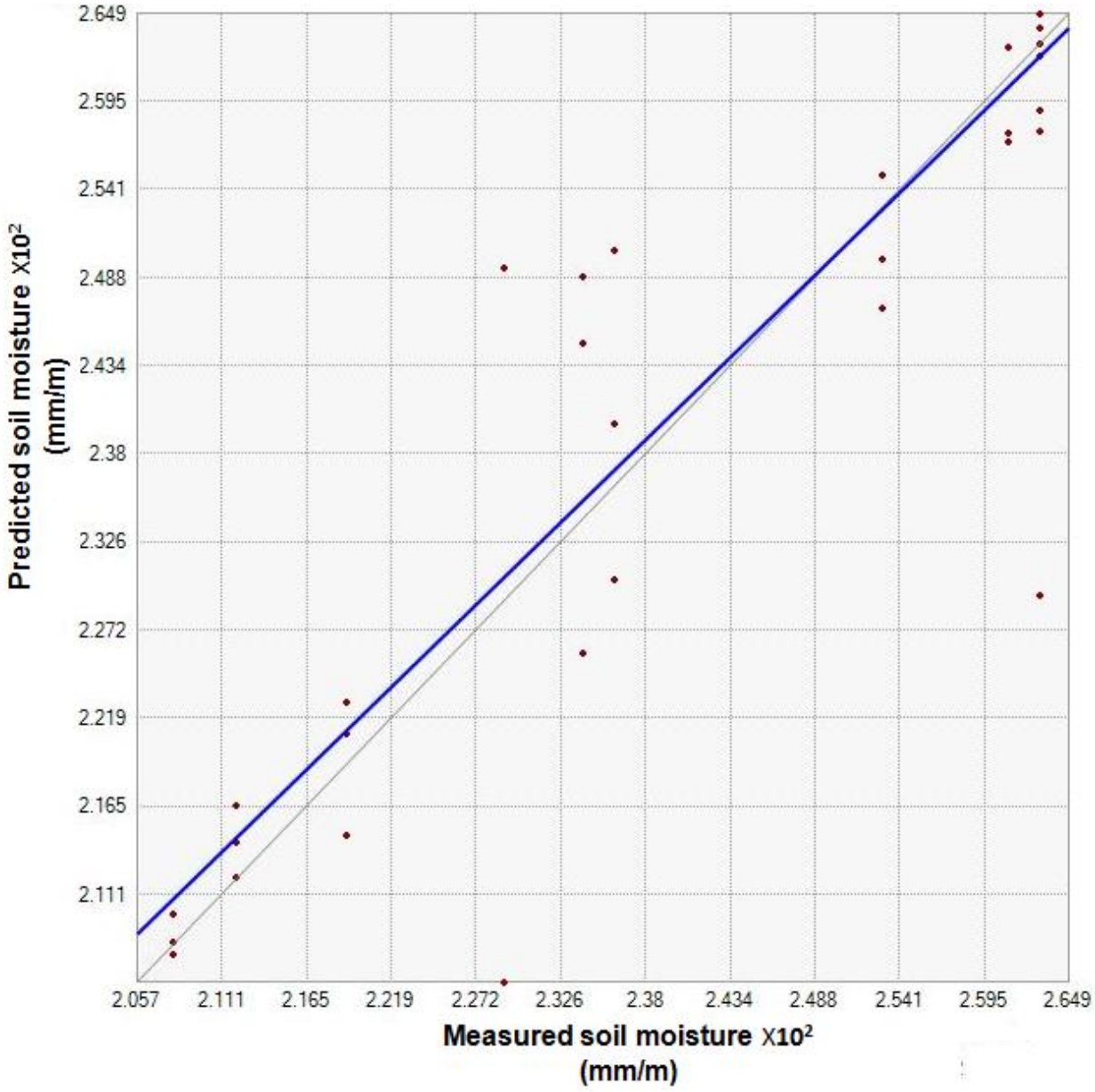

SPAW predicted soil moisture versus measured spatially distributed soil moisture on the date of (17-09-2013)

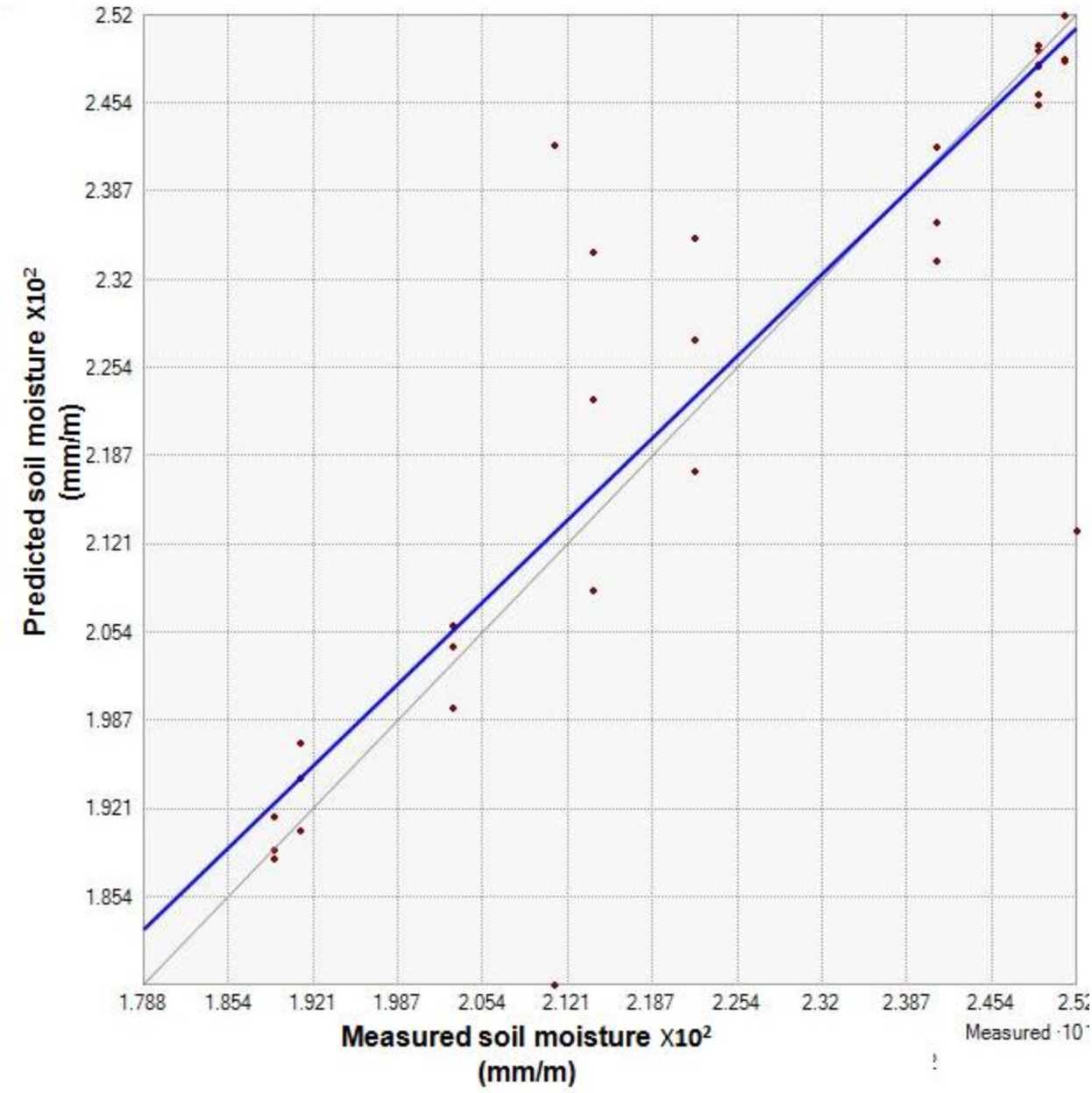

SPAW predicted soil moisture versus measured spatially distributed soil moisture on the date of (24-09-2013)

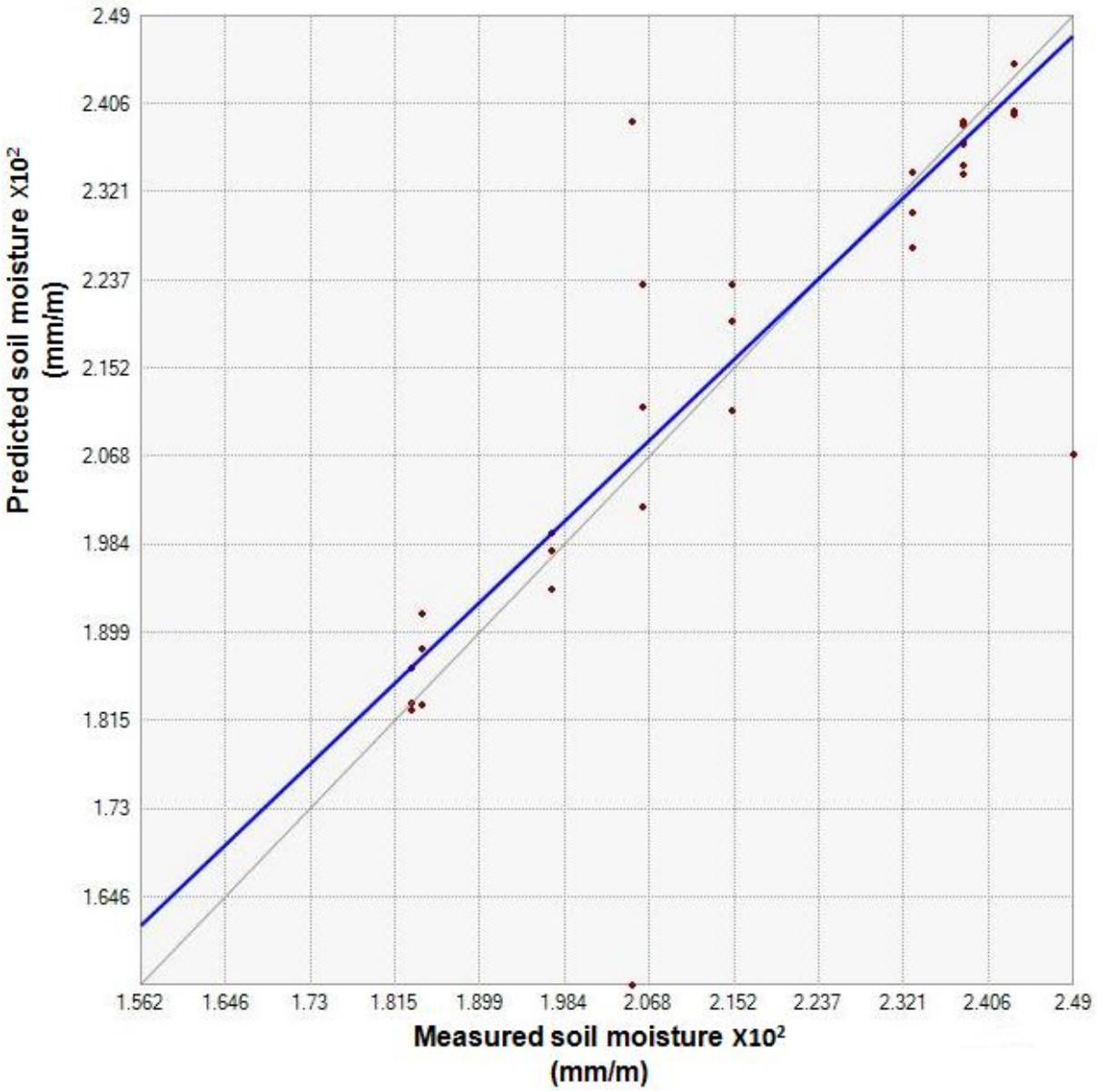

SPAW predicted soil moisture versus measured spatially distributed soil moisture on the date of (02-10-2013)

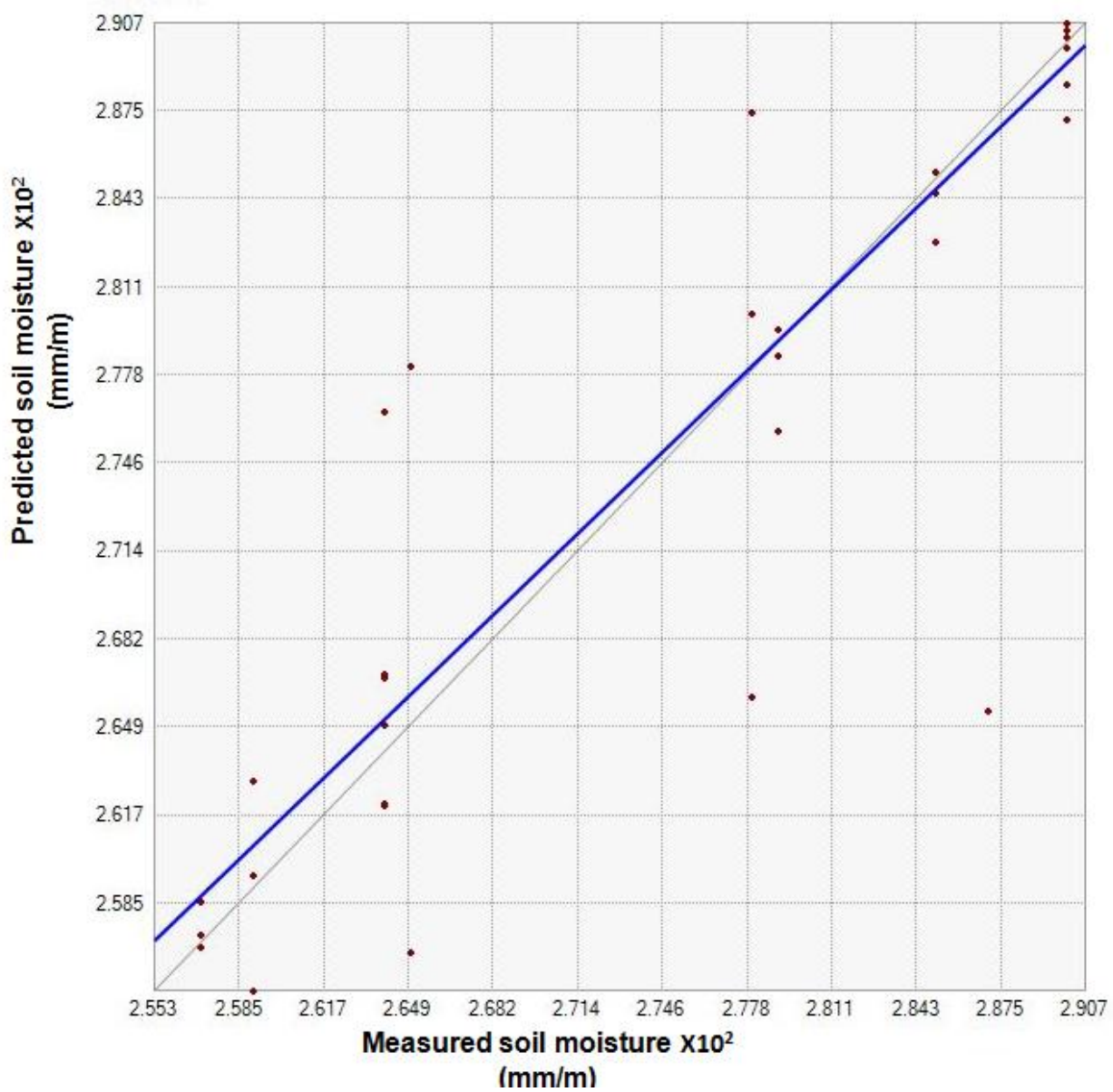

SPAW predicted soil moisture versus measured spatially distributed soil moisture on the date of (09-10-2013)

Appendix v: Comparison of SPAW predicted and Co-kriged soil moisture distribution on days where prediction was done.

Comparison of SPAW predicted and Co-kriged soil moisture distribution on 4th of September 2013.

SPAW predicted (mm/m)	Co-kriged (mm/m)	residual error	Squared residual error	SPAW predicted ($P-P_{mean}$)	Co-kriged ($P-P_{mean}$)	SPAW predicted $(P-P_{mean})^2$	Co-kriged $(P-P_{mean})^2$
322	322.9	-0.9	0.81	-10	-10	95	110
322	319.6	2.4	5.76	-10	-7	95	52
304	309.9	-5.9	34.81	8	3	68	6
304	297.5	6.5	42.25	8	15	68	223
304	322.8	-18.8	353.44	8	-10	68	108
326	325.8	0.2	0.04	-14	-13	190	179
318	306.3	11.7	136.89	-6	6	33	37
326	327.1	-1.1	1.21	-14	-15	190	215
326	323.5	2.5	6.25	-14	-11	190	123
318	329.8	-11.8	139.24	-6	-17	33	302
326	326.2	-0.2	0.04	-14	-14	190	190
326	326.5	-0.5	0.25	-14	-14	190	198
318	320.5	-2.5	6.25	-6	-8	33	65
326	322.3	3.7	13.69	-14	-10	190	98
309	298.7	10.3	106.09	3	14	10	188
296	301.5	-5.5	30.25	16	11	264	119
296	291.4	4.6	21.16	16	21	264	442
318	318.1	-0.1	0.01	-6	-6	33	32
318	318.1	-0.1	0.01	-6	-6	33	32
318	316.8	1.2	1.44	-6	-4	33	19
300	301.2	-1.2	1.44	12	11	150	126
300	299.3	0.7	0.49	12	13	150	172
322	320.6	1.4	1.96	-10	-8	95	67
300	301.5	-1.5	2.25	12	11	150	119
309	307.3	1.7	2.89	3	5	10	26
309	311.4	-2.4	5.76	3	1	10	1
309	308.9	0.1	0.01	3	4	10	12
299	299.4	-0.4	0.16	13	13	175	170
299	303.5	-4.5	20.25	13	9	175	80
299	294.3	4.7	22.09	13	18	175	328

Comparison of SPAW predicted and Co-kriged soil moisture distribution on 9th of September 2013.

SPAW predicted (mm/m)	Co-kriged (mm/m)	residual error	Squared residual error	SPAW predicted $(P-P_{mean})$	Co-kriged $(P-P_{mean})$	SPAW predicted $(P-P_{mean})^2$	Co-kriged $(P-P_{mean})^2$
285	285.3	-0.3	0.09	-11	-12	125	139
285	282.7	2.3	5.29	-11	-9	125	84
264	266.7	-2.7	7.29	10	7	97	47
264	262	2	4	10	12	97	133
264	276.5	-12.5	156.25	10	-3	97	9
290	290.1	-0.1	0.01	-16	-17	261	275
278	266	12	144	-4	8	17	57
290	290.5	-0.5	0.25	-16	-17	261	288
290	287.2	2.8	7.84	-16	-14	261	187
278	280	-2	4	-4	-6	17	42
290	290.7	-0.7	0.49	-16	-17	261	295
290	289.8	0.2	0.04	-16	-16	261	265
278	287.4	-9.4	88.36	-4	-14	17	193
290	288.4	1.6	2.56	-16	-15	261	221
287	265.5	21.5	462.25	-13	8	173	64
265	278.1	-13.1	171.61	9	-5	78	21
265	256.6	8.4	70.56	9	17	78	286
279	278.5	0.5	0.25	-5	-5	27	25
279	279.5	-0.5	0.25	-5	-6	27	36
279	275.8	3.2	10.24	-5	-2	27	5
257	256.8	0.2	0.04	17	17	283	280
257	257.3	-0.3	0.09	17	16	283	263
285	284.5	0.5	0.25	-11	-11	125	120
257	258.5	-1.5	2.25	17	15	283	226
264	262.1	1.9	3.61	10	11	97	131
264	265	-1	1	10	9	97	73
264	266.8	-2.8	7.84	10	7	97	45
259	255.2	3.8	14.44	15	18	220	336
259	262.9	-3.9	15.21	15	11	220	113
259	259.35	-0.35	0.123	15	14	220	201

Comparison of SPAW predicted and Co-kriged soil moisture distribution on 17th of September 2013.

SPAW predicted (mm/m)	Co-kriged (mm/m)	residual error	Squared residual error	SPAW predicted ($P-P_{mean}$)	Co-kriged ($P-P_{mean}$)	SPAW predicted $(P-P_{mean})^2$	Co-kriged $(P- P_{mean})^2$
261	262.9	-1.9	4	-22	-25	487	602
261	257	4	16	-22	-19	487	347
236	239.8	-3.8	14	3	-1	9	2
236	230.3	5.7	32	3	8	9	65
236	250.4	-14.4	207	3	-12	9	145
263	262.3	0.7	0	-24	-24	579	573
234	225.8	8.2	67	5	13	24	158
263	264.9	-1.9	4	-24	-27	579	704
263	259	4	16	-24	-21	579	426
234	244.8	-10.8	117	5	-6	24	41
263	264	-1	1	-24	-26	579	657
263	263	0	0	-24	-25	579	607
234	248.8	-14.8	219	5	-10	24	109
263	257.7	5.3	28	-24	-19	579	374
263	229.3	33.7	1136	-24	9	579	82
229	249.3	-20.3	412	10	-11	99	120
229	205.7	23.3	543	10	33	99	1067
253	249.8	3.2	10	-14	-11	198	131
253	255	-2	4	-14	-17	198	277
253	246.9	6.1	37	-14	-9	198	73
208	209.9	-1.9	4	31	28	957	810
208	207.4	0.6	0	31	31	957	959
261	257.6	3.4	12	-22	-19	487	370
208	208.2	-0.2	0	31	30	957	910
212	214.2	-2.2	5	27	24	725	584
212	212.1	-0.1	0	27	26	725	690
212	216.5	-4.5	20	27	22	725	478
219	220.9	-1.9	4	20	17	397	305
219	222.8	-3.8	14	20	16	397	242
219	214.7	4.3	18	20	24	397	560

Comparison of SPAW predicted and Co-kriged soil moisture distribution on 24th of September 2013.

SPAW predicted (mm/m)	Co-kriged (mm/m)	Residual error	Squared residual error	SPAW predicted ($P-P_{mean}$)	Co-kriged ($P-P_{mean}$)	SPAW predicted $(P-P_{mean})^2$	Co-kriged $(P-P_{mean})^2$
251	252	-1	1	-28	-29	764	847
251	248.5	2.5	6.25	-28	-26	764	655
222	227.5	-5.5	30.25	1	-5	2	21
222	217.5	4.5	20.25	1	5	2	29
222	235.1	-13.1	171.61	1	-12	2	149
249	248.1	0.9	0.81	-26	-25	657	635
214	208.5	5.5	30.25	9	14	88	207
249	249.7	-0.7	0.49	-26	-27	657	718
249	246	3	9	-26	-23	657	534
214	222.9	-8.9	79.21	9	0	88	0
249	249	0	0	-26	-26	657	681
249	248.3	0.7	0.49	-26	-25	657	645
214	234.1	-20.1	404.01	9	-11	88	125
249	245.2	3.8	14.44	-26	-22	657	497
252	213.1	38.9	1513.21	-29	10	820	96
211	242.2	-31.2	973.44	12	-19	153	372
211	178.7	32.3	1043.29	12	44	153	1954
241	236.3	4.7	22.09	-18	-13	311	180
241	242.1	-1.1	1.21	-18	-19	311	369
241	233.5	7.5	56.25	-18	-11	311	112
189	191.4	-2.4	5.76	34	31	1181	992
189	188.2	0.8	0.64	34	35	1181	1204
251	248.7	2.3	5.29	-28	-26	764	666
189	188.9	0.1	0.01	34	34	1181	1156
191	194.3	-3.3	10.89	32	29	1048	818
191	190.4	0.6	0.36	32	32	1048	1056
191	197	-6	36	32	26	1048	671
203	204.3	-1.3	1.69	20	19	415	346
203	205.9	-2.9	8.41	20	17	415	289
203	199.6	3.4	11.56	20	23	415	543

Comparison of SPAW predicted and Co-kriged soil moisture distribution on 2nd of October 2013.

SPAW predicted (mm/m)	Co-kriged (mm/m)	residual error	Squared residual error	SPAW predicted ($P-P_{mean}$)	Co-kriged ($P-P_{mean}$)	SPAW predicted $(P-P_{mean})^2$	Co-kriged $(P-P_{mean})^2$
243	244	-1	1	-27	-30	747	874
243	239.5	3.5	12.25	-27	-25	747	628
215	219.7	-4.7	22.09	1	-5	0	28
215	211.2	3.8	14.44	1	3	0	10
215	223.3	-8.3	68.89	1	-9	0	78
238	236.8	1.2	1.44	-22	-22	499	500
206	201.9	4.1	16.81	10	13	93	157
238	238.9	-0.9	0.81	-22	-24	499	598
238	234.5	3.5	12.25	-22	-20	499	402
206	211.5	-5.5	30.25	10	3	93	9
238	238.5	-0.5	0.25	-22	-24	499	579
238	236.8	1.2	1.44	-22	-22	499	500
206	223.2	-17.2	295.84	10	-9	93	77
238	233.8	4.2	17.64	-22	-19	499	375
249	207	42	1764	-33	7	1111	55
205	238.9	-33.9	1149.21	11	-24	114	598
205	156.1	48.9	2391.21	11	58	114	3404
233	230.2	2.8	7.84	-17	-16	300	248
233	234	-1	1	-17	-20	300	383
233	226.7	6.3	39.69	-17	-12	300	150
183	186.5	-3.5	12.25	33	28	1067	781
183	182.5	0.5	0.25	33	32	1067	1020
243	239.9	3.1	9.61	-27	-25	747	648
183	183.1	-0.1	0.01	33	31	1067	982
184	188.4	-4.4	19.36	32	26	1003	678
184	183.1	0.9	0.81	32	31	1003	982
184	191.8	-7.8	60.84	32	23	1003	513
197	197.8	-0.8	0.64	19	17	348	277
197	199.5	-2.5	6.25	19	15	348	223
197	194.1	2.9	8.41	19	20	348	414
216	214	1		0	0	500	539

Appendix vi: Daily weather (minimum and maximum Temperature, Rainfall, default monthly evaporation, estimated PET) and initial soil moisture for an input of SPAW model

Daily rainfall (mm)

Date (dd/mm/yy)	Rainfall (mm)	Date (dd/mm/yy)	Rainfall (mm)	Date (dd/mm/yy)	Rainfall (mm)	Date (dd/mm/yy)	Rainfall (mm)
13/6/13	0	14/7/13	13	14/8/13	8.5	14/9/13	0.6
14/6/13	0	15/7/13	11	15/8/13	0.4	15/9/13	0
15/6/13	0	16/7/13	19	16/8/13	7.5	16/9/13	0
16/6/13	0	17/7/13	1.4	17/8/13	21	17/9/13	0
17/6/13	0	18/7/13	7	18/8/13	1.4	18/9/13	0.2
18/6/13	0	19/7/13	18	19/8/13	0.6	19/9/13	0.4
19/6/13	0	20/7/13	12	20/8/13	21	20/9/13	0
20/6/13	20	21/7/13	0	21/8/13	18	21/9/13	0
21/6/13	0	22/7/13	12	22/8/13	0	22/9/13	0
22/6/13	25	23/7/13	1.4	23/8/13	0.6	23/9/13	0
23/6/13	0	24/7/13	0	24/8/13	0.4	24/9/13	0
24/6/13	20	25/7/13	0	25/8/13	0.6	25/9/13	0
25/6/13	0	26/7/13	12	26/8/13	0	26/9/13	0
26/6/13	21	27/7/13	0.6	27/8/13	0	27/9/13	0
27/6/13	25	28/7/13	12	28/8/13	18	28/9/13	0
28/6/13	0	29/7/13	13	29/8/13	11	29/9/13	0
29/6/13	10	30/7/13	0	30/8/13	2.4	30/9/13	0
30/6/13	0	31/7/13	16	31/8/13	6.5	1/10/2013	0
1/7/2013	28	1/8/2013	0.6	1/9/2013	0.8	2/10/2013	12
2/7/2013	0	2/8/2013	12	2/9/2013	0.6	3/10/2013	2
3/7/2013	0	3/8/2013	1.8	3/9/2013	0	4/10/2013	1
4/7/2013	27	4/8/2013	18	4/9/2013	20	5/10/2013	0
5/7/2013	16	5/8/2013	16	5/9/2013	0	6/10/2013	0
6/7/2013	15	6/8/2013	20	6/9/2013	8.5	7/10/2013	0
7/7/2013	2.4	7/8/2013	11	7/9/2013	5.5	8/10/2013	0
8/7/2013	0.8	8/8/2013	2.8	8/9/2013	0.6	9/10/2013	0
9/7/2013	0	9/8/2013	0.2	9/9/2013	1.2	10/10/2013	0
10/7/2013	14	10/8/2013	24	10/9/2013	0		
11/7/2013	21	11/8/2013	7.5	11/9/2013	0		
12/7/2013	3.4	12/8/2013	6.5	12/9/2013	0		
13/7/13	16	13/8/13	8.5	13/9/13	0		

Daily estimated Potential Evapotranspiration (PET)

Date (dd/mm/yy)	Calculated Penman ETP(mm)	Date (dd/mm/yy)	Calculated Penman ETP(mm)	Date (dd/mm/yy)	Calculated Penman ETP (mm)	Date (dd/mm/yy)	Calculated Penman ETP (mm)
13/06/13	3.46	14/07/13	2.94	14/08/13	3.1	14/09/13	3.83
14/06/13	3.35	15/07/13	2.97	15/08/13	3.32	15/09/13	4.04
15/06/13	3.43	16/07/13	2.99	16/08/13	3.27	16/09/13	3.76
16/06/13	3.48	17/07/13	2.85	17/08/13	3.25	17/09/13	3.86
17/06/13	3.98	18/07/13	2.76	18/08/13	3.35	18/09/13	3.71
18/06/13	4.19	19/07/13	2.9	19/08/13	3.34	19/09/13	3.89
19/06/13	3.93	20/07/13	3.08	20/08/13	3.25	20/09/13	4.04
20/06/13	3.57	21/07/13	3.15	21/08/13	3.35	21/09/13	4.2
21/06/13	3.58	22/07/13	2.99	22/08/13	3.43	22/09/13	4.21
22/06/13	3.45	23/07/13	3.19	23/08/13	3.31	23/09/13	4.07
23/06/13	3.31	24/07/13	3.23	24/08/13	3.36	24/09/13	3.92
24/06/13	3.27	25/07/13	3.15	25/08/13	3.61	25/09/13	4.06
25/06/13	3.4	26/07/13	2.88	26/08/13	3.26	26/09/13	4.03
26/06/13	3.42	27/07/13	3.06	27/08/13	3.23	27/09/13	3.96
27/06/13	3.46	28/07/13	3.22	28/08/13	3.38	28/09/13	4.02
28/06/13	3.45	29/07/13	3.08	29/08/13	3.38	29/09/13	3.95
29/06/13	3.41	30/07/13	3.21	30/08/13	3.21	30/09/13	3.74
30/06/13	3.45	31/07/13	3.2	31/08/13	3.42	01/10/13	3.8
01/07/13	3.15	01/08/13	3	01/09/13	3.89	02/10/13	3.78
02/07/13	3.28	02/08/13	2.93	02/09/13	3.93	03/10/13	3.71
03/07/13	3.22	03/08/13	3.15	03/09/13	3.73	04/10/13	3.96
04/07/13	3.21	04/08/13	2.93	04/09/13	3.96	05/10/13	3.76
05/07/13	3.13	05/08/13	2.98	05/09/13	3.86	06/10/13	3.59
06/07/13	2.94	06/08/13	2.96	06/09/13	3.63	07/10/13	3.58
07/07/13	3.1	07/08/13	3.03	07/09/13	3.97	08/10/13	3.7
08/07/13	3.38	08/08/13	3.32	08/09/13	4.02	09/10/13	3.66
09/07/13	3.18	09/08/13	3.6	09/09/13	3.8	10/10/13	3.55
10/7/13	3.13	10/08/13	3.33	10/09/13	3.5		
11/7/13	3.12	11/08/13	3.3	11/09/13	4		
12/7/13	3.22	12/08/13	3.2	12/09/13	3.93		
13/7/13	2.96	13/08/13	3.23	13/09/13	3.85		

Monthly evaporation defaults (mm)

Month	January	February	March	April	May	June
Evporation (mm)	159	144	142	142	156	137
Month	July	August	September	October	November	December
Evporation (mm)	126	123	112	130	138	130

Soil moisture (v/v) data for an initial condition of SPAW model (calibration)

Sampling Date	Soil moisture @10cm	Soil moisture @20cm	Soil moisture @30cm	Soil moisture @40cm	Soil moisture @60cm	Soil moisture @100cm
30/07/2013	0.18	0.24	0.31	0.33	0.37	0.40
08/08/2013	0.18	0.26	0.32	0.34	0.38	0.41
13/08/2013	0.18	0.26	0.33	0.34	0.39	0.40
20/08/2013	0.19	0.27	0.33	0.35	0.38	0.40
29/08/2013	0.20	0.28	0.34	0.35	0.38	0.40

Daily maximum temperature (ºc)

Date (dd/mm/yy)	Maximum Temp. (ºc)	Date (dd/mm/yy)	Maximum Temp. (ºc)	Date (dd/mm/yy)	Maximum Temp. (ºc)	Date (dd/mm/yy)	Maximum Temp. (ºc)
13/06/13	22.6	14/07/13	20.9	14/08/13	19.9	14/09/13	24.8
14/06/13	22.2	15/07/13	21.0	15/08/13	23.1	15/09/13	27.2
15/06/13	24.3	16/07/103	21.6	16/08/13	22.7	16/09/13	23.7
16/06/13	23.9	17/07/13	18.9	17/08/13	22.3	17/09/13	25.0
17/06/13	26.2	18/07/13	18.6	18/08/13	23.3	18/09/13	23.3
18/06/13	26.3	19/07/13	20.8	19/08/13	24.1	19/09/13	26.3
19/06/13	25.7	20/07/13	22.6	20/08/13	21.9	20/09/13	27.8
20/06/13	25.8	21/07/13	23.4	21/08/13	23.3	21/09/13	28.2
21/06/13	23.5	22/07/13	21.9	22/08/13	25.2	22/09/13	28.6
22/06/13	24.7	23/07/13	23.4	23/08/13	22.7	23/09/13	27.5
23/06/13	23.6	24/07/13	23.7	24/08/13	23.2	24/09/13	26.4
24/06/13	21.4	25/07/13	22.6	25/08/13	25.8	25/09/13	28.1
25/06/13	23.2	26/07/13	20.4	26/08/13	21.1	26/09/13	27.5
26/06/13	24.3	27/07/13	22.0	27/08/13	22.2	27/09/13	27.1
27/06/13	25.1	28/07/13	22.8	28/08/13	24.5	28/09/13	27.9
28/06/13	25.0	29/07/13	22.8	29/08/13	23.8	29/09/13	28.0
29/06/13	25.3	30/07/13	24.2	30/08/13	21.9	30/09/13	25.0
30/06/13	25.3	31/07/13	22.8	31/08/13	23.9	01/10/13	24.9
01/07/13	22.9	01/08/13	18.2	01/09/13	25.0	02/10/13	25.2
02/07/13	24.3	02/08/13	18.0	02/09/13	26.8	03/10/13	23.8
03/07/13	24.1	03/08/13	21.0	03/09/13	24.4	04/10/13	26.8
04/07/13	24.0	04/08/13	17.7	04/09/13	26.5	05/10/13	24.5
05/07/13	23.0	05/08/13	19.6	05/09/13	25.8	06/10/13	22.7
06/07/13	21.2	06/08/13	19.2	06/09/13	22.7	07/10/13	22.9
07/07/13	23.2	07/08/13	19.5	07/09/13	25.5	08/10/13	24.7
08/07/13	25.1	08/08/13	23.8	08/09/13	26.2	09/10/13	24.7
09/07/13	22.8	09/08/13	25.7	09/09/13	24.6	10/10/13	23.1
10/07/13	23.4	10/08/13	23.3	10/09/13	21.0		
11/07/13	22.9	11/08/13	23.3	11/09/13	26.3		
12/07/13	23.9	12/08/13	22.0	12/09/13	26.0		
13/07/13	21.4	13/08/13	22.1	13/09/13	25.5		

Daily minimum temperature (ºc)

Date (dd/mm/yy)	Minimum Temp. (ºc)	Date (dd/mm/yy)	Minimum Temp. (ºc)	Date (dd/mm/yy)	Minimum Temp. (ºc)	Date (dd/mm/yy)	Minimum Temp. (ºc)
13/06/13	15.0	14/07/13	15.0	14/8/13	16.0	14/09/13	16.3
14/06/13	16.4	15/07/13	14.8	15/8/13	15.0	15/09/13	15.1
15/06/13	15.1	16/07/13	14.1	16/8/13	15.5	16/09/13	16.3
16/06/13	14.6	17/07/13	14.7	17/8/13	14.5	17/09/13	15.7
17/06/13	14.3	18/07/13	14.3	18/8/13	15.0	18/09/13	15.0
18/06/13	14.5	19/07/13	13.3	19/8/13	13.9	19/09/13	13.2
19/06/13	16.0	20/07/13	15.0	20/8/13	14.9	20/09/13	13.0
20/06/13	14.3	21/07/13	15.9	21/8/13	15.3	21/09/13	13.9
21/06/13	16.2	22/07/13	14.5	22/8/13	15.3	22/09/13	12.4
22/06/13	16.2	23/07/13	14.8	23/8/13	16.2	23/09/13	13.0
23/06/13	15.3	24/07/13	14.3	24/8/13	15.6	24/09/13	13.5
24/06/13	15.2	25/07/13	15.9	25/8/13	13.2	25/09/13	12.6
25/06/13	14.9	26/07/13	15.1	26/8/13	14.9	26/09/13	14.0
26/06/13	15.9	27/07/13	14.4	27/8/13	13.3	27/09/13	13.1
27/06/13	15.7	28/07/13	14.8	28/8/13	12.7	28/09/13	14.1
28/06/13	15.2	29/07/13	15.0	29/8/13	13.5	29/09/13	13.3
29/06/13	15.1	30/07/13	14.7	30/8/13	14.8	30/09/13	15.7
30/06/13	15.1	31/07/13	15.5	31/8/13	13.5	01/10/13	14.1
01/07/13	15.6	01/08/13	15.0	01/09/13	13.1	02/10/13	12.8
02/07/13	14.2	02/08/13	14.1	02/09/13	14.0	03/10/13	14.0
03/07/13	14.5	03/08/13	13.6	03/09/13	15.2	04/10/13	13.3
04/07/13	15.1	04/08/13	14.4	04/09/13	14.6	05/10/13	15.3
05/07/13	14.3	05/08/13	14.2	05/09/13	14.6	06/10/13	16.4
06/07/13	15.2	06/08/13	14.2	06/09/13	14.7	07/10/13	15.2
07/07/13	14.4	07/08/13	14.9	07/09/13	14.7	08/10/13	13.6
08/07/13	14.3	08/08/13	12.8	08/09/13	13.8	09/10/13	12.3
09/07/13	14.9	09/08/13	15.8	09/09/13	14.2	10/10/13	13.7
10/07/13	14.0	10/08/13	14.9	10/09/13	15.1		
11/07/13	13.9	11/08/13	14.3	11/09/13	14.1		
12/07/13	14.1	12/08/13	15.8	12/09/13	13.4		
13/07/13	15.3	13/08/13	15.8	13/09/13	14.6		

Appendix vii. Infiltration rate of soils cropped with sorghum, mixed cropping of sorghum and faba bean, and tef *(eragrostis Tef)*

Location 1 (Sorghum)		Location 2 (Mixed cropping of Sorghum & faba bean)				Location 3 (Tef)			
Time (min)	Infiltration rate (mm/h)	Time (min)	Infiltration rate (mm/h)	Time (min)	Infiltration rate (mm/h)	Time (min)	Infiltration rate (mm/h)	Time (min)	Infiltration rate (mm/h)
0	900	0	600	73	115	0	480	71	60
1	550	1	530	77	109	1	422	75	56.6
3	525	3	480	81	103.5	3	389	79	53.4
5	459	5	430	85	98.5	5	341	83	50.2
7	407	7	380	89	95.3	7	301	87	47.2
9	373	9	355	93	93.7	9	279	91	44.4
11	343	11	339	97	90.9	11	248	95	42
13	317	13	323	101	89.5	13	229	99	39.6
15	297	15	315	105	87.9	15	213	103	37.6
17	281	17	307	109	86.3	17	205	107	35.6
19	265	19	299	113	85.3	19	197	111	34.5
21	249	21	292	117	85.1	21	191	115	34.6
23	233	23	289	121	85.1	23	183	119	34.6
25	217	25	275	125	85.1	25	175	123	34.6
27	201	27	269	129	85.1	27	166	127	34.6
29	185	29	259	133	85.1	29	158	131	34.6
31	169	31	251	137	85.1	31	149	135	34.6
33	159	33	243			33	142		
35	132	35	236			35	134		
37	120	37	229			37	125		
41	108	41	215			41	109		
45	80	45	201			45	97		
47	63	49	187			47	93		
51	59	53	173			51	85		
55	55	57	159			55	77		
59	50	61	145			59	72		
63	50	65	133			63	68		
67	50	69	123			67	64		